UNIVERSITÀ
DEGLI STUDI
DI PADOVA

Administrative unit: **University of Padova**

Department: **Land, Environment, Agriculture and Forestry (TESAF)**

PhD Program: **Land, Environment, Resources and Health (LERH)**

Batch: XXXV

WINDSTORMS IMPACTS ON PROTECTIVE FORESTS: ASSESSING VULNERABILITY AND DEFINING INTERVENTION STRATEGIES

PhD Program Coordinator: Prof. Marco Borga

Supervisor: Prof. Emanuele Lingua

PhD candidate: Maximiliano Costa

Sede Amministrativa: Università degli Studi di Padova

Dipartimento Territorio e Sistemi Agro-Forestali (TESAF)

CORSO DI DOTTORATO DI RICERCA: **Land, Environment, Resources, Health (LERH)**

Ciclo: **XXXV**

WINDSTORMS IMPACTS ON PROTECTIVE FORESTS: ASSESSING VULNERABILITY AND DEFINING INTERVENTION STRATEGIES

Coordinatore: Prof. Marco Borga

Supervisore: Prof. Emanuele Lingua

Dottorando: Maximiliano Costa

Index

1. General introduction

1.1 Introduction

Mountains cover more than 40% of the European continent and they are covered for almost 40% of their extent by mountain forests (Price et al., 2004, Price et al., 2011). Mountain forests have been widely studied under different perspectives, from their ecological characteristics to historical and present utilisation, since local communities always relied on ecosystem services provided by these forest stands (Kräuchi et al., 2000).

Among the ecosystem services that are provided by a mountain forest there are three main categories (Price et al., 2011):

- Provisioning services
- Cultural services
- Regulating and supporting services

Some examples of provisioning services are timber production, fuelwood production, or Non-Timber Forest Products - NTFPs (Price et al. 2011). Cultural services are related with an intrinsic aesthetic value of stands which may provide a recreational function and that can have a touristic value (Price et al. 2011).

Lastly, regulating and supporting services are related to the interaction of mountain forests with gravitative hazards or with the hydrological cycle. Some examples of these services are the prevention of soil erosion, the maintenance of the hydrological cycle on large catchments with the limitation of peak stream flow rates. One of these services is the protective function against gravitative hazards like avalanches or rockfall (Kräuchi et al., 2000; Motta and Haudemand, 2000). This function's importance increased in the last years according to some authors (Kräuchi et al., 2000; Mina et al., 2017) due to the impact of disturbances regime on mountain forests (Bebi et al., 2017; Hanewinkel et al., 2008). Forest management should evaluate which management strategies are better to increase forest resistance and resilience against natural disturbances and at the same time maintain the protective function with a sufficient efficiency.

Going into the specifics of this thesis work, the topic will concern the impact of wind disturbances on protection forests in the Alps. This specific disturbance was chosen because this is the disturbance that impacts European forests the most, and it is expected that wind damage will increase in the coming years (Patacca et al., 2022).

Figure 1 exemplifies the concepts so far; the figure represents the effects of a windstorm in the Dolomite area. It is possible to observe a damaged protective forest and two different management strategies, non-intervention above the village, and complete salvage logging under the village and closer to forest roads. It is clear that different management strategies will lead to different outcomes, and these practices will be discussed within this thesis.

Figure 1. Example of wind disturbance in a protective forest in the Dolomites, Italian Alps.

An example is the non-intervention option: it will be discussed how leaving deadwood on the ground may help to maintain the protective efficiency in a damaged stand, however this practice will lead to an increase of bark beetle outbreak risk (Dobor et al. 2020). Recent studies focussed on how to manage bark beetles' outbreaks in protective forests, with a specific focus on protective from avalanches (Teich et al. 2019). Moreover, experiences of wind damages within protective stands have been observed and studied in the north of the Alps, after the Vivian and Lothar storms in Switzerland (Schönenberger et al., 2005; Wohlgemuth et al., 2017), this thesis represents a first study of this kind on the southern side of the Alps focusing on the case study of the storm Vaia. The storm Vaia hit Italy at the end of October 2018 hitting more than 40'000 ha of forests and causing the loss of at least 10 million m^3 of timber (Piragnolo et al., 2021; Udali et al., 2021). Moreover, this thesis will focus on the mapping of vulnerability to wind disturbances. Some authors observed using dynamic vegetation models how climate change will threaten the efficiency of protective forests in the Alps in the next years (Moos et al. 2021); these results, although limited to a case study, can give insight into the importance of assessing the vulnerability of mountain forests to wind damage.

1.2 Structure of the thesis

The general workflow of the thesis is represented in Figure 2, the four points that are highlighted in the figure represent the four chapters of the work.

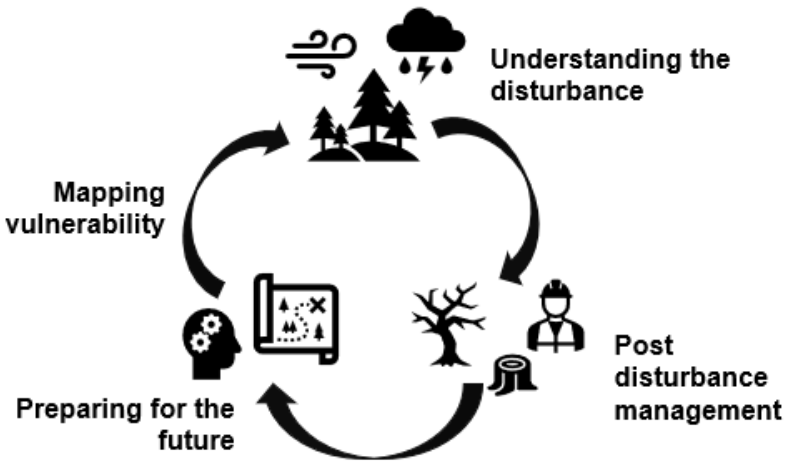

Figure 2. Workflow of the thesis

The starting chapter is focused on the understanding of disturbances, with a specific focus on disturbances legacies, in Figure 1 it is reported as '*Understanding the disturbance*'. Starting from a very broad point of view concerning natural disturbances in general, this chapter aims to present the state of the art regarding the definition of disturbance legacies and what the studied roles of these are. The aim of the chapter is also to identify possible gaps of knowledge.

From the next chapter, the thesis will deal more specifically with wind disturbances in protective forests. The aim of this chapter is to analyse the role of biological legacies in post disturbance management, hence the chapter title *'Post disturbance management'*. The main research questions of this chapter are:

- Do biological legacies maintain the protective efficiency in a damaged forest stand?
- How can post disturbance management take advantage of the presence of biological legacies?

The case study that is reported in this chapter is related to the windstorm Vaia, which hit the north-eastern Italian Alps in October 2018.

The last two chapters address not post-disturbance management in the strict sense, but the prevention of future disturbances and the planning of forest management for this purpose.

The first step, set out in the chapter *'Preparing for the future'*, aims to deepen knowledge of the stability of trees growing in sloping terrain, which is typical of mountain forests. Field tests conducted

on spruce specimens, one of the main species in Alpine forests, were aimed at studying the difference in plant overturning resistance as a function of growth site. The results of this study made it possible to implement a new parameterisation in a model for estimating susceptibility to wind damage. The validation of this new parameterisation is contained in the chapter *'Mapping vulnerability'*. The objective of this last chapter is the creation of susceptibility maps, maps that can help to target forest planning and forest operation in order to enhance forest resistance and resilience against future disturbance.

The structure of the thesis is presented as a cycle, because disturbances recur cyclically, due to climate change their frequency is expected to increase. The overall objective of this thesis is to improve actual knowledge so that we can start with the cycle with more specific expertise concerning natural disturbances and their management in the context of protective forests in the Alps.

1.3 References

Bebi, P., Seidl, R., Motta, R., Fuhr, M., Firm, D., Krumm, F., Conedera, M., Ginzler, C., Wohlgemuth, T., Kulakowski, D., 2017. Changes of forest cover and disturbance regimes in the mountain forests of the Alps. For. Ecol. Manage. 388, 43–56. https://doi.org/10.1016/j.foreco.2016.10.028

Dobor, L., Hlásny, T., Rammer, W., Zimová, S., Barka, I., & Seidl, R. (2020). *Spatial configuration matters when removing windfelled trees to manage bark beetle disturbances in Central European forest landscapes. J. of Env. Man., 254, 109792.* doi:10.1016/j.jenvman.2019.109792

Hanewinkel, M., Breidenbach, J., Neeff, T., Hanewinkel, E.K.M., 2008. Seventy-seven years of natural disturbances in a mountain forest area - The influence of storm, snow, and insect damage analysed with a long-term time series. Can. J. For. Res. 38, 2249–2261. https://doi.org/10.1139/X08-070

Kräuchi, N., Brang, P., Schönenberger, W., 2000. Forests of mountainous regions: Gaps in knowledge and research needs. For. Ecol. Manage. 132, 73–82. https://doi.org/10.1016/S0378-1127(00)00382-0

Mina, M., Bugmann, H., Cordonnier, T., Irauschek, F., Klopcic, M., Pardos, M., Cailleret, M., 2017. Future ecosystem services from European mountain forests under climate change. J. Appl. Ecol. 54, 389–401. https://doi.org/10.1111/1365-2664.12772

Moos, C., Guisan, A., Randin, C.F., Lischke, H., 2021. Climate Change Impacts the Protective Effect of Forests: A Case Study in Switzerland. Front. For. Glob. Chang. 4. https://doi.org/10.3389/ffgc.2021.682923

Motta, R., Haudemand, J.-C., 2000. Protective Forests and Silvicultural Stability. Mt. Res. Dev. 20, 180–187. https://doi.org/10.1659/0276-4741(2000)020[0180:PFASS]2.0.CO;2

Patacca, M., Lindner, M., Lucas-Borja, M.E., Cordonnier, T., Fidej, G., Gardiner, B., Hauf, Y., Jasinevičius, G., Labonne, S., Linkevičius, E., Mahnken, M., Milanovic, S., Nabuurs, G.J., Nagel, T.A., Nikinmaa, L., Panyatov, M., Bercak, R., Seidl, R., Ostrogović Sever, M.Z., Socha, J., Thom, D., Vuletic, D., Zudin, S., Schelhaas, M.J., 2022. Significant increase in natural disturbance impacts on European forests since 1950. Glob. Chang. Biol. 1–18. https://doi.org/10.1111/gcb.16531

Piragnolo, M., Pirotti, F., Zanrosso, C., Lingua, E., Grigolato, S., 2021. Responding to large-scale forest damage in an alpine environment with remote sensing, machine learning, and Web-GIS. Remote Sens. 13. https://doi.org/10.3390/rs13081541

Price, M., Lysenko, I., Gloersen, E., 2004. Delineating Europe's mountains. Rev. géographie Alp. 92, 75–86. https://doi.org/10.3406/rga.2004.2294

Price, Martin F, Georg Gratzer, Lalisa Alemayehu Duguma, Thomas Kohler, Daniel Maselli, and Rosalaura Romeo (editors) (2011). Mountain Forests in a Changing World - Realizing Values,

addressing challenges. Published by FAO/MPS and SDC, Rome

Schönenberger, W., Noack, A., Thee, P., 2005. Effect of timber removal from windthrow slopes on the risk of snow avalanches and rockfall. For. Ecol. Manage. 213, 197–208. https://doi.org/10.1016/j.foreco.2005.03.062

Teich, M., Giunta, A. D., Hagenmuller, P., Bebi, P., Schneebeli, M., & Jenkins, M. J. (2019). Effects of bark beetle attacks on forest snowpack and avalanche formation – Implications for protection forest management. For. Ecol. and Manage. 438, 186–203. doi: 10.1016/j.foreco.2019.01.052

Udali, A., Andrighetto, N., Grigolato, S., Gatto, P., 2021. Economic impacts of forest storms—taking stock of after-vaia situation of local roundwood markets in northeastern italy. Forests 12. https://doi.org/10.3390/f12040414

Wohlgemuth, T., Schwitter, R., Bebi, P., Sutter, F., Brang, P., 2017. Post-windthrow management in protection forests of the Swiss Alps. Eur. J. For. Res. 136, 1029–1040. https://doi.org/10.1007/s10342-017-1031-x

2. Understanding the disturbance

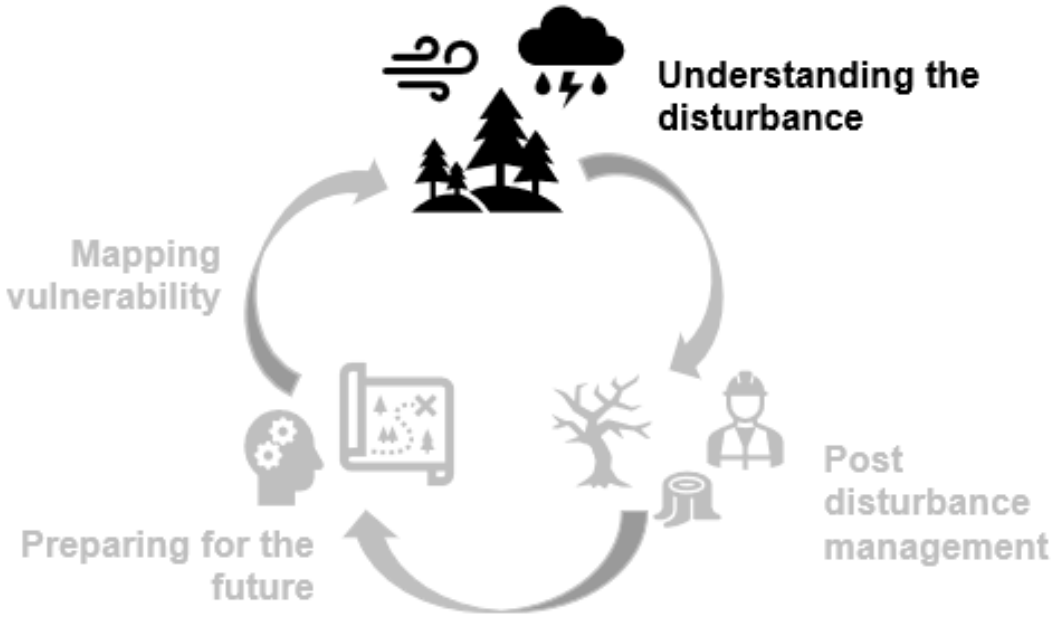

Natural disturbances are key events in ecosystems dynamics, and they represent a widely studied topic. Disturbances can have both biotic or abiotic origin and they will modify ecosystem processes leaving legacies. Disturbance legacies may help ecological recovery processes or slow other processes, they can also lead to a drastic change in the ecosystem. Currently disturbance legacies are divided in two categories: information legacies and material legacies. Information legacies are mainly the result of the interaction between an organism and its environment; material legacies are what physically remain after a disturbance, they can be subdivided in survivors, structural legacies, and spatial derived patterns. Each disturbance will produce different type of legacies and each legacy will play a different role, both in the short and in the long term. To understand the role of these legacies is of key importance both for having a deeper knowledge of ecosystem processes and their response to natural disturbances, both for managing disturbed ecosystems for enhancing their resistance and resilience against external stresses when needed.

The aim of this chapter is to present an up-to-date state of the art on disturbance legacies in forest environments and their roles, with a focus on the most studied roles and those that are less investigated. A deeper knowledge, as well as a more systemic categorisation, of the roles of biological legacies can lead to a clear improvement in the management of an ecosystem after a disturbance.

2.1 Introduction

Natural disturbances are discrete events of biotic or abiotic origin that cause tree mortality and loss of vegetation biomass in a forest environment (White and Pickett, 1985). Natural disturbances have a key role in the dynamics of ecological processes of many ecosystems. Disturbances have been widely studied for what concerns their effect on ecosystem services, public safety, and economy (Bebi et al., 2017; Hanewinkel et al., 2008; Schelhaas et al., 2010). The triggers of disturbances have been studied as well by means of providing risk maps and prevention/mitigation strategies. One aspect less studied, if not more recently than the others, is what is remaining after a disturbance, so the legacy of a disturbance, and how could this legacy influence post disturbances processes.

The key concept of biological legacy was developed by Franklin (Franklin et al., 2000) considering the case study of Mount St. Helens eruption. Some years after the event he observed how ecological recovery processes were linked with remnant organisms, biological legacies were defined as "*the organisms, organic materials, and organically-generated environmental patterns that persist through a disturbance and are incorporated into the recovering ecosystem*" (Franklin et al., 2000).
In the first definition it was possible to differentiate biological legacies in three categories, each category has different characteristics and different role in post disturbance processes. The three categories recognized by Franklin are listed below and some examples are synthetised below:

- survivors
    - these legacies provide *in situ inocula*, for instance a green island of trees is a seed source after the disturbance event, rendering migration to the site unnecessary.
- structural legacies
    - structural legacies promote provide critical habitat, substrate and food sources and moderate microclimatic conditions; examples are reported in Figure 3 where deadwood provides shelter for natural regeneration, and in Figure 4 where snags and lying logs after a windstorm can be observed.
- biologically generated spatial patterns
    - their contribution goes beyond the early stages of recovery
    - they enhance the structural complexity which has practical importance for the recovery of species diversity and ecosystem functions.

Figure 3. Early regeneration of Norway spruce (Picea abies (L.) Karst) in the red circles, it was found close to deadwood two years after a windthrow event. San Lucano valley in Belluno province, Dolomites, Italy.

Figure 4. Example of biological legacies. Lying logs and snags after the windstorm Vaia, Colle Santa Lucia (BL), Dolomites, Italy

Some examples of biological legacies are synthetically reported in Figure 5.

Survivors	**Structural legacies**	**Biologically generated spatial patterns**
- Complete organisms (e.g. single trees)	- snags	- roots, pits and mounds
- Perennating parts (roots, rhizomes, hyphae ecc)	- logs and coarsy woody debris	- understory community patterns
- Propagules (seeds, spores, eggs)	- large soil aggregates	- soil physical, chemical and microbiological patterns
	- dead animal bodies	

Figure 5. Examples of biological legacies, divided into the three categories introduced by Franklin (Franklin 2000).

After Franklin, Johnstone et al. (2016) expanded the concept of biological legacies to the one of disturbance legacies, the concepts are akin, but Johnstone introduces a new perspective. Legacies can

be differentiated in two main classes: material legacies (in which the three categories introduced by Franklin can be found) and information legacies. Information legacies are related to the interaction of the organisms with their environment, like species life history traits, i.e., the result of an adaptive process of the species to the environment. Material legacies have among their role the one of for the perpetuation of the information legacies. Both classes of legacies (material and information), contribute to create the ecological memory of an ecosystem. The ecological memory of an ecosystem is what built resistance and resilience against natural disturbances and, according to Johnstone, help maintaining a "*safe operating space for ecosystem recovery*" (Johnstone et al., 2016). The concept of ecological memory is influenced either by the disturbance history of a system, because over large temporal and spatial scales it shapes information legacies, and by specific disturbance events, because they produce material legacies.

Summarizing all these concepts it is possible to schematize a categorization of biological legacies combining the definition provided by Franklin and by Johnstone. Figure 6 shows this schematic division with the last columns indicating some of their role in a post disturbance scenario.

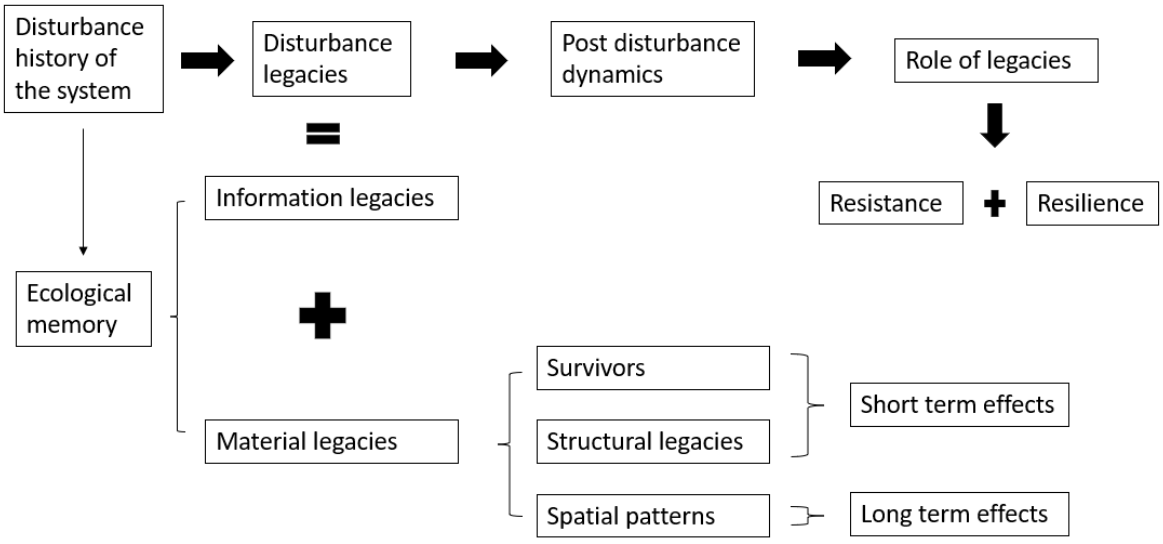

Figure 6. Scheme of biological legacies, their categorizations, and some roles that they can play in a post disturbance scenario (based on Franklin et al. 2000 and Johnstone et al. 2016).

To conclude it is clear that any changes to local climate, to the disturbance regimes and to the number and distribution of biological legacies have an influence on the forest landscape and ecosystem services (Seidl et al., 2014a). Any change may potentially modify, or even disrupt, the interaction or the feedbacks that confer resilience to the forest ecosystem, as well as it may trigger state changes.

The objective of the current review is to put together the actual knowledge about biological legacies that remain after natural disturbances in a forest environment. This review aims to the creation of a

frame for the identification of biological legacies and the identification of their role after a disturbance thus to create some guidelines that may help local managers to identify the best strategies for fulfilling their management goals.

2.2 Materials & methods

The reviewing process was based on the Prisma procedure (Moher et al., 2009), so as to adopt a rigorous procedure to limit bias and criticality. The same procedure has been used by numerous authors (Leverkus et al., 2021, 2018) within the forest ecology field, it is based on broad research through keywords.

The first step consists in the individuation of the keywords, in this specific case the objective of this work Is to investigate the role of biological legacies after a natural disturbance, with a specific focus on forests and recovery processes, so the search string that was selected is:

Search string: **forest AND recovery AND (disturbance OR "biological legac*" OR *wood OR log?)**

The search string was run on two major databases, Scopus, and Web of Science. Other minor databases were used but the results were already included in the previous. A similar approach was adopted by Leverkus (Leverkus et al., 2021). The first step of Prisma's procedure is the analysis of results by title, the idea is to exclude or include papers according to the title. Then the procedure is moving to the second step.

The second step is focused on the selection by abstract. After reading the abstract the papers were selected for the next step, the third one, in which the whole papers were read and analysed for eligibility. The eligible papers were included in the final analysis for the review's results.

The criteria for eligibility that were used are listed below:

- The studied environment must be a forest and the disturbance may be natural or anthropogenic.

- Biological legacies must be quantified, even if they are not clearly defined as legacies they must, however, fall into one of Franklin's three categories (survivors, structural legacies, biologically generated spatial pattern).

- The role played by the studied biological legacies, categorised as: recovery, life boating, c cycle, ecosystem services, structure, resilience, soil properties, must be made explicit. The functions of biological legacies and some examples are reported in Figure 7.

- The reviews are excluded from the general analysis but read and analysed to create the framework of the analysis matrix, and to get an overview of the state of the art.

For each eligible paper some data were noted and put in a matrix: year of the publication, location of the study area, type of forest, type of disturbance, type of biological legacy, role of biological legacy.

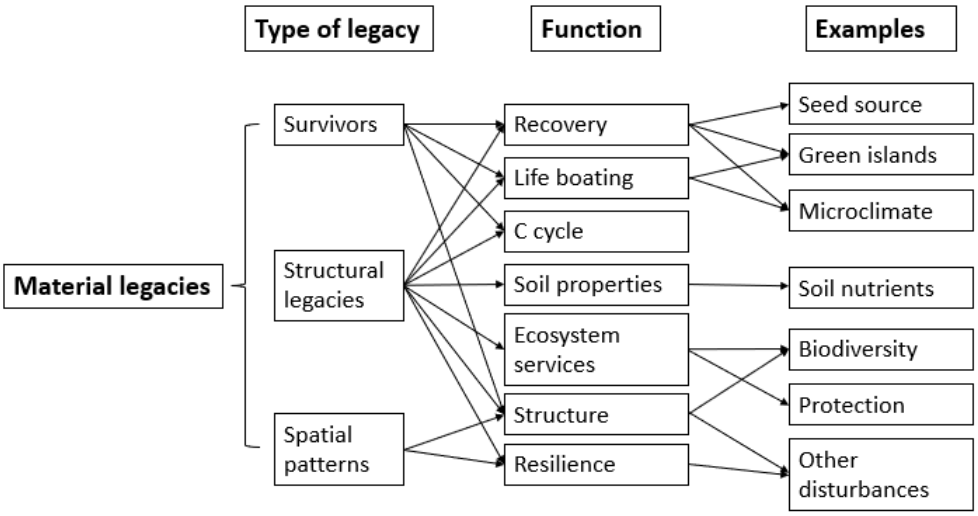

Figure 7. Scheme of material legacies classification by type and function. The last column reports some examples

From the final matrix data were elaborated to observe the most studied type of legacy and the most studied functions. Moreover, some analyses were carried on the type of forest that were studied and for which disturbances. In the discussion section some further qualitative analyses are reported.

2.3 Results

The research through keywords identified 3425 results on Scopus and 3777 results on Web of Sciences. Merging the results and eliminating doubles the final result was of 5396 papers to screen.

Of these papers 4672 were excluded based on the title, the remaining 724 were selected according to the abstract. In this phase 574 papers were excluded and only 150 papers remained to be read and selected for eligibility. At the end of the process 95 papers were assessed as eligible.

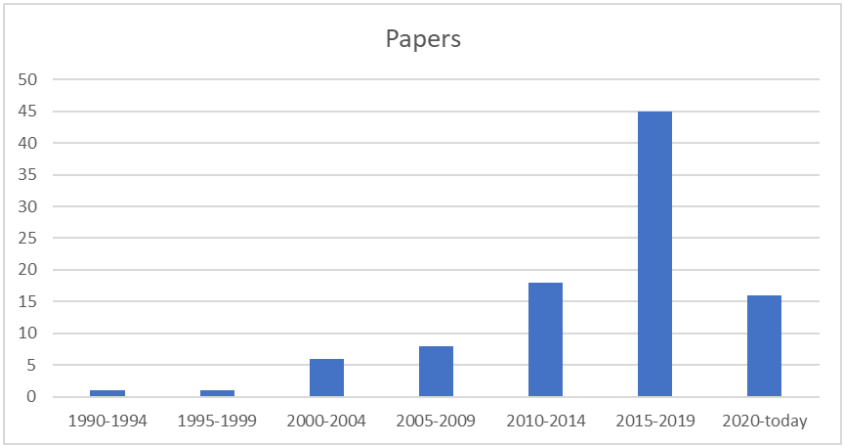

Figure 8. Number of papers identified in the reviewing process for years of publication

Most of the eligible papers were published in the last decade, as it can be seen in Figure 8, only 2 eligible papers were found in the 90's, before the most famous definition of biological legacies developed by Franklin (2000).

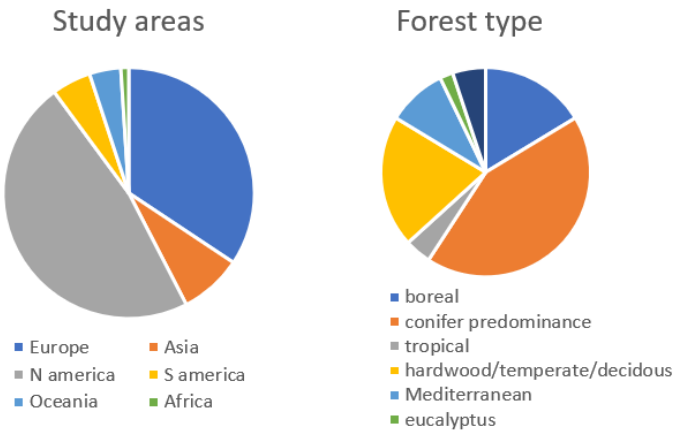

Figure 9. Study areas and forest type in literature

The most studied areas appeared to be North America and Europe (Figure 9). The less represented continent is Africa. In these areas the most studied forest types are conifer forests and deciduous forests. The less represented forest type was found to be plantations of eucalyptus.

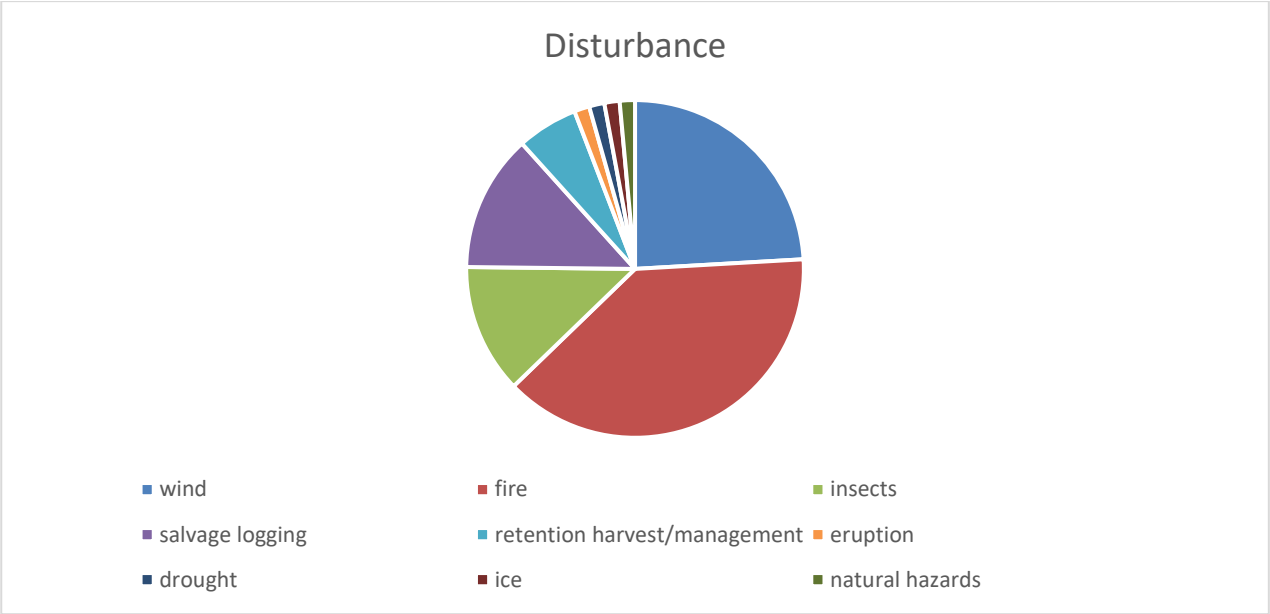

Figure 9. Natural and anthropogenic disturbances that were found by the Prisma procedure

The natural and anthropogenic disturbances that were found in the review are reported in Figure 10. The most studied disturbances are wildfires and windthrow. Salvage logging is at third place followed by insect outbreaks. Less studied disturbances are drought, ice storms, natural hazards (rockfall or avalanches) and eruptions.

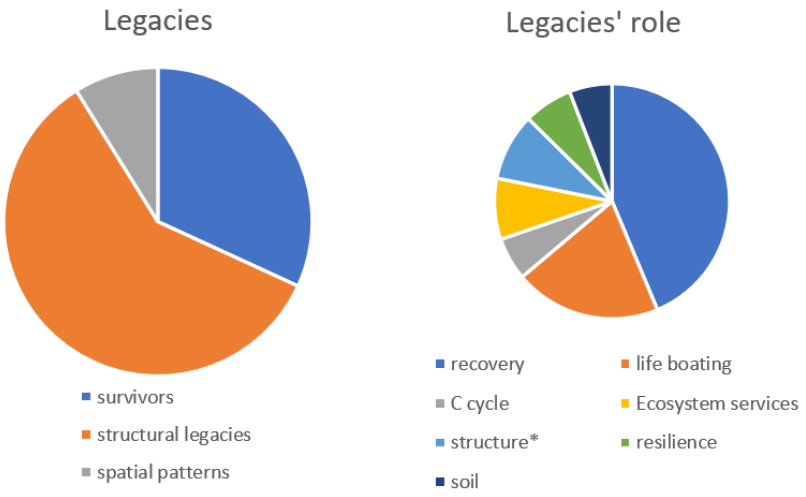

Figure 10. Type of material legacies and their observed role.

The most studied legacies are structural legacies, most of the studies were focused on deadwood, from lying logs to coarse woody debris, and snags. A good number of studies were also focused on survivors, on individual level and on green islands. Biologically generated spatial patterns, i.e., legacies which effects can be observed on larger time scales were less studied (see Figure 11).

The most studied role of biological legacies is linked to recovery processes, for instance like microclimate or facilitation for natural regeneration. The second most studied role is biological legacies as lifeboats for species, from fungi to bird species as well as for maintaining biodiversity in general. The other roles that are studied and observed are the maintaining of the forest structure, the provision of ecosystem services, the enhancing of resilience of the forest ecosystem, the balance of carbon cycle, the effects on soil.

2.4 Discussion

The first result to be noted is the growing interest toward the topic. Interest on disturbance legacies in forestry research has been increasingly growing along the years, mainly starting after the 'official' definition of biological legacies (Franklin et al., 2000) and increasing significantly over the last 5/7 years, when also a new and broader definition of disturbance legacies was introduced (Johnstone et al., 2016). A note to be made is that the review mainly only identified papers that explicitly refer to biological legacies or disturbance legacies, however, it was noted during the reading and analysis of the papers that some authors deal with the topic without using this terminology. The incorrect use of terminology may have prevented the identification of other papers that observed and studied the roles of biological legacies. Most of the studies come from North America and Europe, and the papers identified by the research focus mainly on macro-areas of these continents: boreal forests, temperate forests, and the Mediterranean area. Consequently, the forest types that can be traced back to these areas are the most studied. The most studied disturbances resulted to be wind and fire, fire was especially studied in the Mediterranean basin in Europe (García-Tejero et al., 2013; José Martínez-Sánchez et al., 1999; Marzano et al., 2012; Rost et al., 2009). Among less studied disturbances we found eruptions (Ferreiro et al., 2018; Iida et al., 2021), ice storms (Mou and Warrillow, 2020), drought (Kannenberg et al., 2019; Krawchuk et al., 2020) and natural hazard, e.g. debris flow (McGuire and Youberg, 2019; Sass et al., 2006a).

Among the disturbances studied in the papers identified by the Prisma procedure, not only natural disturbances but also two main anthropogenic disturbances were identified: salvage logging and retention harvesting. Salvage logging has been introduced as a disturbance according to recent studies (Hernández-Hernández et al., 2017; Leverkus et al., 2015; Royo et al., 2016) and during the review it always appeared together with other natural disturbances, following them as a management option and as secondary disturbance (Kleinman et al., 2019; Royo et al., 2016; Taeroe et al., 2019). For what concerns retention harvest all the various studies identified are from Canada (Lindenmayer et al., 2019; Palik and D'Amato, 2019).

Turning to the categories of biological legacies, structural legacies are the most studied category, followed by survivors. Spatial derived patterns are less studied, perhaps also because of the longer temporal span over which they act (Seidl et al., 2014b). For what concerns the different roles played by biological legacies they will briefly explain in the sections below.

Disturbance legacies and recovery processes

One of the most studied roles played by biological legacies after a disturbance is related to the early recovery processes. The presence of biological legacies may enhance and facilitate the persistence and the presence of species on a disturbed stand, even when the severity of the event was extreme. For tree species, for instance, the presence of survivors or green islands (groups of survivors) can provide seeds that are fundamental for the early successional recovery processes, especially if advanced regeneration is missing (Franklin et al., 2000; Lindenmayer et al., 2019). Moreover, disturbance legacies can accelerate the rate of recolonization during these early stages (Lindenmayer et al., 2019).

Among the type of legacies, structural legacies play a key role into the recovery processes. Elements like deadwood or snags may provide protection and may create ideal microclimatic conditions that help early regeneration recruitment (Beghin et al., 2010; Marzano et al., 2013). Post disturbance management can take advantage of these legacies, for instance using deadwood elements as natural shelters for new seedlings (Marangon et al., 2022). Some studies focus on how the regeneration is delayed on steep terrains due to superficial movements of debris, small rocks and snow (Sass et al., 2006b), the presence of deadwood may protect seedlings from material downward movements. Moreover, deadwood influence on the establishment of natural or artificial regeneration is greatly important in water limited environment: where seedlings are subject to water stress issues, the presence of material legacies may reduce soil temperature, providing a shading effect and may protect plants from wind, avoiding loss of water through transpiration, moreover the relative humidity of microsites may increase (Castro et al., 2011).

Disturbance legacies as species lifeboats

Material legacies, especially survivors and some structural legacies, may have a life boating function for some species, either animal, vegetation or fungi (Rudolphi et al., 2014).
For instance, the presence of green islands after a natural or anthropogenic disturbance influence the response of nesting birds (Lindenmayer et al., 2018), the influence of biological legacies on birds population may also be reflected on the seed dispersal after an event, considering that snags or survivors can be used as perching sites (Rost et al., 2009). Biological legacies may also have a positive

influence on the presence of gastropods communities (Bros et al., 2011) as well as fungi communities (Mediavilla et al., 2014).

Some authors observed the influence of legacies in the limitation of damages on fungi communities after wildfires: disturbances may impact these communities slowing recovery processes and it was observed how survivors can play as lifeboats for fungi (Owen et al., 2019).

Disturbance legacies and ecosystem services

The results of the review show that disturbance legacies may improve or, on the contrary, disrupt the provision of ecosystem services. It was observed that up to ten years after natural disturbances the provisioning of ecosystem services, regulating ecosystem services, and cultural services were registered to be lower than before the disturbance event (Fleischer et al., 2017).

For what concerns disturbances impacts on regulating services some authors focus on how these can modify the water cycle improving the risk of floods or debris flow (McGuire and Youberg, 2019). About this topic, a less studied effect of legacies is their effect on the terrain roughness, especially on steep terrains. An increasing of soil roughness due to deadwood material may also provide a protective function against some natural hazards in a mountain scenario (rockfall, avalanches): some studies carried in an alpine scenario describe some possible interaction among biological legacies, e.g. deadwood and lying logs, and natural hazards (Costa et al., 2021; Schönenberger et al., 2005; Wohlgemuth et al., 2017).

Disturbance legacies and carbon cycle

Structural legacies, mainly snags and deadwood, may have an impact on carbon dynamics of a forest stand affected by a disturbance. Deadwood loss of C is impacting on the carbon balance of the system, as well as it could be balanced by the C stored by early regeneration establishment. Some studies focus on these dynamics, investigating how the sink/source dynamics are balanced after wildfire events (Rothstein et al., 2004; Yue et al., 2016), for instance it was observed that, after a natural disturbance, survivors may enhance the recovery of total ecosystem carbon (TEC) stock (Seidl et al., 2014b). Moreover, the past disturbances history of a stand may influence the carbon balance as well (Yue et al., 2016).

Disturbance legacies and soil properties

Depending on the type of disturbance, some events can alter soil composition and soil related dynamics. For instance, bark beetle outbreaks will cause an accumulation of litter on the forest ground;

these legacies of the disturbance will modify both carbon and nitrogen cycle (Boggs Lynch et al., 2021). Other studies focused on the effect of wildfires and their legacies on soil fungal communities (Alem et al., 2020; Smith et al., 2017), on nitrogen concentration (Durán et al., 2010) and on soil hydraulic properties, which increase the danger of natural hazards as previously mentioned (McGuire and Youberg, 2019). Some authors also observed the influence of different disturbance severities, which bring different quantities of legacies, on soil dynamic. In all these study cases structural legacies, and in one case survivors, played a critical role.

Lastly, some authors observed the interaction of windstorms legacies with soil properties, in sites were no intervention were made and in sites were salvage logging was applied (Gáfriková et al., 2019).

Legacies and multiple disturbances

The interaction among natural disturbances is a widely studied topic in ecology: in this interaction disturbance legacies, and their management, may play a key role considering that they can link multiple disturbances in different ways (Buma, 2015; Buma and Wessman, 2011; Kleinman et al., 2019). As a matter of fact, disturbance interactions consist in the interplay between the drivers of the natural disturbance (wind, fire etc.), ecosystem properties, such as resistance against specific disturbance or general resilience of the system, and material legacies left by previous disturbances (Buma, 2015). The link from a first disturbance to a second one mainly relies on structural legacies (e.g., presence of deadwood on the ground is increasing fuel loading of a site), but they may be due also to other biological or environmental factors (altered community structure, water temperature etc.). Specifically, these interactions develop when biological legacies are functionally connected to the type of the event, either in terms of disturbance drivers or recovery processes. Many studies focus on these interactions and their dynamics, to give some examples: in northern Colorado it was observed that the increased presence of coarse woody debris in a stand after a windthrown event triggered a stand replacing fire 5 years later (Buma and Wessman, 2011). Other studies on fires after blowdowns show how the interaction among the two disturbances leads to the destruction of advanced regeneration and the elimination by fire of seeds previously fallen on the ground: this interaction fails to provide the material legacies needed for the recovery of a conifer forest, leaving ground for broadleaves, which rely on wind-dispersal seeds like aspen or birch (Frelich and Reich, 1999). In this example material legacies fail in providing information from past events after the combination of two different disturbances, this may degrade the general resilience of the damaged forest stand, opening the way to new recovery trajectories (Buma, 2015). Other interactions that are studied are linked to bark beetles outbreaks, after wildfire (Stevens-Rumann et al., 2015) or after windstorm events (Vanická et al., 2020).

As already mentioned, another important anthropogenic disturbance that may interact with natural disturbances and that may link different natural disturbances is salvage logging. The impact of this practice is widely studied, some reviews show how the impact of biological legacies removal is different considering the natural disturbance type (fire, wind, bark beetles), the forest type (Mediterranean forest, subalpine forest, boreal forest etc.), and the time scale of the observations (Leverkus et al., 2018; Lindenmayer and Noss, 2006; Taeroe et al., 2019).

For a better comprehension of disturbance interaction dynamics Buma (2015) divided the composite disturbances into two classes: linked disturbances and compound disturbances. The interaction that leads to a linked disturbance is when "*disturbance legacies that alter resistance, by increasing or decreasing the likelihood of the subsequent disturbance, its spatial extent (likelihood at a location), intensity, or severity can drive an interaction among events. More precisely, the term "linked" implies a spatial and/or temporal aspect to the relationship, whereby changes in the spatial/temporal scale or intensity of a disturbance is affected by the legacies of a previous disturbance*" (Buma, 2015). On the other hand, if disturbances interaction alters the ecosystem resilience, directly affecting the recovery processes, the interaction leads to a compound disturbance. Shortly, the interaction among natural disturbances may are grouped into two categories: those interactions which will alter ecosystem resistance (linked disturbances) and those interactions which will alter resilience (compound disturbances). Both categories, linked and compound disturbances, may have additive, synergistic or negative effects (Buma, 2015). Some authors highlighted how in some occasions multiple disturbance may increase the system resilience (Kleinman et al., 2019).

2.5 Conclusions

The results presented in this review show the multifunctionality of disturbance legacies, especially material legacies, i.e. biological legacies.

Every disturbance, natural or anthropogenic, that hits a forest ecosystem will leave legacies and these will have a role in post event dynamics, from recovery processes to the provision of ecosystem services. It was possible to observe that each disturbance has its own legacies depending on the severity of it and the forest type. To know the role of these legacies is of key importance for post disturbance management in order to fulfil management goals effectively.

Some of the main findings of this review are listed below:

- problems were encountered with the nomenclature. We found some studies about disturbance legacies where this term was not used, instead other terms were used (e.g. remnants). We suggest in the future to use the existing terminology more strictly, we hope

that the introduction to this study will help in understanding the current state of the art in this regard.

- For what concerns study areas Europe and North America are overrepresented. Studies from disturbances from other parts of the world are lacking.
- Some disturbances, e.g. wildfires, windstorms and salvage logging, are well studied and many reviews are available in literature. Future research should focus on other disturbances, e.g. ice storms, drought.
- Future studies should consider the interaction among legacies and secondary disturbances, e.g. linked and compound effects, in order to identify guidelines for risk management in areas of interest.

2.6 References

Alem, D., Dejene, T., Oria-de-Rueda, J.A., Geml, J., Castaño, C., Smith, J.E., Martín-Pinto, P., 2020. Soil fungal communities and succession following wildfire in Ethiopian dry Afromontane forests, a highly diverse underexplored ecosystem. For. Ecol. Manage. 474. https://doi.org/10.1016/j.foreco.2020.118328

Bebi, P., Seidl, R., Motta, R., Fuhr, M., Firm, D., Krumm, F., Conedera, M., Ginzler, C., Wohlgemuth, T., Kulakowski, D., 2017. Changes of forest cover and disturbance regimes in the mountain forests of the Alps. For. Ecol. Manage. 388, 43–56. https://doi.org/10.1016/j.foreco.2016.10.028

Beghin, R., Lingua, E., Garbarino, M., Lonati, M., Bovio, G., Motta, R., Marzano, R., 2010. Pinus sylvestris forest regeneration under different post-fire restoration practices in the northwestern Italian Alps. Ecol. Eng. 36, 1365–1372. https://doi.org/10.1016/j.ecoleng.2010.06.014

Boggs Lynch, L.A., Norton, U., van Diepen, L.T.A., 2021. Legacy of bark beetles (Dendroctonus spp.) on soil carbon and nitrogen cycling seven years after forest infestation. For. Ecol. Manage. 489, 119064. https://doi.org/10.1016/j.foreco.2021.119064

Bros, V., Moreno-Rueda, G., Santos, X., 2011. Does postfire management affect the recovery of Mediterranean communities? The case study of terrestrial gastropods. For. Ecol. Manage. 261, 611–619. https://doi.org/10.1016/j.foreco.2010.11.014

Buma, B., 2015. Disturbance interactions: Characterization, prediction, and the potential for cascading effects. Ecosphere 6, 1–15. https://doi.org/10.1890/ES15-00058.1

Buma, B., Wessman, C.A., 2011. Disturbance interactions can impact resilience mechanisms of forests. Ecosphere 2, 1–13. https://doi.org/10.1890/ES11-00038.1

Castro, J., Allen, C.D., Molina-Morales, M., Marañón-Jiménez, S., Sánchez-Miranda, Á., Zamora, R., 2011. Salvage Logging Versus the Use of Burnt Wood as a Nurse Object to Promote Post-Fire Tree Seedling Establishment. Restor. Ecol. 19, 537–544. https://doi.org/10.1111/j.1526-100X.2009.00619.x

Costa, M., Marchi, N., Bettella, F., Bolzon, P., Berger, F., Lingua, E., 2021. Biological legacies and rockfall: The protective effect of a windthrown forest. Forests 12, 1–16. https://doi.org/10.3390/f12091141

Durán, J., Rodríguez, A., Fernández-Palacios, J.M., Gallardo, A., 2010. Long-term decrease of organic and inorganic nitrogen concentrations due to pine forest wildfire. Ann. For. Sci. 67, 207–207. https://doi.org/10.1051/forest/2009100

Ferreiro, N., Satti, P., Mazzarino, M.J., 2018. Biological legacies promote succession and soil development on tephra from the Puyehue-Cordon Caulle eruption (2011). Austral Ecol. 43, 435–446. https://doi.org/10.1111/aec.12580

Franklin, J.F., Lindenmayer, D., Macmahon, J.A., Mckee, A., Perry, D.A., Waide, R., Foster, D., 2000. Threads of Continuity: Ecosystem disturbance, recovery, and the theory of biological legacies. Conserv. Pract. 1, 8–17.

Frelich, L.E., Reich, P.B., 1999. Neighborhood effects, disturbance severity, and community stability in forests. Ecosystems 2, 151–166. https://doi.org/10.1007/s100219900066

Gáfriková, J., Hanajík, P., Vykouková, I., Zvarík, M., Ferianc, P., Drahovská, H., Puškárová, A., 2019. Dystric Cambisol properties at windthrow sites with secondary succession developed after 12 years under different conditions in Tatra National Park. Biologia (Bratisl). 74, 1099–1114. https://doi.org/10.2478/s11756-019-00275-2

García-Tejero, S., Taboada, A., Tárrega, R., Salgado, J., Marcos, E., 2013. Differential responses of ecosystem components to a low-intensity fire in a Mediterranean forest: A three-year case study. Community Ecol. 14, 110–120. https://doi.org/10.1556/ComEc.14.2013.1.12

Hanewinkel, M., Breidenbach, J., Neeff, T., Hanewinkel, E.K.M., 2008. Seventy-seven years of natural disturbances in a mountain forest area - The influence of storm, snow, and insect damage analysed with a long-term time series. Can. J. For. Res. 38, 2249–2261. https://doi.org/10.1139/X08-070

Hernández-Hernández, R., Castro, J., Del Arco Aguilar, M., Fernández-López, Á.B., González-Mancebo, J.M., 2017. post-fire salvage logging imposes a new disturbance that retards succession: The case of bryophyte communities in a Macaronesian laurel forest. Forests 8, 1–16. https://doi.org/10.3390/f8070252

Iida, K., Hayasaka, D., Suzuki, Y., Uchida, T., Sawahata, T., Hashimoto, K., 2021. Legacy of pre-eruption vegetation affects ground-dwelling arthropod communities after different types of volcanic disturbance. Ecol. Evol. 11, 9110–9122. https://doi.org/10.1002/ece3.7755

Johnstone, J.F., Allen, C.D., Franklin, J.F., Frelich, L.E., Harvey, B.J., Higuera, P.E., Mack, M.C., Meentemeyer, R.K., Metz, M.R., Perry, G.L.W., Schoennagel, T., Turner, M.G., 2016. Changing disturbance regimes, ecological memory, and forest resilience. Front. Ecol. Environ. 14, 369–378. https://doi.org/10.1002/fee.1311

José Martínez-Sánchez, J., Ferrandis, P., De Las Heras, J., María Herranz, J., 1999. Effect of burnt wood removal on the natural regeneration of Pinus halepensis after fire in a pine forest in Tus Valley (SE Spain). For. Ecol. Manage. 123, 1–10. https://doi.org/10.1016/S0378-1127(99)00012-2

Kannenberg, S.A., Maxwell, J.T., Pederson, N., D'Orangeville, L., Ficklin, D.L., Phillips, R.P., 2019. Drought legacies are dependent on water table depth, wood anatomy and drought timing across the eastern US. Ecol. Lett. 22, 119–127. https://doi.org/10.1111/ele.13173

Kleinman, J.S., Goode, J.D., Fries, A.C., Hart, J.L., 2019. Ecological consequences of compound

disturbances in forest ecosystems: a systematic review. Ecosphere 10. https://doi.org/10.1002/ecs2.2962

Krawchuk, M.A., Meigs, G.W., Cartwright, J.M., Coop, J.D., Davis, R., Holz, A., Kolden, C., Meddens, A.J.H., 2020. Disturbance refugia within mosaics of forest fire, drought, and insect outbreaks. Front. Ecol. Environ. 18, 235–244. https://doi.org/10.1002/fee.2190

Leverkus, A.B., Buma, B., Wagenbrenner, J., Burton, P.J., Lingua, E., Marzano, R., Thorn, S., 2021. Tamm review: Does salvage logging mitigate subsequent forest disturbances? For. Ecol. Manage. 481, 118721. https://doi.org/10.1016/j.foreco.2020.118721

Leverkus, A.B., Gustafsson, L., Lindenmayer, D.B., Thorn, S., 2018. Salvage logging in the world ' s forests : Interactions between natural disturbance and logging need recognition 1140–1154. https://doi.org/10.1111/geb.12772

Leverkus, A.B., Gustafsson, L., Rey Benayas, J.M., Castro, J., 2015. Does post-disturbance salvage logging affect the provision of ecosystem services? A systematic review protocol. Environ. Evid. 4. https://doi.org/10.1186/s13750-015-0042-7

Lindenmayer, D., Blair, D., McBurney, L., 2019. Variable retention harvesting in Victoria's Mountain Ash (Eucalyptus regnans) forests (southeastern Australia). Ecol. Process. 8. https://doi.org/10.1186/s13717-018-0156-2

Lindenmayer, D.B., McBurney, L., Blair, D., Wood, J., Banks, S.C., 2018. From unburnt to salvage logged: Quantifying bird responses to different levels of disturbance severity. J. Appl. Ecol. 55, 1626–1636. https://doi.org/10.1111/1365-2664.13137

Lindenmayer, D.B., Noss, R.F., 2006. Salvage logging, ecosystem processes, and biodiversity conservation. Conserv. Biol. 20, 949–958. https://doi.org/10.1111/j.1523-1739.2006.00497.x

Lindenmayer, D.B., Westgate, M.J., Scheele, B.C., Foster, C.N., Blair, D.P., 2019. Key perspectives on early successional forests subject to stand-replacing disturbances. For. Ecol. Manage. 454, 117656. https://doi.org/10.1016/j.foreco.2019.117656

Marangon, D., Marchi, N., Lingua, E., 2022. Windthrown elements: a key point improving microsite amelioration and browsing protection to transplanted seedlings. For. Ecol. Manage. 508. https://doi.org/10.1016/j.foreco.2022.120050

Marzano, R., Garbarino, M., Marcolin, E., Pividori, M., Lingua, E., 2013. Deadwood anisotropic facilitation on seedling establishment after a stand-replacing wildfire in Aosta Valley (NW Italy). Ecol. Eng. 51, 117–122. https://doi.org/10.1016/j.ecoleng.2012.12.030

Marzano, R., Lingua, E., Garbarino, M., 2012. Post-fire effects and short-term regeneration dynamics following highseverity crown fires in a Mediterranean forest. IForest 5, 93–100. https://doi.org/10.3832/ifor0612-005

McGuire, L.A., Youberg, A.M., 2019. Impacts of successive wildfire on soil hydraulic properties:

Implications for debris flow hazards and system resilience. Earth Surf. Process. Landforms 44, 2236–2250. https://doi.org/10.1002/esp.4632

Mediavilla, O., Oria-de-Rueda, J.A., Martín-Pinto, P., 2014. Changes in sporocarp production and vegetation following wildfire in a Mediterranean Forest Ecosystem dominated by Pinus nigra in Northern Spain. For. Ecol. Manage. 331, 85–92. https://doi.org/10.1016/j.foreco.2014.07.033

Moher, D., Liberati, A., Tetzlaff, J., Altman, D.G., Altman, D., Antes, G., Atkins, D., Barbour, V., Barrowman, N., Berlin, J.A., Clark, J., Clarke, M., Cook, D., D'Amico, R., Deeks, J.J., Devereaux, P.J., Dickersin, K., Egger, M., Ernst, E., Gøtzsche, P.C., Grimshaw, J., Guyatt, G., Higgins, J., Ioannidis, J.P.A., Kleijnen, J., Lang, T., Magrini, N., McNamee, D., Moja, L., Mulrow, C., Napoli, M., Oxman, A., Pham, B., Rennie, D., Sampson, M., Schulz, K.F., Shekelle, P.G., Tovey, D., Tugwell, P., 2009. Preferred reporting items for systematic reviews and meta-analyses: The PRISMA statement. PLoS Med. 6. https://doi.org/10.1371/journal.pmed.1000097

Mou, P., Warrillow, M.P., 2020. Ice Storm Damage to a Mixed Hardwood Forest and Its Impacts on Forest Regeneration in the Ridge and Valley Region of Southwestern Virginia Author (s): Pu Mou and Michael P . Warrillow Source : The Journal of the Torrey Botanical Society , Vol . 127 , No 127, 66–82.

Owen, S.M., Patterson, A.M., Gehring, C.A., Sieg, C.H., Baggett, L.S., Fulé, P.Z., 2019. Large, high-severity burn patches limit fungal recovery 13 years after wildfire in a ponderosa pine forest. Soil Biol. Biochem. 139. https://doi.org/10.1016/j.soilbio.2019.107616

Palik, B.J., D'Amato, A.W., 2019. Variable retention harvesting in Great Lakes mixed-pine forests: emulating a natural model in managed ecosystems. Ecol. Process. 8. https://doi.org/10.1186/s13717-019-0171-y

Rost, J., Pons, P., Bas, J.M., 2009. Can salvage logging affect seed dispersal by birds into burned forests? Acta Oecologica 35, 763–768. https://doi.org/10.1016/j.actao.2009.08.004

Rothstein, D.E., Yermakov, Z., Buell, A.L., 2004. Loss and recovery of ecosystem carbon pools following stand-replacing wildfire in Michigan jack pine forests. Can. J. For. Res. 34, 1908–1918. https://doi.org/10.1139/X04-063

Royo, A.A., Peterson, C.J., Stanovick, J.S., Carson, W.P., 2016. Evaluating the ecological impacts of salvage logging: Can natural and anthropogenic disturbances promote coexistence? Ecology 97, 1566–1582. https://doi.org/10.1890/15-1093.1

Rudolphi, J., Jönsson, M.T., Gustafsson, L., 2014. Biological legacies buffer local species extinction after logging. J. Appl. Ecol. 51, 53–62. https://doi.org/10.1111/1365-2664.12187

Sass, O., Wetzel, K.F., Friedmann, A., 2006a. Landscape dynamics of sub-alpine forest fire slopes in the Northern Alps - Preliminary results. Zeitschrift fur Geomorphol. Suppl. 142, 207–227.

Sass, O., Wetzel, K.F., Friedmann, A., 2006b. Landscape dynamics of sub-alpine forest fire slopes in

the Northern Alps - Preliminary results. Zeitschrift fur Geomorphol. Suppl. 142, 207–227.

Schelhaas, M.J., Hengeveld, G., Moriondo, M., Reinds, G.J., Kundzewicz, Z.W., ter Maat, H., Bindi, M., 2010. Assessing risk and adaptation options to fires and windstorms in European forestry. Mitig. Adapt. Strateg. Glob. Chang. 15, 681–701. https://doi.org/10.1007/s11027-010-9243-0

Schönenberger, W., Noack, A., Thee, P., 2005. Effect of timber removal from windthrow slopes on the risk of snow avalanches and rockfall. For. Ecol. Manage. 213, 197–208. https://doi.org/10.1016/j.foreco.2005.03.062

Seidl, R., Rammer, W., Spies, T.A., 2014a. Disturbance legacies increase the resilience of forest ecosystem structure, composition, and functioning. Ecol. Appl. 24, 2063–2077. https://doi.org/10.1890/14-0255.1

Seidl, R., Rammer, W., Spies, T.A., 2014b. Disturbance legacies increase the resilience of forest ecosystem structure, composition, and functioning. Ecol. Appl. 24, 2063–2077. https://doi.org/10.1890/14-0255.1

Smith, J.E., Kluber, L.A., Jennings, T.N., McKay, D., Brenner, G., Sulzman, E.W., 2017. Does the presence of large down wood at the time of a forest fire impact soil recovery? For. Ecol. Manage. 391, 52–62. https://doi.org/10.1016/j.foreco.2017.02.013

Stevens-Rumann, C., Morgan, P., Hoffman, C., 2015. Bark beetles and wildfires: How does forest recovery change with repeated disturbances in mixed conifer forests? Ecosphere 6, 1–17. https://doi.org/10.1890/ES14-00443.1

Taeroe, A., Koning, J.H.C. De, Löf, M., Tolvanen, A., Heiðarsson, L., 2019. Forest Ecology and Management Recovery of temperate and boreal forests after windthrow and the impacts of salvage logging . A quantitative review. For. Ecol. Manage. 446, 304–316. https://doi.org/10.1016/j.foreco.2019.03.048

Vanická, H., Holuša, J., Resnerová, K., Ferenčík, J., Potterf, M., Véle, A., Grodzki, W., 2020. Interventions have limited effects on the population dynamics of Ips typographus and its natural enemies in the Western Carpathians (Central Europe). For. Ecol. Manage. 470–471. https://doi.org/10.1016/j.foreco.2020.118209

White, P.S., Pickett, S.T.A., 1985. Natural Disturbance and Patch Dynamics: An Introduction, The Ecology of Natural Disturbance and Patch Dynamics. ACADEMIC PRESS, INC. https://doi.org/10.1016/b978-0-12-554520-4.50006-x

Wohlgemuth, T., Schwitter, R., Bebi, P., Sutter, F., Brang, P., 2017. Post-windthrow management in protection forests of the Swiss Alps. Eur. J. For. Res. 136, 1029–1040. https://doi.org/10.1007/s10342-017-1031-x

Yue, C., Ciais, P., Zhu, D., Wang, T., Peng, S.S., Piao, S.L., 2016. How have past fire disturbances contributed to the current carbon balance of boreal ecosystems? Biogeosciences 13, 675–690.

https://doi.org/10.5194/bg-13-675-2016

3. Post disturbance management in protective forests

Based on **Costa, M.**; Marchi, N.; Bettella, F.; Bolzon, P.; Berger, F.; Lingua, E. Biological Legacies and Rockfall: The Protective Effect of a Windthrown Forest. Forests 2021, 12, 1141. https://doi.org/10.3390/f12091141

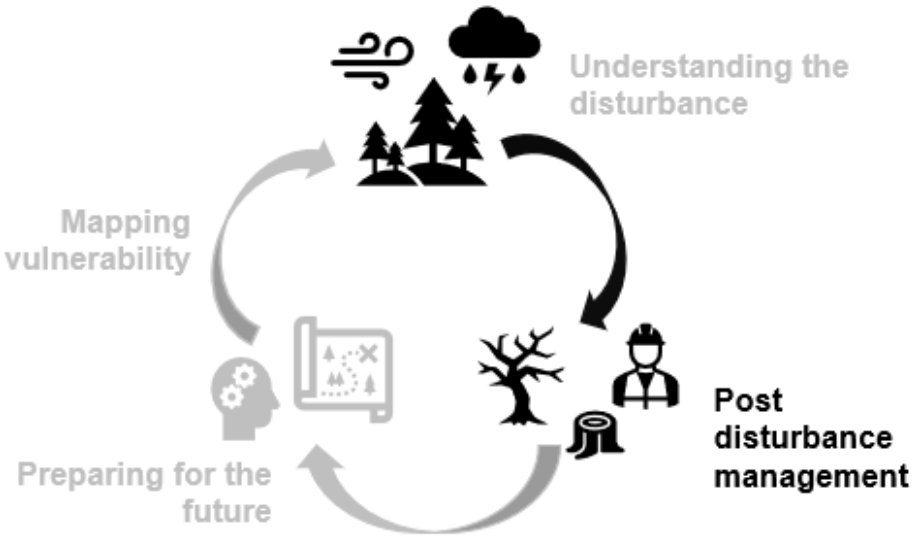

Windstorms represent one of the main large-scale disturbances that shape the European landscape and influence its forest structure, so post-event restoration activities start to gain a major role in mountain forests management. After a disturbance event, biological legacies may enhance or maintain multiple ecosystem services of mountain forests such as protection against natural hazards, biodiversity conservation or erosion mitigation. However, the conservation of all these ecosystem services after stand-replacing events could go against traditional management practices, such as salvage logging. Thus far, the impact of salvage logging and removal of biological legacies on the protective function of mountain stands has been poorly studied. Structural biological legacies may provide protection for natural regeneration and may also increase the terrain roughness providing a shielding effect against gravitational hazards like rockfall. The aim of this chapter is to understand the dynamics of post-windthrow recovery processes, to investigate how biological legacies affect the multifunctionality of mountain forests, in particular the protective function. To observe the role of biological legacies we performed 3000 simulations of rockfall activity on windthrown areas. Results show the active role of biological legacies in preventing gravitational hazards, providing a barrier effect and an energy reduction effect on rockfall activity. To conclude, we underline how forest management should take into consideration the protective function of structural legacies. A suggestion is to avoid salvage logging in order to maintain the multifunctionality of damaged stands during the recovery process

3.1. Introduction

Mountain forests provide multiple services, from timber production to the protection of infrastructures against natural hazards like rockfall, landslides or avalanches (Motta and Haudemand, 2000). Considering the protective function, forests should always fulfil their role minimizing the risk exposure of local populations, therefore the interaction among natural hazards and mountain forests, as well as their management, has been widely studied (Berger et al., 2002; Brang, 2001; Briones-Bitar et al., 2020; Moos et al., 2017b; Motta and Haudemand, 2000). Recently rockfall research has been heading toward the study of simulation models (Dorren, 2003; Moos et al., 2019, 2017b), quantification of the protective effect of forests (Dupire et al., 2016a; Moos et al., 2017b) and the influence of rockfall on the forest structure (Moos et al., 2021). Natural disturbances (e.g., wildfires, windstorms, or insect outbreaks) may greatly affect the provision of ecosystem services by Alpine stands. Disturbances may undermine the mitigation effect that forests play as was observed after the windstorm Vivian in central Europe in the 1990s (Frey and Thee, 2002; Schönenberger, 2002; Wohlgemuth et al., 2017). Moreover, natural disturbances are expected to increase in frequency and intensity in the coming years, especially in coniferous forests, mainly due to climate change (Seidl et al., 2017). A correct forest management should consider natural disturbances in order to plan a rapid and efficient post-event restoration of a damaged area, in order to minimize the risk exposure and shortening of the protection gap (Beghin et al., 2010; Wohlgemuth et al., 2017). It is thus fundamental to recognize the role of biological legacies left by disturbances (Franklin et al., 2000), since they can strongly influence both the post-disturbance recovery pattern (Johnstone et al., 2016; Lindenmayer et al., 2019) and the residual provision of ecosystem services through their type, number and spatial arrangement. Considering windstorm, the main disturbance affecting European forests (Bebi et al., 2017; Forzieri et al., 2021; Gardiner et al., 2013; Seidl et al., 2017), the main structural legacies that are present on a windthrown site are lying logs, stumps and snags or snapped trees. After the Vivian storm in Switzerland it was observed that the presence of deadwood could have a positive effect in scattering the energy of falling blocks, due to an increase of terrain roughness (Schönenberger et al., 2005). However, a quantification of this effect is still lacking, and it is not clear how long this effect may last. Although wood decaying processes may decrease the protection provided by these material legacies over time (Frey and Thee, 2002), some studies suggest that lying logs may provide a barrier effect against snow and rocks even up to 30 years after the disturbance event (Rammig et al., 2006). In this paper we present a case study of a protective forest located on the eastern Italian Alps. The target stand provided protection against rockfall until the 30th October 2018 when a massive windstorm, named Vaia, hit northern Italy, causing a loss of more than 10 million cubic meters of timber (Cadei et al., 2020; Chirici et al., 2019; Pellegrini et al., 2021) and severely damaging the study

site. This event modified the dynamics of interaction between the forested slope and rockfall events, hence the aim of this paper is to quantify the role played by biological legacies in providing a protective function in damaged protective forests. Results will allow to evaluate the effects of different post-disturbance management options, the first of which is salvage logging.

3.2 Materials and method

Study area

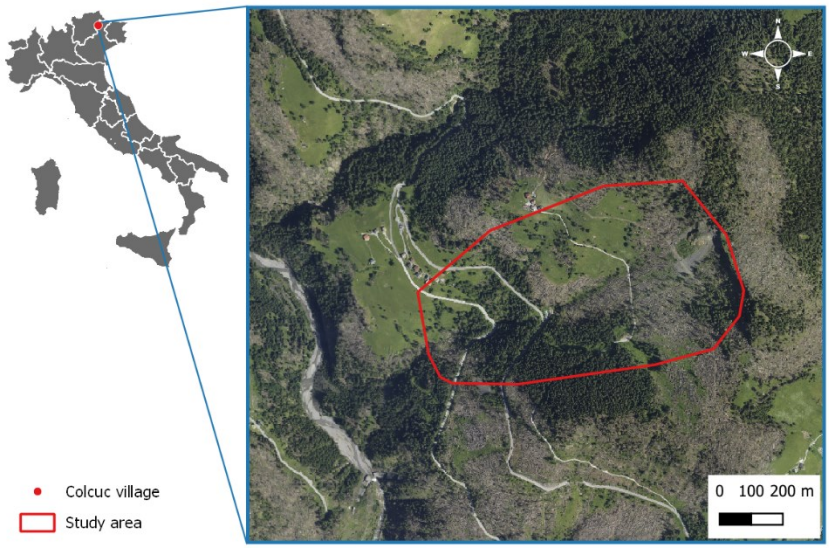

Figure 11. Location of the Colcuc study site

The study site is located in the Dolomites, specifically on Monte Pore, close to Colcuc village (46° 27' 21"N, 11° 59' 45"E), municipality of Colle Santa Lucia, in Belluno province, NE Italy (Figure 12). The site is on a south-western slope and has an elevation ranging from 1360 to 1710 m a.s.l. The main forest species is Norway spruce (*Picea abies*(L.)Karst.), with the sporadic presence of European larch (*Larix decidua* Mill.) at higher elevations. On the 2nd of April 2004 the site was affected by a massive landslide (around 4000 m^3 of material) that defined the site as "active" for rockfall concern. The study site is crossed at different altitudes by a hiking/biking trail, a local and a regional road. After the event, some concrete infrastructures and rockfall nets were built to minimize the risk for stakeholders (users of the trail and the local population). Some studies were started in the autumn of 2018 in order to evaluate and quantify the protective function of the forest stands of the area. However, on the 30th October 2018 the storm "Vaia" blew down most of the selected stands.

Field data

Rockfall activity

To simulate rockfall events and study their interaction with the protective forest we used the probabilistic process-based model Rockyfor3D (Dorren, 2016). A field survey was conducted in summer 2018 in order to characterize the rockfall activity within the protective forest and to collect data required for the calibration of the rockfall model. Two transects were identified in the transit zone, one following the line of slope (vertical transect) and the other perpendicular to it (horizontal transect). The transects were 10 m wide and long enough to cover the entire length and width of the protective forest, equal to 440 m and 175 m respectively. Stakes were installed along the transects (one stake every 20-30 m) to aid relocation over time. The positions of the stakes were determined through RTK-DGPS measurements (TopConHiPerV DGPS system). All the rockfall deposits within each transect and with one dimension (x, y or z) larger than 50 cm were measured. For each deposit we collected the three dimensions of the block, using a measuring tape ($\pm$ 1cm), and its relative position with respect to a fixed georeferenced stake (horizontal distance and azimuth) using Trupulse 360°B Laser Technology. For each deposit we classified the rock's shape, using categories based on Dorren (Dorren, 2016) and the stopping cause. The stopping cause must identify why an individual rock stopped at a certain location. The main causes may be classified using the object where the rock stopped, e.g., another rock, a tree, a lying log, a flat area etc., it may also be classified as undefined when the stop is due to the total loss of kinetic energy. If the falling block was stopped by a tree, we also measured the tree DBH. In addition, for all the impacted trees within the transects, data on DBH, tree position, and characteristics (height and dimension) of the scars were recorded.

Slope surface parameters

To define ground and forest stand parameters required as input in the software package Rockyfor3D, field investigations were conducted during summer 2018 setting up 16 circular plots with a radius of 12 m (Figure 13). In each plot, we collected the position of the centre (using a TopCon DGPS system). Within each plot, we recorded species, DBH and relative position to the centre for each tree with a DBH larger than 7.5 cm. We also collected the heights of the five trees closest to the centre, in order to create a local tree height-diameter curve. For each plot we evaluated the surface roughness (hereafter *RG*), expressed as the size of the material covering the slope's surface and assessing the three size probability classes named *rg70*, *rg20* and *rg10*; these parameters are an expression of the different MOHs (Mean Object Heights, (Dorren et al., 2006)). We recorded the main soil type for each plot following the classification provided in the Rockyfor3D Manual (Dorren, 2016).

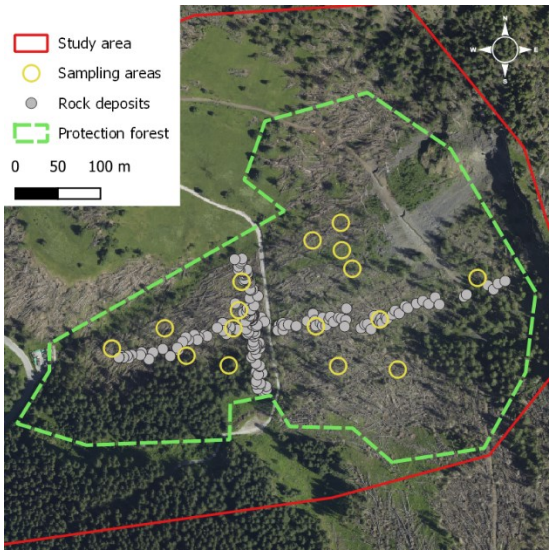

Figure 12. Localization of transects, surveyed rockfall deposits, and circular plots surveyed within the considered protective forest.

Remote sensing data

The area has been flown over with different sensors both in pre-event and post-event conditions. A first campaign was performed by means of a high-density LiDAR scan in 2015 (appr. 12 pts/m^2) and a UAV flight that provided high resolution imagery and a Structure-from-Motion (SfM) point cloud. Because of the storm event, during 2019 the area was re-scanned with LiDAR sensor, adding a new very high detailed data source (appr. 25 pts/m^2 for the study site).

Data pre-processing

Rockyfor3D simulations require a stack of raster layers with the same resolution and extent. For this specific purpose, the resolution has been set to a pixel size of 2 metres. The DTM (*dem.asc*) derived from the ground-classified point cloud collected during 2015 has been used as a base layer. We selected the four roads crossing the study area as local checkpoints (calculation screens) to evaluate the number of passages and rock energy, while the conifer percentage (*conif_percent.asc*) and soil type (*soiltype.asc*) parameters were derived from field measurements and photo interpretation. Differently from the usual subdivision of the study area into subzones with homogeneous values, the *RG* files (*rg10.asc*, *rg20.asc*, and *rg70.asc*) have been produced hypothesizing a linear relation between slope and *RG* values measured in the field, offering a more realistic distribution across the site. We observed higher values of *RG* associated to lower values of slope, where we found a high presence of rock deposits. Finally, the file related to the position of trees (*treefile.txt*) has been created extracting the single tree locations using the software FINT (ecorisq.org) from the CHM derived from the SfM point cloud.

Post-event layers

All the input layers had to be updated to match the post-event configuration of the site. This required the delineation of the damaged area, in order to mask the windthrown areas and add the newly calculated input values. The damaged area has been defined by the difference between CHMs, where all the areas with a decrease in height greater than 5 metres have been considered as "damaged", in order to avoid fine local bias from misaligned scans/pixels. If for the tree positions the update meant a simple difference, the *RG* layers had to be elaborated from scratch. The point cloud has been filtered for first returns, height normalised on the DTM and then all the points above 2.5 metres have been removed. This height threshold has been set according to the estimated most frequent maximum height of the downed material; the threshold value was verified on the field. Hence, in order to be consistent with the Rockyfor3D parameter, the RG values have been calculated as the 10th, 20th and 70th percentile of the points' distribution starting from the maximum value (i.e. 2.5 m) to the lowest and then regularised according to the standard thresholds (*see* Manual's Annex I [26]). Finally, to validate the new *RG* rasters, we collected in the field the values of *rg10*, *rg20* and *rg70* at 103 different locations in the study area. Field sampled data and LiDAR data were compared in order to understand the pros and cons of both methodologies. For the statistical analysis we used the free software PAST (Hammer et al., 2009). The rasters obtained through this methodology provides values of *RG* with a resolution of 2m, allowing the interaction between falling blocks and deadwood to be investigated.

Simulations

The rockfall analysis has been performed using Rockyfor3D (Dorren, 2016), running 1000 simulations for each of the following scenarios:

- no forest (NFOR; reference): free-falling rocks; it is used to determine the potential energy, distance and trajectory of rocks,
- with forest (FPRE; pre-event): rock falling under pre-event conditions, simulating the presence of the protective forest,
- with forest (FPOS; post-event): rock falling under post-event conditions, simulating the presence of biological legacies in the windthrown stand.

As concerns the other parameters that are necessary to the model, i.e. the shape of the test rock and its dimensions, these were based on the average size of rocks measured in the field. Rock density was set to 2700 kg/m^3 (calcareous rock).

Ultimately, we set some checkpoints in order to collect data of passing rocks at different slope length from the hazard source. Each checkpoint collects mainly the number of rockfall passages, the kinetic

energy of falling blocks, their velocity, and their passing heights. The position of checkpoints is shown in Figure 14.

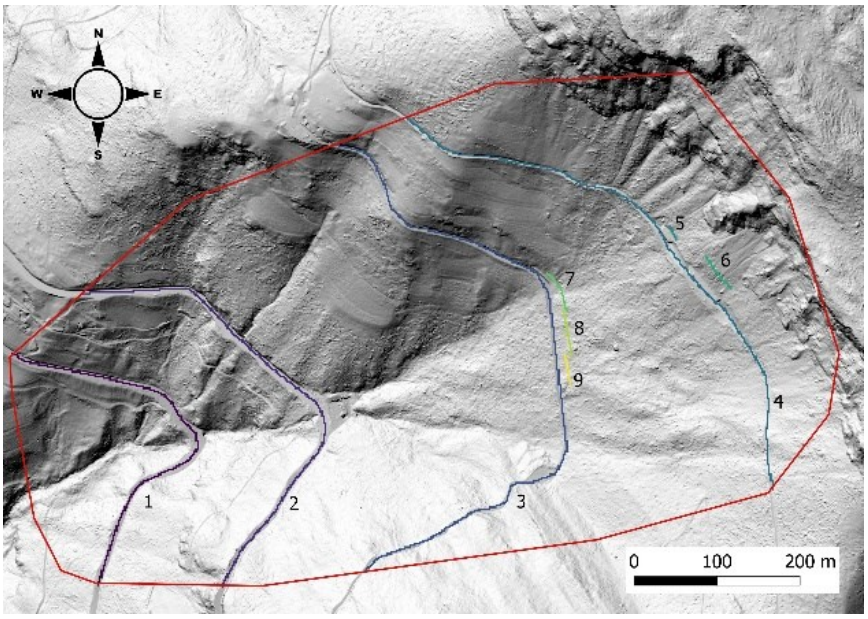

Figure 13. Position of the checkpoints used for computation of the indices. We identified the main roads and the real nets present in the study area as checkpoints. The red line contours the study site while the numbers indicate the ID of each checkpoint.

Protective effect

For the assessment of the protective effect of the stand (both standing and windthrown) we used the indices introduced by Dupire et al. (Dupire et al., 2016b). The first index is the BARI (BARrier effect Index), it is computed using formula (1) and is aimed at an assessment of the barrier effect of trees or lying logs (i.e. the capacity of stopping rocks in the transit zone). The second index is the MIRI (Maximum Intensity Reduction Index), it is computed using formula (2) and assesses the reduction of kinetic energy due to the presence of trees or logs in the transit area (i.e. the loss of kinetic energy after impact with obstacles). The last one is the ORPI (Overall Rockfall Protection Index), it is computed using formula (3) and quantifies the overall protection of the upslope stand.

$$BARI(x) = 100 \times \left(1 - \frac{N_{rock_{forest}}(x)}{N_{rock_{no-forest}}(x)}\right) \quad (1)$$

$$MIRI(x) = 100 \times \left(1 - \frac{E95_{forest}(x)}{E95_{no-forest}(x)}\right) \quad (2)$$

$$ORPI(x) = 100 \times \left(1 - \frac{\sum_{i=1}^{n\ forest} E(x)}{\sum_{k=1}^{n\ no-forest} E(x)}\right) \quad (3)$$

Where, in formula (1)$N_{rock_{forest}}(x)$ indicates the number of rocks that passed through a checkpoint in the FPRE, or FPOS, simulations, $N_{rock_{no-forest}}(x)$ indicates the number of rocks that passed through a checkpoint in the NFOR simulations. In formula (2)$E95_{forest}(x)$ and $E95_{no-forest}(x)$ respectively indicate the 95th percentile of kinetic energy of the rocks that passed through a checkpoint in the FPRE,

or FPOS scenario and in the NFOR scenario. In formula (3) $\sum_{i=1}^{n\ forest} E(x)$ indicates the total sum of the kinetic energy of each block that passed through a checkpoint in the FPRE, or FPOS, scenario, $\sum_{k=1}^{n\ no-forest} E(x)$ refers to the NFOR scenario.

We computed the three indices for each checkpoint, for the FPRE and FPOS scenarios, using the NFOR scenario as the reference scenario. Considering the small sample size we applied the non-parametric Kolmogorov-Smirnov test to observe any difference among the three scenarios. For the statistical analysis we used the software PAST (Hammer et al., 2009).

3.3 Results

Field results

In the pre-Vaia forest stands, tree mean DBH was 30.5 cm with a standard deviation of 12.9 cm, and the mean tree density was 720 trees/ha. 100% were conifers. Inside the transects, we recorded 242 rocks with an average size of 1.5 m x 1.0 m x 0.8 m. The main stop cause (51% of cases) was classified as undefined, i.e. most of the rocks simply stopped due to the loss of their kinetic energy, 18% of rocks stopped on other rock deposits, 12% stopped on stumps, 10% stopped on a tree and 9% stopped in a flat area. The shape of falling blocks was undefined (not relatable to any known geometric form) in the majority of the cases (48%), 26% were rectangular, 14% spheric and 12% discoid.

Validation of LiDAR derived roughness values

The *RG* values collected in the field have been compared to the ones derived from the LiDAR point cloud. The field estimations have been associated to the mean value of the LiDAR-derived raster cells that were within a circular area of 2 m radius.

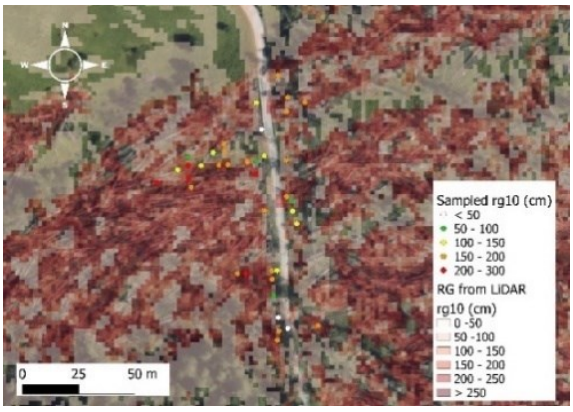

Figure 14. Comparison among roughness (rg10) data extracted by LiDAR and sampled in the field. The map shows the spatialization of RG data obtained through a LiDAR source and of RG data sampled in the field.

After the removal of outliers, we compared rg10 values, we observed a mean value of 1.69 m for the sampled data and a mean value of 1.44m for the LiDAR derived data. The average difference between

the two sets of data (sampled data – LiDAR data) was 0.25 m, that is circa 30% of the smallest dimension of the average falling rock. We did the same comparison for the rg20: the mean value of sampled data is 1.06 m, and the mean value of LiDAR derived data is 1.25 m, in this case the average difference between data was -0.18 m, 22.5% of the smallest dimension of the average falling rock. Lastly, for rg 70 we observed a mean value of sampled data of 0.70 m and a mean value of LiDAR derived data of 0.64 m. The average difference resulted to be 0.06 m, in this case 7.5% of the smallest dimension of falling rocks.

Considering the acceptable difference among field collected data and LiDAR derived raster and since it was a general underestimation leading to more conservative simulations (i.e., lower rg values) we adopted the LiDAR derived *rg* values for running the simulations in order to detect and take into account the spatial variability of windthrown material (Figure 15).

Simulations results

The results of the 'no forest scenario' show a potential severe rockfall activity in the study area, where falling rocks converge into a main gully, located in the centre of the area.

Table 1. Summary of Rockyfor3D simulations outputs for the NFOR scenario. For each checkpoint the table reports: n, the total number of registered passages of falling rocks; E_95, the 95th percentile of the energy of registered falling rocks; Ph_95, the 95th percentile of passing height values recorded at the checkpoint; V_95, the 95th percentile of the speed of recorded falling rocks.

Checkpoint	n (-)	E_95 (kJ)	Ph_95 (m)	V_95 (m/s)
1	776'172	1080	1.3	20.3
2	586'053	953	2.6	20.0
3	2'796'600	1971	2.7	25.8
4	3'180'107	1843	4.0	26.1
5	192'933	1807	1.8	25.6
6	530'231	1984	1.9	26.3
7	1'216'722	2126	3.1	26.7
8	390'563	1969	2.8	25.3
9	606'256	1722	2.2	24.0

The main source of activity is recognizable in the north-eastern part of the study area above the main trail and the roads where a rock cliff is located.

The first set of simulations, the NFOR scenario, show rockfall dynamics considering only the morphology of the study area, without taking into account the presence of trees or biological legacies. Simulation results are reported in Table 1.

The highest rockfall activity was registered at checkpoint 4, the one closest to the source area. The registered number of passages was 3'180'107 with a 95th percentile of kinetic energy of 1'843 kJ, a 95th percentile height of passage of 4.0 m and a 95th percentile of velocity of 26.1 m/s. It may be observed that increasing the distance from the source, so increasing the slope length, the number of rockfall passages decreases. On the other hand, the values of energy, passing height and velocity show less variability, mainly because we are reporting the 95th percentile.

The outputs of the simulation with forest data, FPRE scenario, show how rockfall activity interacted with the forest stand. Results show a reduction in the number of passages and a decrease in the mean kinetic energy of the falling block in the lower part of the main catchment, where the forest is present. The energy and speed of falling blocks also show lower values if compared to the upper part, where tree density is lower (Table 2).

Regarding passing heights and velocity values we can observe a reduction in most of the cases. Where the forest stand has a lower tree density, or where the forest is not present, Ph_95 and V_95 values remain constant. Checkpoint 4 registered 2'671'715 passages with a 95th percentile of kinetic energy of 1'733 kJ, a 95th percentile of passing heights of 4.1 m and a 95th percentile of velocity of 25.3 m/s. While a reduction in the number of passages, kinetic energy and velocity may be observed, if compared to the NFOR scenario, Ph_95 doesn't show an appreciable change.

Table 2. Summary of Rockyfor3D simulations outputs in the FPRE scenario. For each checkpoint the table reports: n, the total number of registered passages of falling rocks; E_95, the 95th percentile of the energy of registered falling rocks; Ph_95, the 95th percentile of passing height values recorded at the checkpoint; V_95, the 95th percentile of the speed of registered falling rocks.

Checkpoint	n (-)	E_95 (kJ)	Ph_95 (m)	V_95 (m/s)
1	478'121	816	0.9	17.1
2	490'779	578	1.3	15.7
3	1'523'292	1'773	2.4	24.1
4	2'671'715	1'733	4.1	25.3
5	191'329	1'782	1.8	25.4
6	519'953	1'965	1.9	26.2
7	792'383	1'927	2.8	25.3
8	228'081	1'787	2.5	23.9
9	141'892	1'600	2.0	22.8

The outputs of the FPOS scenario shows the interaction of rockfall activity with the biological legacies of the damaged forest. In the upper part, where the forest had a lower density of trees the number of passages and the energy of falling blocks are higher than in the lower part, where the forest stand had a higher density (Table 3).

Table 3. Summary of Rockyfor3D simulations outputs in the FPOS scenario. For each checkpoint the table reports: n, the total number of registered passages of falling rocks; E_95, the 95th percentile of the energy of registered falling rocks; Ph_95, the 95th percentile of passing height values recorded at the checkpoint; V_95, the 95th percentile of the speed of registered falling rocks.

Checkpoint	n (-)	E_95 (kJ)	Ph_95 (m)	V_95 (m/s)
1	291’697	658	0.8	14.7
2	430’738	401	1.1	13.1
3	228’487	1’140	1.5	20.0
4	901’333	1’626	4.5	24.2
5	116’717	1’537	1.5	23.9
6	464’749	1’951	1.8	26.0
7	6’492	2’098	2.6	26.2
8	22’996	1’839	2.4	24.1
9	1’042	1’819	1.9	24.1

The highest number of passages was always registered at checkpoint 4, where it was 901’333. In the same checkpoint the registerd E_95 and V_95 were 1'626 kJ and 24.2 m/s, in both cases the values decreased if compared with the previous scenarios (NFOR and FPRE); the registered value of Ph_95 was slightly higher and was equal to 4.5 m.

The outputs of all the simulations are reported in Figure 16: it is possible to observe that the presence of deadwood influences the rockfall trajectories and the kinetic energy of falling blocks.

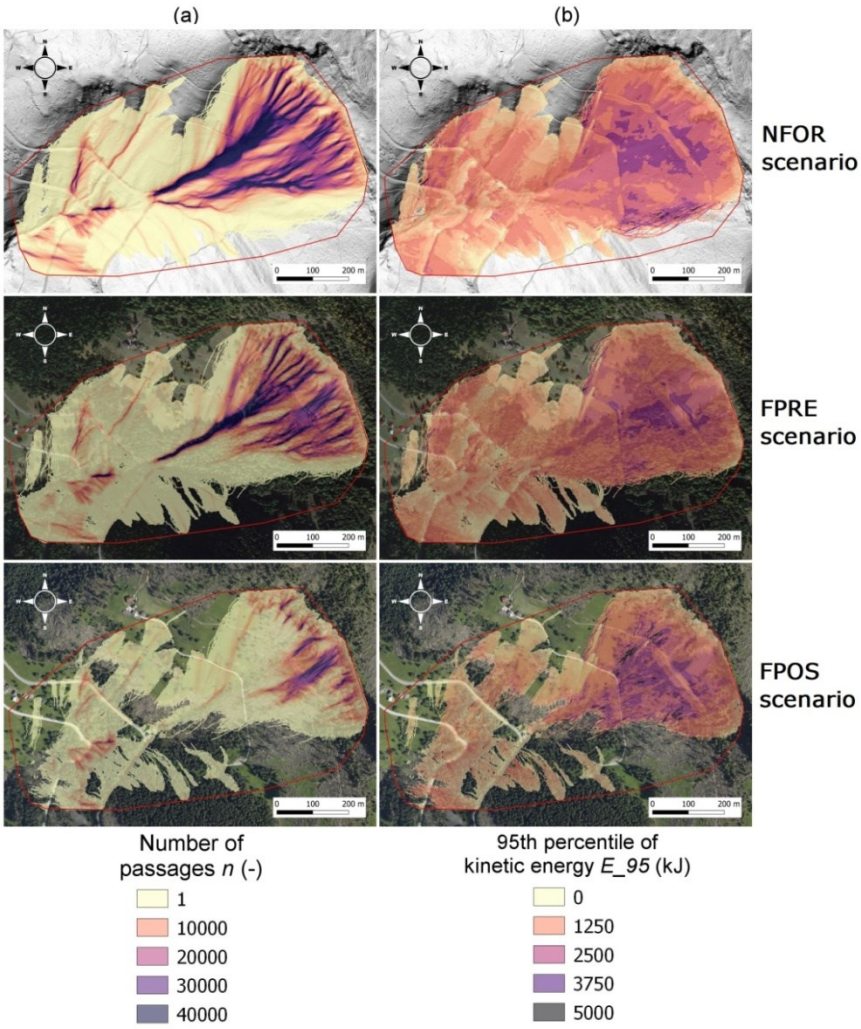

Figure 15. Output of Rockyfor3D simulations. In the first row the simulation in a 'no forest' scenario, in the second row the simulation in a 'with forest' scenario, in the third row the simulation in a 'post windstorm' scenario. Column (a) represents the number of passages of rockfall activity while column (b) represents the 95th percentile of the kinetic energy of falling blocks. The red line delimits the computational domain boundary of the numerical simulations.

Indices computation

To evaluate and quantify the protective efficiency of the forest and the biological legacies against rockfall, we computed the Dupire's indices [29] for the FPRE and FPOS scenarios, using NFOR scenario as a reference. The values of the indices are reported in Table 4, as well as the classification of the protective effect provided by the forested slope, both before and after the storm. These categories vary from Low Protective Effect to High Protective Effect (Dupire et al., 2016a) (as reported also in Figure 6). After the storm, there has been a clear increment in BARI, MIRI, and ORPI values. Considering the ORPI index and the protective efficiency (PE), in seven cases out of nine we have an improvement from a lower protection class to a higher one (from low to medium and from medium to high).

Table 4. Summary of Dupire's indices. For each checkpoint the table shows the results of the three indices computation, BARI, MIRI, ORPI for both the FPRE scenario and the FPOS scenario. The last column reports the classification of the protective efficiency (PE) of the forest stand according to the scenario (the categories are based on (Dupire et al., 2016a)).

Checkpoint	Scenario	BARI (-)	MIRI (-)	ORPI (-)	Classification
1	FPRE	38.4	24.4	52.6	Medium PE
	FPOS	62.4	39.1	76.0	Medium PE
2	FPRE	16.3	39.3	41.1	Low PE
	FPOS	26.5	57.9	59.8	Medium PE
3	FPRE	45.5	10.0	54.4	Medium PE
	FPOS	91.8	42.2	97.4	High PE
4	FPRE	16	6.0	26.4	Low PE
	FPOS	71.7	11.8	77.2	Medium PE
5	FPRE	0.8	1.4	2.4	Low PE
	FPOS	39.5	14.9	58.4	Medium PE
6	FPRE	1.9	1.0	3.1	Low PE
	FPOS	12.3	1.7	14.5	Low PE
7	FPRE	34.9	9.4	45.3	Low PE
	FPOS	99.5	1.3	99.6	High PE
8	FPRE	41.6	9.2	51.1	Medium PE
	FPOS	94.1	6.6	94.9	High PE
9	FPRE	76.6	7.1	78.9	Medium PE
	FPOS	99.8	-5.6	99.8	High PE

Moreover, results show that lying logs mainly provide a barrier effect rather than an energy reduction of falling blocks. As can be observed in Figure 17, the variation among BARI indices is higher than the variation of MIRI indices. Kolmogorov-Smirnov test was used to compare the two scenarios (p-value ≤ 0.1): the difference between FPRE and FPOS is significant in the cases of BARI and ORPI indices. Instead, the MIRI indices do not present significant differences between the two scenarios.

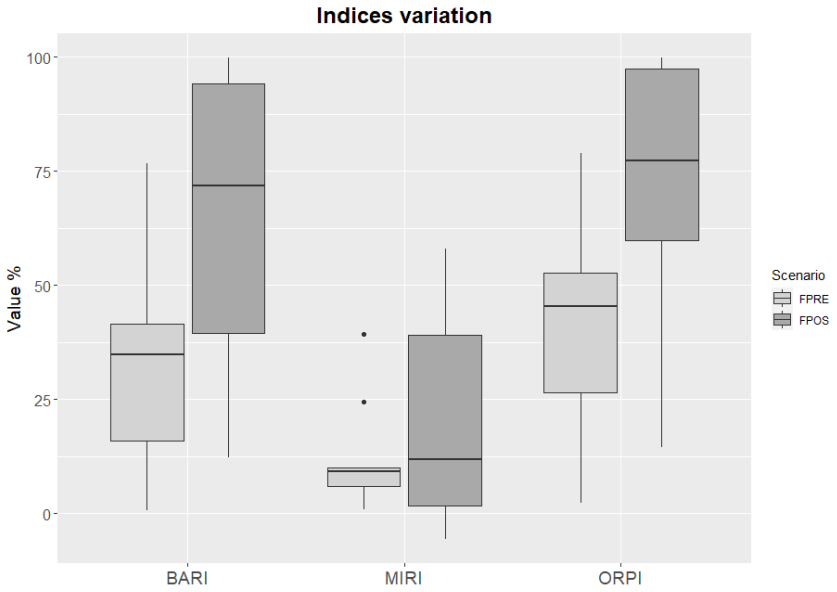

Figure 16. Boxplot of the values for the three indices BARI, MIRI, and ORPI in the scenarios FPRE, in light grey, and FPOS, in dark grey. The first index quantifies the barrier effect played by the protective forest, the second index is related to the maximum intensity reduction and the last one is related to the overall protective effect.

3.4 Discussion

The role of a forested slope in the mitigation of rockfall hazard highlighted by the results of this study is aligned with the current literature (Bianchi et al., 2018; Briones-Bitar et al., 2020; Moos et al., 2017a; Scheidl et al., 2020). We could observe and quantify the reduction of rockfall passages and their energy due to the presence of a protective forest, underlining the importance of these stands for risk assessment (Moos et al., 2017b). Moreover, our results provide an innovative detailed analysis of the impact of a windstorm on the protective efficiency of an alpine stand. Thanks to the use of indicators of protective efficiency (Dupire et al., 2016b) we have been able to compare how the interaction between a forested slope and rockfall hazard changed after a windthrow. Our results may help the understanding of the interaction of natural disturbances with the multifunctionality of mountain forests, a topic that is currently investigated in the literature, especially as concerns evaluation of the development of the provision of ecosystem services in a changing climate (Irauschek et al., 2017).

The results of the FPRE scenario show clearly that there is an effect of the forest in the reduction of the magnitude of rockfall activity. Figure 5 illustrates the barrier effect played by trees, as shown by the values of BARI and ORPI indices (Table 4). Moreover, concerning the kinetic energy of the falling blocks, the presence of the forest could lead to an energy reduction. Thanks to different positioning of the checkpoints, it was possible to evaluate the influence of the slope length on the magnitude of rockfall activity. According to the ORPI index the forest stand varies from a low to a medium protective effect where the forested slope is longer. Our results also show that where the slope length is short the protective forest didn't affect the passing heights of rocks.

Considering the FPOS scenario, the use of LiDAR-derived data represented an innovative way to study rockfall hazard. The methodology that we used for the creation of the *RG* rasters appeared to be efficient for a precise localization of biological legacies after the windstorm Vaia. Currently, remote sensing applications are starting to become more commonly used in forestry (Marchi et al., 2018) and they may provide a high precision detection of biological legacies positions after a storm. The obtained *RG* rasters resulted as more accurate than data provided by field surveys: they present a better spatialization that leads to a good localization of lying logs. Moreover, during the surveys we understood the difficulty of the estimation of *RG* values in the field. As a consequence, we think that the definition of a stricter procedure may avoid mistakes during the operations of data collection in the field.

The mean values of *RG* sampled in the field were slightly higher than LiDAR derived data. Consequently, the adoption of LiDAR derived *RG* as input for the numerical modelling provides a more conservative scenario. Using the raster produced with the LiDAR data we have been able to simulate the post windstorm scenario with high accuracy, considering the presence of biological legacies such as lying logs and stumps.

Moreover, the results of FPOS scenario show that the windthrown stand still provides an important protective function against rockfall. We expected this result considering previous studies that were carried out after other storms in the alpine area, e.g. Vivian or Lothar (Schönenberger et al., 2005; Wohlgemuth et al., 2017). In addition, we observed that immediately after a windthrown event the protective efficiency of the damaged stand is even higher than the previous forest, although the current literature affirms that the protective efficiency of a forested slope should start to decrease after a disturbance (Wohlgemuth et al., 2017).

Our observations suggest that biological legacies, like lying logs, provide mainly a barrier effect rather than an energy reduction of falling blocks, as can be observed in Figure 6. The barrier effect played by deadwood has already been observed and analysed by Fuhr et al. (Fuhr et al., 2015) and by Olmedo et al. (Olmedo et al., 2016): the presence of lying logs significantly improves the surface roughness of a forested slope, in particular in a windthrown stand where all trees act like natural barriers on the ground.

Furthermore, biological legacies may provide a protective function against other gravitational hazards, for instance avalanches. It was observed that, in Switzerland, after the storm Vivian, uncleared areas prevented avalanches release (Frey and Thee, 2002; Wohlgemuth et al., 2017). As concerns shallow landslides, it was observed that structural legacies cannot provide any protective effect, mainly because the removal of the roots contribution to soil stability in windthrown areas may enhance the potential risk (Bebi et al., 2019; Wohlgemuth et al., 2017).

Knowing the spatial arrangements and conditions of deadwood we could define the PE of the windthrown stand at different slope length level with a good accuracy. We observed an improvement of the PE for the majority of the checkpoints. This improvement of the protective role could last for a few years, before lying logs start to rot and the height of the logs from the ground starts to decrease, as observed in Wohlgemuth (Wohlgemuth et al., 2017). Moreover, with a reduction of deadwood height above the ground and with a higher portion of logs in direct contact with the soil the wood decaying processes may accelerate (Petrillo et al., 2016), leading to lower protective efficiency of biological legacies.

Some empirical studies show that, after some branches breakage in the first years, the downslope movement of lying logs may be relatively small (Frey and Thee, 2002). However, some tensile tests showed a reduction of the breaking point of logs, mainly due to the decay of wood. It was also observed that the level of decay was related to the microsite, mainly the height above ground of logs and their vegetation cover (Bebi et al., 2015); the presence of bark on logs may also influence the speed of decaying processes (Hagge et al., 2019). Although we were able to observe and quantify the protective role played by structural legacies, it is important to underline that this role is strictly connected with the type of disturbance that hit the protective forest. Other kinds of natural disturbances may create different biological legacies, with a different spatial arrangement, which may not provide the same barrier effect. For instance it was observed that after a wildfire burnt logs and snags may behave in a different manner (Maringer et al., 2016).

Furthermore the presence of biological legacies in a post-disturbance scenario, like a windthrown stand, may provide other important functions, from the protection of new seedlings (Marzano et al., 2013; Wohlgemuth et al., 2002), to the conservation of biodiversity and structural complexity of the forest [17,33,34]. The facilitation effect provided by deadwood can be fundamental for speeding up natural regeneration processes. The presence of biological legacies, indeed, may not only provide protection but also create the condition for shortening the protection gap, which should be the main target of management strategies for a damaged protective forest (Bebi et al., 2015; Motta and Haudemand, 2000; Wohlgemuth et al., 2017).

The current literature investigates the impacts of traditional salvage logging practice, considering this management strategy as a second disturbance event (Leverkus et al., 2021; Taeroe et al., 2019) that can modify the provision of some ecosystem services. Our results may introduce a new element in the evaluation of the outcomes of this practice, suggesting that the removal of lying logs may eliminate the protective effect of the forested slope exposing infrastructures to rockfall hazard. Moreover, we would suggest adopting management strategies that aim to reach a resistant and resilient forest structure, considering i) local environmental conditions, ii) the multifunctionality of

alpine forests, iii) the interaction and the possible future interactions of these stands with natural disturbances and climate change.

3.5 Conclusions

With this study, we evaluated the influence of structural biological legacies on rockfall activity after a windstorm in an alpine stand. After a natural disturbance, the protective function efficiency of a mountain forest may change drastically, and according to the severity of the event it may lead to a protection gap. However, we observed that in a short period of time after the event, the protective efficiency of the disturbed slope can be higher than before the event. This is because of lying logs and stumps, i.e. the structural biological legacies, which play an important role in providing a barrier effect against rockfall. Legacies characteristics, and consequently the barrier effect, depend on the type of disturbance (e.g. wind). In addition, the time, or rather wood decay, is the other variable mainly affecting the protective function after a disturbance event, as observed in other studies (Frey and Thee, 2002; Rammig et al., 2006; Schönenberger et al., 2005; Wohlgemuth et al., 2017). We recommend that future research should focus on the protective role of structural biological legacies, considering other gravitational hazards, like shallow landslides and avalanches. Moreover, future studies should take into account the time span of the protection gap, in order to understand when wood decaying processes will undermine the protection provided by deadwood on damaged slopes.

Finally, from an operative point of view, we would suggest avoiding traditional practices like salvage logging. Where a gravitational hazard is present forest managers should consider other options with the target of enhancing the natural restoration of protective forests, in order to shorten the protection gap.

3.6 References

Bebi, P., Bast, A., Ginzler, C., Rickli, C., Schöngrundner, K., Graf, F., 2019. Forest dynamics and shallow landslides: A large-scale gis-analysis. Schweizerische Zeitschrift fur Forstwes. 170, 318–325. https://doi.org/10.3188/szf.2019.0318

Bebi, P., Putallaz, J.M., Fankhauser, M., Schmid, U., Schwitter, R., Gerber, W., 2015. Die Schutzfunktion in Windwurfflächen. Schweizerische Zeitschrift fur Forstwes. 166, 168–176. https://doi.org/10.3188/szf.2015.0168

Bebi, P., Seidl, R., Motta, R., Fuhr, M., Firm, D., Krumm, F., Conedera, M., Ginzler, C., Wohlgemuth, T., Kulakowski, D., 2017. Changes of forest cover and disturbance regimes in the mountain forests of the Alps. For. Ecol. Manage. 388, 43–56. https://doi.org/10.1016/j.foreco.2016.10.028

Beghin, R., Lingua, E., Garbarino, M., Lonati, M., Bovio, G., Motta, R., Marzano, R., 2010. Pinus sylvestris forest regeneration under different post-fire restoration practices in the northwestern Italian Alps. Ecol. Eng. 36, 1365–1372. https://doi.org/10.1016/j.ecoleng.2010.06.014

Berger, F., Quetel, C., Dorren, L.K.A., 2002. Forest : a natural protection mean against rockfalls , but with which efficiency? Interpraevent 2002 Pacific Rim Matsumoto/Japan 2, 815–826.

Bianchi, E., Accastello, C., Trappmann, D., Blanc, S., Brun, F., 2018. The Economic Evaluation of Forest Protection Service Against Rockfall: A Review of Experiences and Approaches. Ecol. Econ. 154, 409–418. https://doi.org/10.1016/j.ecolecon.2018.08.021

Brang, P., 2001. Resistance and elasticity: Promising concepts for the management of protection forests in the European Alps. For. Ecol. Manage. 145, 107–119. https://doi.org/10.1016/S0378-1127(00)00578-8

Briones-Bitar, J., Carrión-Mero, P., Montalván-Burbano, N., Morante-Carballo, F., 2020. Rockfall research: A bibliometric analysis and future trends. Geosci. 10, 1–25. https://doi.org/10.3390/geosciences10100403

Cadei, A., Mologni, O., Röser, D., Cavalli, R., Grigolato, S., 2020. Forwarder productivity in salvage logging operations in difficult terrain. Forests 11, 341. https://doi.org/10.3390/f11030341

Chirici, G., Giannetti, F., Travaglini, D., Nocentini, S., Francini, S., D'Amico, G., Calvo, E., Fasolini, D., Broll, M., Maistrelli, F., Tonner, J., Pietrogiovanna, M., Oberlechner, K., Andriolo, A., Comino, R., Faidiga, A., Pasutto, I., Carraro, G., Zen, S., Contarin, F., Alfonsi, L., Wolynski, A., Zanin, M., Gagliano, C., Tonolli, S., Zoanetti, R., Tonetti, R., Cavalli, R., Lingua, E., Pirotti, F., Grigolato, S., Bellingeri, D., Zini, E., Gianelle, D., Dalponte, M., Pompei, E., Stefani, A., Motta, R., Morresi, D., Garbarino, M., Alberti, G., Valdevit, F., Tomelleri, E., Torresani, M., Tonon, G., Marchi, M., Corona, P., Marchetti, M., 2019. Forest damage inventory after the "Vaia" storm in Italy. For. - Riv. di Selvic. ed Ecol. For. 16, 3–9. https://doi.org/10.3832/efor3070-016

Dorren, L.K. a, 2016. Rockyfor3D (v5.2) revealed – Transparent description of the complete 3D rockfall model. ecorisQ Pap.

Dorren, L.K.A., 2003. A review of rockfall mechanics and modelling approaches. Prog. Phys. Geogr. 27, 69–87. https://doi.org/10.1191/0309133303pp359ra

Dorren, L.K.A., Berger, F., Putters, U.S., 2006. Real-size experiments and 3-D simulation of rockfall on forested and non-forested slopes. Nat. Hazards Earth Syst. Sci. 6, 145–153. https://doi.org/10.5194/nhess-6-145-2006

Dupire, S., Bourrier, F., Monnet, J.M., Bigot, S., Borgniet, L., Berger, F., Curt, T., 2016a. Novel quantitative indicators to characterize the protective effect of mountain forests against rockfall. Ecol. Indic. 67, 98–107. https://doi.org/10.1016/j.ecolind.2016.02.023

Dupire, S., Bourrier, F., Monnet, J.M., Bigot, S., Borgniet, L., Berger, F., Curt, T., 2016b. Novel quantitative indicators to characterize the protective effect of mountain forests against rockfall. Ecol. Indic. 67, 98–107. https://doi.org/10.1016/j.ecolind.2016.02.023

Fischer, A., Fischer, H.S., 2012. Individual-based analysis of tree establishment and forest stand development within 25 years after wind throw. Eur. J. For. Res. 131, 493–501. https://doi.org/10.1007/s10342-011-0524-2

Fischer, A., Lindner, M., Abs, C., Lasch, P., 2002. Vegetation dynamics in Central European forest ecosystems (near-natural as well as managed) after storm events. Folia Geobot. 37, 17–32. https://doi.org/10.1007/BF02803188

Forzieri, G., Girardello, M., Ceccherini, G., Spinoni, J., Feyen, L., Hartmann, H., Beck, P.S.A., Camps-Valls, G., Chirici, G., Mauri, A., Cescatti, A., 2021. Emergent vulnerability to climate-driven disturbances in European forests. Nat. Commun. 12, 1081. https://doi.org/10.1038/s41467-021-21399-7

Franklin, J.F., Lindenmayer, D., Macmahon, J.A., Mckee, A., Perry, D.A., Waide, R., Foster, D., 2000. Threads of Continuity: Ecosystem disturbance, recovery, and the theory of biological legacies. Conserv. Pract. 1, 8–17.

Frey, W., Thee, P., 2002. Avalanche protection of windthrow areas: A ten year comparison of cleared and uncleared starting zones. For. Snow Landsc. Res. 77, 89–107.

Fuhr, M., Bourrier, F., Cordonnier, T., 2015. Protection against rockfall along a maturity gradient in mountain forests. For. Ecol. Manage. 354, 224–231. https://doi.org/10.1016/j.foreco.2015.06.012

Gardiner, B., Schuck, A., Schelhaas, M.-J., Orazio, C., Blennow, K., Nicoll, B., 2013. Living with Storm Damage to Forests. What Science Can Tell Us 3. https://doi.org/10.1007/s10342-006-0111-0

Hagge, J., Bässler, C., Gruppe, A., Hoppe, B., Kellner, H., Krah, F.S., Müller, J., Seibold, S., Stengel, E., Thorn, S., 2019. Bark coverage shifts assembly processes of microbial decomposer communities

in dead wood. Proc. R. Soc. B Biol. Sci. 286. https://doi.org/10.1098/rspb.2019.1744

Hammer, O., Harper, D.A.T., Ryan, P.D., 2009. PAST–Palaeontological statistics, ver. 1.89.

Irauschek, F., Rammer, W., Lexer, M.J., 2017. Evaluating multifunctionality and adaptive capacity of mountain forest management alternatives under climate change in the Eastern Alps. Eur. J. For. Res. 136, 1051–1069. https://doi.org/10.1007/s10342-017-1051-6

Johnstone, J.F., Allen, C.D., Franklin, J.F., Frelich, L.E., Harvey, B.J., Higuera, P.E., Mack, M.C., Meentemeyer, R.K., Metz, M.R., Perry, G.L.W., Schoennagel, T., Turner, M.G., 2016. Changing disturbance regimes, ecological memory, and forest resilience. Front. Ecol. Environ. 14, 369–378. https://doi.org/10.1002/fee.1311

Leverkus, A.B., Buma, B., Wagenbrenner, J., Burton, P.J., Lingua, E., Marzano, R., Thorn, S., 2021. Tamm review: Does salvage logging mitigate subsequent forest disturbances? For. Ecol. Manage. 481, 118721. https://doi.org/10.1016/j.foreco.2020.118721

Lindenmayer, D.B., Westgate, M.J., Scheele, B.C., Foster, C.N., Blair, D.P., 2019. Key perspectives on early successional forests subject to stand-replacing disturbances. For. Ecol. Manage. 454, 117656. https://doi.org/10.1016/j.foreco.2019.117656

Marchi, N., Pirotti, F., Lingua, E., 2018. Airborne and terrestrial laser scanning data for the assessment of standing and lying deadwood: Current situation and new perspectives. Remote Sens. 10, 1356. https://doi.org/10.3390/rs10091356

Maringer, J., Ascoli, D., Dorren, L., Bebi, P., Conedera, M., 2016. Temporal trends in the protective capacity of burnt beech forests (Fagus sylvatica L.) against rockfall. Eur. J. For. Res. 135, 657–673. https://doi.org/10.1007/s10342-016-0962-y

Marzano, R., Garbarino, M., Marcolin, E., Pividori, M., Lingua, E., 2013. Deadwood anisotropic facilitation on seedling establishment after a stand-replacing wildfire in Aosta Valley (NW Italy). Ecol. Eng. 51, 117–122. https://doi.org/10.1016/j.ecoleng.2012.12.030

Moos, C., Dorren, L., Stoffel, M., 2017a. Quantifying the effect of forests on frequency and intensity of rockfalls. Nat. Hazards Earth Syst. Sci. 17, 291–304. https://doi.org/10.5194/nhess-17-291-2017

Moos, C., Fehlmann, M., Trappmann, D., Stoffel, M., Dorren, L., 2017b. Integrating the mitigating effect of forests into quantitative rockfall risk analysis - Two case studies in Switzerland. Int. J. Disaster Risk Reduct. https://doi.org/10.1016/j.ijdrr.2017.09.036

Moos, C., Khelidj, N., Guisan, A., Lischke, H., Randin, C.F., 2021. A quantitative assessment of rockfall influence on forest structure in the Swiss Alps. Eur. J. For. Res. 140, 91–104. https://doi.org/10.1007/s10342-020-01317-0

Moos, C., Thomas, M., Pauli, B., Bergkamp, G., Stoffel, M., Dorren, L., 2019. Economic valuation of ecosystem-based rockfall risk reduction considering disturbances and comparison to structural

measures. Sci. Total Environ. 697, 134077. https://doi.org/10.1016/j.scitotenv.2019.134077

Motta, R., Haudemand, J.-C., 2000. Protective Forests and Silvicultural Stability. Mt. Res. Dev. 20, 180–187. https://doi.org/10.1659/0276-4741(2000)020[0180:PFASS]2.0.CO;2

Olmedo, I., Bourrier, F., Bertrand, D., Berger, F., Limam, A., 2016. Discrete element model of the dynamic response of fresh wood stems to impact. Eng. Struct. 120, 13–22. https://doi.org/10.1016/j.engstruct.2016.03.025

Pellegrini, G., Martini, L., Cavalli, M., Rainato, R., Cazorzi, A., Picco, L., 2021. The morphological response of the Tegnas alpine catchment (Northeast Italy) to a Large Infrequent Disturbance. Sci. Total Environ. 770, 145209. https://doi.org/10.1016/j.scitotenv.2021.145209

Petrillo, M., Cherubini, P., Fravolini, G., Marchetti, M., Ascher-Jenull, J., Schärer, M., Synal, H.A., Bertoldi, D., Camin, F., Larcher, R., Egli, M., 2016. Time since death and decay rate constants of Norway spruce and European larch deadwood in subalpine forests determined using dendrochronology and radiocarbon dating. Biogeosciences 13, 1537–1552. https://doi.org/10.5194/bg-13-1537-2016

Rammig, A., Fahse, L., Bugmann, H., Bebi, P., 2006. Forest regeneration after disturbance: A modelling study for the Swiss Alps. For. Ecol. Manage. 222, 123–136. https://doi.org/10.1016/j.foreco.2005.10.042

Scheidl, C., Heiser, M., Vospernik, S., Lauss, E., Perzl, F., Kofler, A., Kleemayr, K., Bettella, F., Lingua, E., Garbarino, M., Skudnik, M., Trappmann, D., Berger, F., 2020. Assessing the protective role of alpine forests against rockfall at regional scale. Eur. J. For. Res. 139, 969–980. https://doi.org/10.1007/s10342-020-01299-z

Schönenberger, W., 2002. Windthrow research after the 1990 storm Vivian in Switzerland: Objectives, study sites, and projects. For. Snow Landsc. Res. 77, 9–16.

Schönenberger, W., Noack, A., Thee, P., 2005. Effect of timber removal from windthrow slopes on the risk of snow avalanches and rockfall. For. Ecol. Manage. 213, 197–208. https://doi.org/10.1016/j.foreco.2005.03.062

Seidl, R., Thom, D., Kautz, M., Martin-Benito, D., Peltoniemi, M., Vacchiano, G., Wild, J., Ascoli, D., Petr, M., Honkaniemi, J., Lexer, M.J., Trotsiuk, V., Mairota, P., Svoboda, M., Fabrika, M., Nagel, T.A., Reyer, C.P.O., 2017. Forest disturbances under climate change. Nat. Clim. Chang. 7, 395–402. https://doi.org/10.1038/nclimate3303

Taeroe, A., de Koning, J.H.C., Löf, M., Tolvanen, A., Heiðarsson, L., Raulund-Rasmussen, K., 2019. Recovery of temperate and boreal forests after windthrow and the impacts of salvage logging. A quantitative review. For. Ecol. Manage. 446, 304–316. https://doi.org/10.1016/j.foreco.2019.03.048

Wohlgemuth, T., Kull, P., Wüthrich, H., 2002. Disturbance of microsites and early tree regeneration

after windthrow in Swiss mountain forests due to the winter storm Vivian 1990. For. Snow Landsc. Res. 77, 17–47.

Wohlgemuth, T., Schwitter, R., Bebi, P., Sutter, F., Brang, P., 2017. Post-windthrow management in protection forests of the Swiss Alps. Eur. J. For. Res. 136, 1029–1040. https://doi.org/10.1007/s10342-017-1031-x

4. Tree stability in steep terrain

Based on Marchi, L.; **Costa M.**; Grigolato S.; Lingua, E.

Overturning resistance of large diameter Norway spruce (Picea abies (L.) Karst) on sloped conditions

Forest Ecology and Management 524 (2022) 120531

https://doi.org/10.1016/j.foreco.2022.120531

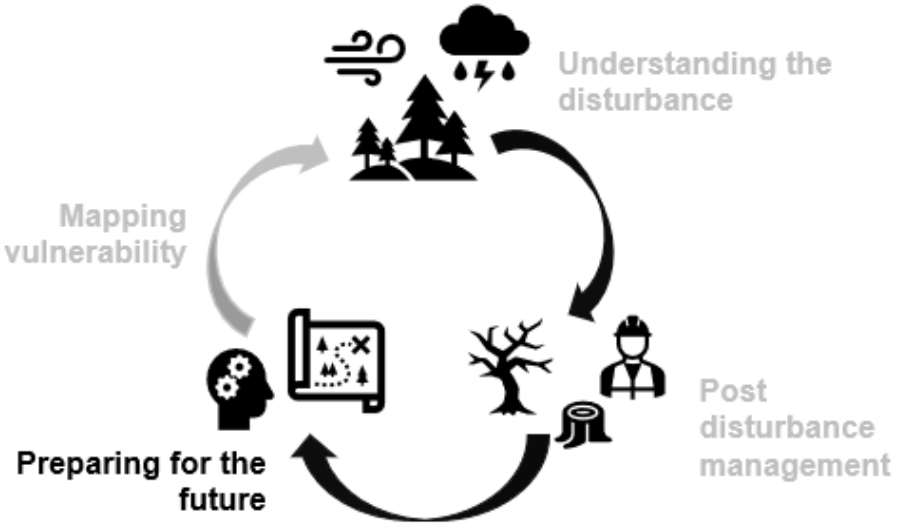

Increasing knowledge on tree stability in the forest environment has two major objectives: the first is to provide detailed information to help the decision-making processes that aim to maximize the efficiency of localized silvicultural interventions; the second is to provide useful information and safety guidelines for those who operate in these forests. With this aim, the mechanical response of large diameter Norway Spruce (*Picea abies* (L.) Karst) trees was investigated in the north-eastern Italian Alps. The aim of the study was to define the mechanical parameters necessary to model the overturning propensity of shallowly rooted mature trees growing on steep terrain characterized by soils with limited cohesion. Twelve standing trees (mean DBH=50.6 cm) were equipped with sensors at their base and pulled until their complete overturning. Thanks to the pulling method employed and the high precision sensors it was possible to describe the overall overturning behaviour in terms of bending moment vs. rotation curves. The pulling of two additional tree stumps also provided an example of the great contribution of the stem and crown weight to overall stability. Results show an increased resistance of the trees when compared to equivalent conditions but on flat terrain. On the contrary, the equivalent secant stiffness of the root-plate did not manifest significant variations. The obtained outcomes may be directly used as input data for management tools such as predictive models that quantify windthrow risk, protection against rockfall events or avalanches in all alpine contexts having similar characteristics to those dealt with in this study.

4.1 Introduction

Wind disturbance to forest ecosystems has been a widely investigated topic in the last few decades, from single tree resistance to the definition of stand management guidelines for mitigating its impact (Gardiner, 2021). Furthermore, most of the deadwood that can be found in European forests is likely a consequence of wind-related disturbances (Seidl et al., 2014), and is essential in shaping regeneration dynamics by providing suitable substrate or enhanced microsites for seedlings establishment and survival (Marangon et al., 2022). However, the changing climate and increasing vulnerability of European forests to natural disturbances require targeted strategies to mitigate losses in ecosystem services provision (Forzieri et al., 2021; Irauschek et al., 2017; Seidl et al., 2017). Some of the greatest advances in knowledge in this field were related to the understanding of the mechanics of wind-tree interaction. Several recent reviews summarized the many research works available on the topic covering the biomechanics of trees with particular focus on the dynamics of trees struck by wind load (James et al., 2014), providing comprehensive analysis of the reactions that wind produces on the growth of the trees in order to reduce their susceptibility (Gardiner et al., 2016), and highlighting that a high multi-disciplinary approach is required to shed light on the understanding of the interaction between wind and trees (Gardiner et al., 2019).

Another important interaction, when considering tree stability in mountain forests, occurs between trees and gravitative hazards, such as rockfall or avalanches (Brang et al., 2006; Lingua et al., 2020). Here, each single tree performs as a static obstacle to the movement of rocks or snow down the slope and therefore the assessment of the forces (and energies) required to initiate its failure, are a key point in the definition of whether the slope itself may be subjected to a low or high risk of damage (Dorren and Berger, 2006). Such interaction between trees and natural hazards plays a fundamental role in protective forests management (Lingua et al., 2020; Moos et al., 2017), for instance after natural disturbances, like windstorms, structural biological legacies, e.g., lying logs, may provide an effective protective function against avalanches or rockfall (Costa et al., 2021; Schönenberger et al., 2005; Wohlgemuth et al., 2017). The management choice of avoiding salvage logging (removal of lying logs), as well as not removing survivors and green islands, is therefore of great importance (Leverkus et al., 2021). These management choices may help to maintain the protective efficiency of mountain forests after natural disturbances and may link other important research questions: how long will the protective effect of lying logs last? How will this affect slope stability over time? (Schönenberger et al., 2005). This topic links tree stability with slope stability: the interaction of biological legacies with gravitative hazards and slope stability depends on the type of damage that originated the structural legacies: uprooted trees play a different role compared with snapped trees. The nature of the abiotic

damage directly depends on tree stability and the strength of the root plate of each tree, so the interaction with soil (Nicoll et al., 2006).

Finally, tree stability has recently been considered in studies involving the logging industry (Marchi et al., 2018). In this context, cable supported forest operations such as cable logging or winch-assisted machines rely on the resistance of standing trees or stumps that are used as natural anchors for the cables. Their failure, which may lead to fatal injuries, must be avoided by constantly monitoring their movements and relating them to available data of the tree pulling test (Marchi et al., 2021). A better understanding of the real propensity of the tree to failure would also affect the choices made by the loggers to find the safest but economically efficient harvesting technique for each site.

Therefore, improving the knowledge on tree stability in the forest environment has two major objectives: the first is to provide detailed information to help the decision-making processes that aim to maximize the efficiency of localized silvicultural interventions; the second is to provide useful information and safety guidelines for those who operate in these forests.

Mechanistic models of trees

To describe the mechanical response of trees to externally applied forces, mechanistic models (i.e., models considering only physical factors) have been developed by the scientific community. These models, although initially developed in studies concerning wind and trees interaction (Gardiner and Quine, 2000; Peltola et al., 1999), for the sole purpose of defining the critical wind-speed that will lead to the collapse of the tree with a given probability, are now widely applied in risk mitigation and forest management tools concerning also the previously aforementioned topics.

In general, two failure conditions are contemplated within such models: stem breakage or uprooting failure. The first situation is intrinsic mainly to the tree aboveground characteristics and is related to the mechanical properties of the green wood such as modulus of elasticity and rupture, stem dimensions and presence of knots. With respect to the latter case, it has been demonstrated that the root-soil interaction can be considered a more intricate situation and depends on the “scale” over which the problem is approached: root-soil plate mechanics (Fourcaud et al., 2007), root morphology (Fourcaud et al., 2008) and single root mechanical strength (Vergani et al., 2012) are all complex factors that could be taken into account to obtain a detailed perspective of the problem.

However, a simpler but very frequently used approach, foresees the propensity of tree overturning (namely the anchorage strength of the tree to the ground) as directly proportional to specific stem volume predictors (e.g., diameter at breast height (DBH), height (H) or most frequently, a combination of these). A strong experimental background is essential to adopt it. Several authors (Achim and Nicoll, 2009; Blackwell et al., 1990; Coutts, 1986) provided detailed analyses - based on experimental tests – which aimed at identifying the different components to be included in the overturning mechanism of

shallowly rooted trees. Stem, crown and root-plate self-weight, root-soil strength interaction, are these components. This approach still considers that the tree overturning susceptibility is species- and site-specific (namely, soil-specific) (Dupuy et al., 2005; Moore, 2000). Therefore, specific correlations have been built for the most common tree species and the latest mechanistic models account for the possibility to distinguish the root-plate overall behaviour for different root-architecture (e.g., shallow roots or tap root systems) and different soil macro-categories (Hale et al., 2015; Locatelli et al., 2017).

In conclusion, the risk of overturning can be described by two elements: a) a sort of "mechanical resistance" which is measured by the maximum bending moment to be applied to the tree base before its overturning and detected from moment vs. rotation curves; b) the stiffness of the root-plate system which measures the propensity of the stem base to rotate according to a given external applied load. More in detail, the propensity to overturning, consequent on the shift of the centre of gravity of the tree to a less stable position, is based on either the bending capability of the stem or on the stiffness of the root-soil system itself (Neild and Wood, 1999).

Current available data

A key point in the calibration and subsequent exploitation of such models is to build a consistent dataset on which empirical formulations rely. Experimental data (either in-situ or laboratory testing) are still a key component in the successfulness of all mechanistic models for tree stability (Gardiner et al., 2019).

Therefore, a lot of effort has been made to build up a strong and consistent database of tree pulling experiments. Nicoll et al. (2006) provided the summary of nearly two thousand pulling tests performed in the UK region, which covered most tree species present in the European territories. Since then, a few additional tests have been performed to fill the gap left for some common tree species or different sites (extra UK). For example, data on Norway spruce (*Picea abies* (L.) Karst) trees on freely draining soils, which are known to provide less anchorage strength than cohesive ones, are limited to relatively small stem sizes (i.e., below 0.35m of DBH (Nicoll et al., 2006)). More specifically, concerning Norway spruce, one of the most important tree species in Europe both for economic and ecological aspects (Caudullo et al., 2016), current pulling test data include trees having limited age and dimensions. Only two works (Jonsson et al., 2006; Lundström et al., 2007) presented tests on large diameter trees in the Alpine and subalpine environment aimed to identify the regression parameters for this specific condition, but most of them were performed on nearly flat terrain at a relatively low altitude (<620 m a.s.l.).

Moreover, pulling tests data are available for peaty gley soils(Coutts, 1986), Podzols (Gardiner et al., 2000) and mixed Cambisols and Pozsols (Lundström et al., 2007). There is scarce information on the

stability of Norway spruce growing on freely draining mineral soil which is a typical configuration of the Central European alpine and subalpine context, given the fact that anchorage strength appears to be scarcer for this soil condition (Dupuy et al., 2005; Moore, 2000).

Lastly, some interest has been placed on analysing the influence of a sloped terrain on the overall stability of trees. Sloped terrain conditions have been demonstrated to affect the root development systems (Chiatante et al., 2002) and, additionally, some authors found a greater anchorage capacity if trees were pulled uphill rather than downhill, despite the root depth and root-soil plate volume being higher in the latter (Achim et al., 2003; Nicoll et al., 2005). Jonsson et al. (2006) managed to provide a test oin sloped terrain but the results are unclear and deserve more research. Sun et al. (2008) performed tests on small DBH conifers finding a positive correlation between terrain slope and anchoring capacity of the root system. Schütz et al. (2006) observed that steeper slopes caused a significant reduction in susceptibility (by a factor of six for slopes over 50%, in comparison to gentle slopes <20%). It is still unclear if the cause of such evidence should be related to the orography and, consequently, the spread of the wind gusts, or a greater anchoring capacity of the trees should be considered.

Research objectives

This paper aims to provide knowledge on the uprooting resistance of Norway spruce trees, with a particular focus on medium-large diameter stems growing in freely draining mineral soils and on steep terrain. The main objective is to extend the use of predictive models that quantify stem failures for this species in the conditions already described. Our results may be implemented in models employed as ecosystem management tools dealing with windthrow risk, protection against rockfall events or avalanches in alpine contexts, especially in those scenarios that present similar characteristics to the ones dealt with within the framework of this study. Another objective is to quantify the difference in terms of resistance to overturning of Norway spruce trees being pulled on plain and sloped terrain. Furthermore, an estimation of the effect of tree self-weight on the overall stability was provided by pulling two large DBH stumps right after the felling of the tree.

4.2 Materials and methods

Site and trees description

Tree pulling tests were carried out in the Cansiglio forest, a 6,500-hectare area located in Veneto region in the north-eastern Italian Alps (Figure 18) and spread between 1100 m a.s.l. to 1200 m a.s.l.. The experimental campaign was conducted on a south facing slope in Val Menera, in a stand composed of Norway spruce planted approximately 70 years ago. The even-aged forest presented a homogeneous

and regular structure. Given the high stand density, most of the trees developed relatively small crowns, which, combined with small diameters and elevated heights, had enhanced the susceptibility to wind damages of the stand. The study area was hit by a windstorm, named Vaia, in late October 2018, where only in the Cansiglio forest area a total of 30.000 m^3 of windthrown timber was recorded. The study site location was selected approximately 500 m away from a site where pulling tests on flat terrain were performed in 2018 (Marchi et al., 2019), in order to be able to compare the mechanical response of pulled trees in similar weather and soil type conditions. The test site is characterized by slopes ranging from 22 and 30° where major soil groups include Epileptic Calcaric Phaenozem of limited depth (< 0.75 m) on limestone and marlstone bedrocks. Soils mainly develop from alluvial parent material and due to the steep terrain conditions present very shallow mineral horizons rich in coarse gravel (Garlato, 2016).

The testing site was an even-aged Norway spruce forest stand, trees DBH varied between 0.25 m up to 0.70 m while average tree height was approximately 30 m. Twelve Norway spruce trees and two stumps, with a DBH larger than 0.35 m, were randomly selected and pulled downslope. No edge trees were included in the pulling tests, in order to test trees with comparable crown sizes. Tests were conducted in two weeks of July 2020 with a gap of 14 days between them: eight standing trees and one tree stump were pulled on the first date, five standing trees on the other. However, all standing trees will be treated as a single data sample as no noteworthy difference of soil and weather conditions (windless) were reported. Neighbouring trees were felled when necessary to avoid obstruction of crowns and to provide a safe landing of the tree on the ground.

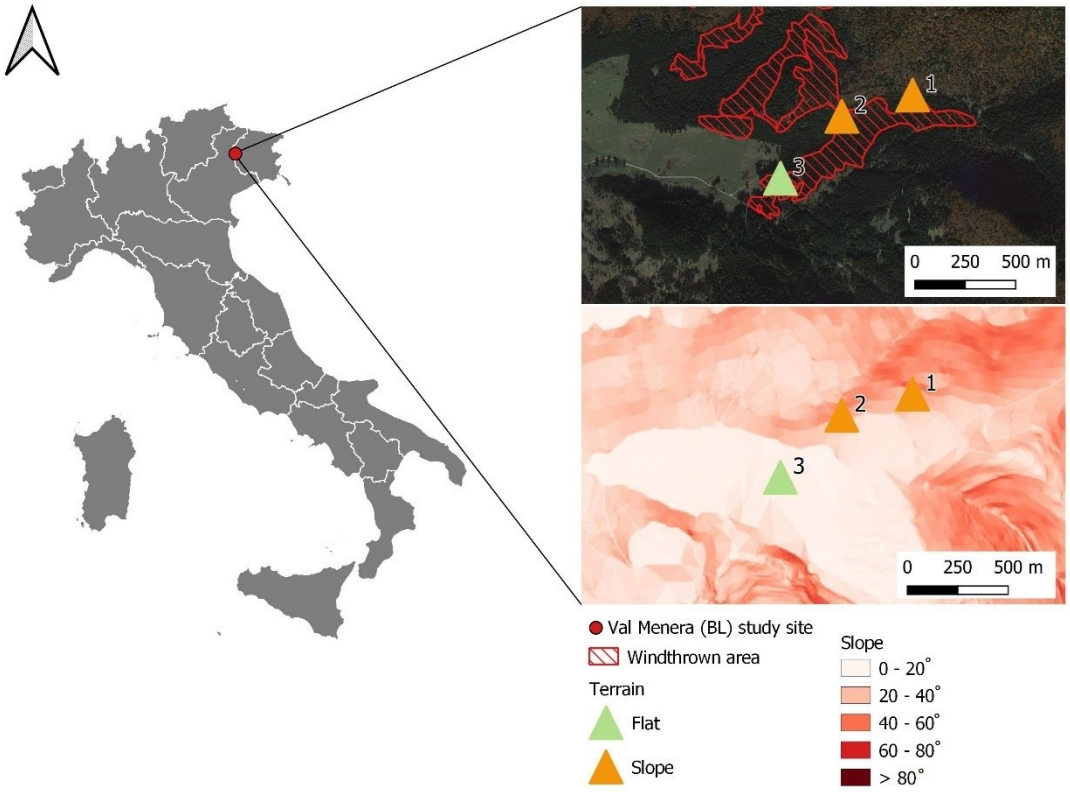

Figure 17. Map of the testing site

Pulling direction and method

The nearby windthrown areas (Figure 18) did not show evidence of a predominant wind direction, which may suggest that the storm Vaia in the site developed strong turbulences. A good availability of anchoring trees at the base of the slope, combined with an easily accessible road to set up the pulley system and to be used as an area safe from the falling trees led to the final choice of pulling the trees in the downslope direction only. Additionally, pulling them upslope would have required the felling of an excessive number of standing trees to obtain the sufficient safety measures for the tests.

A specifically designed pulling system capable of applying tensile forces up to 400kN was adopted, coherently with the expected maximum resistance of large DBH conifers falling by uprooting. A detailed description of the setup system is available in (Marchi et al., 2019). Nevertheless, some adaptations to the use on sloped terrain were undertaken. As all trees were pulled downslope, four trees at the base of the slope served as anchor trees for the pulley system. These were chosen to apply the pulling force in the direction of maximum slope with an admitted azimuthal deviation of ±15°. The two 22-mm pulling cables were wrapped around the tree at a given height from the ground (≤ 1.00 m), directly tightened over the bark, and secured with U-bolt clamps. Only the tree stump was provided

with a notch in which the cables were placed to prevent them from slipping over the tree during the test. The two stumps were pulled right after felling the standing trees.

Instruments and measurements

Tensile force data were collected by means of a load cell applied to the 22-mm cables with a constant recording frequency of 100Hz. The displacement of the tree root-plate was measured with two triaxial accelerometers based on the original work by James et al. (2013). The accelerometers, placed in waterproof canisters, were rigidly attached to the base lateral roots, one on the up-slope side (*windward* in the following) and one in the nearest root orthogonal to the pulling direction. The high gain accelerometers comprised of an internal datalogger to collect the tree root-plate movements during the pulling procedures.

Before each pulling test, cable height, its vertical inclination and azimuth of the pulling force were recorded, as well as the position of the lateral roots. After each test, diameters along the stem were measured at a 5-m interval using tree calipers; stem green density, used to convert stem volume to stem mass (***m)***, was extrapolated from stem cross sections sampled after the removal of the branches and weighed onsite with a digital scale. The dimensions of the overturned root-plate on the leeward (***d_1)*** and windward side (***d_2)*** (side of the pulling force and the opposite one respectively) were measured according to the protocol used by (Nicoll et al., 2005). Total width (***w)*** and depth of the pit (***d_p)*** were also measured (Figure 19).

Measurements of the crown weight and dimensions were not undertaken in this study. In fact, as actual mechanistic models allow the stem base moment due to the overhanging weight to be calculated separately, it was decided to focus on the assessment of the root-soil interaction, which for large sized trees is decisive in the overall calculation of the total anchoring capacity.

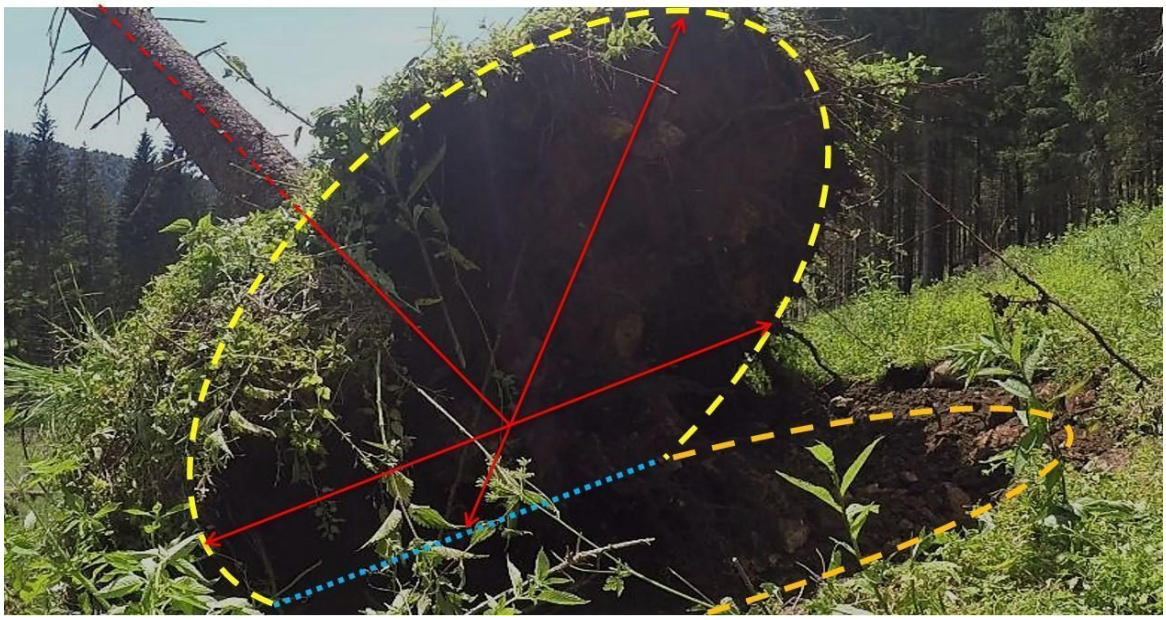

Figure 18. Root-plate of tree during the overturning: yellowish dashed lines highlight the gross shape; red arrows define the measurements undertaken after the test; dotted line represents the fictitious hinge location.

Mechanical model

The advantage of applying the force in proximity to the stem base allows an easier identification of its angles and components applied to the tree. The measurement of the stem deflection, which is essential to correctly evaluate the position and angle of the pulling force can be disregarded in this case, i.e., the stem base and its root-plate is assumed to behave as a unique rigid body. Hereafter, root-plate rotation or stem base rotation are considered the same parameter. On the contrary, with the employed pulling method, the shorter is the lever arm of the pulling force, the higher is the relative error obtained with an imprecise evaluation of the hinge position. Consequently, a camera was placed in proximity to the tree base to continuously record the whole overturning process and to facilitate the visual definition of the root-plate hinge point.

A mechanistic model used in similar studies (e.g., Achim et al., 2003; Nicoll et al., 2005)) was adopted to translate the synchronized rotations and pulling forces into actual equivalent bending moment vs. rotation correlations.

On flat terrain, the pulling force (***F)*** should be considered parallel to terrain and assuming that the hinge (the pivotal point of the root-system) is positioned at ground level, the applied lever arm (***h)*** is equal to the height of the cable from the ground (Figure 20a). The derivation of the equivalent bending moment ($M_)$ is then straightforward (Equation 4). The increased height (***h')***, that results from the progressive overturning of the root-plate, can be neglected in the pre-peak phase: for large DBH trees, the peak load is obtained for small variations of stem base rotation as explained by Equation (5) (namely, below 5°), where l_h is the ground distance of the hinge from the axis of the tree. Conversely,

in the case that the analysis includes the post-peak phase (i.e., large displacement and rotations, Figure 20b) such increase should be accounted for.

$$M = F \cdot h \tag{4}$$

$$M = F \cdot h' = F \cdot (h \cdot \cos\theta \ + l_h \cdot \sin\theta\ ) \approx F \cdot h \tag{5}$$

Finally, on sloped terrain, the pulling angle ***α*** may differ from the slope angle ***β*** (Figure 20c and Figure 20d), and the derivation of the lever arm must be modified accordingly, Equation (6).

$$h' = h \cdot cos\ [(\alpha - \beta) + \theta]\ + l_h\ sin\ [(\alpha - \beta) + \theta] \tag{6}$$

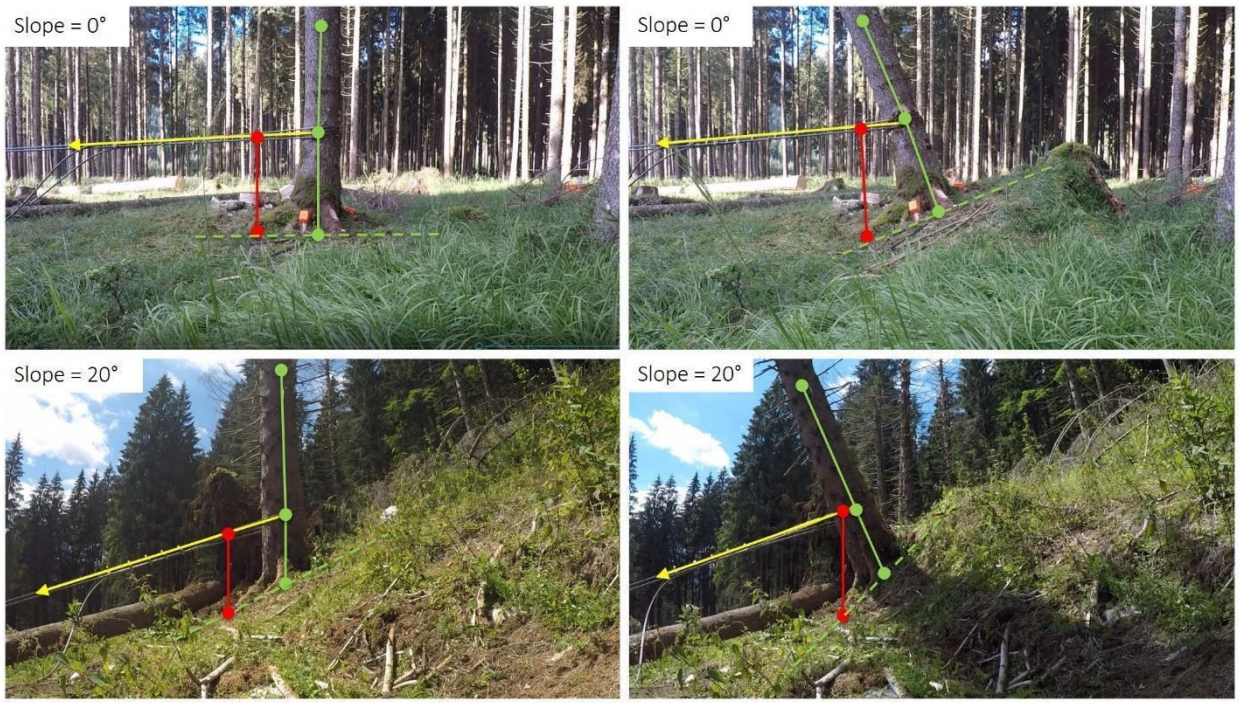

Figure 19. Mechanistic model: yellow arrow represents the direction of the pulling force F; red line is the height h; green line is the stem longitudinal axis; dashed green line shows the rotation of the root plate.

Data analysis and output parameters

Pulling test results are usually expressed through synchronized moment vs. rotation (***M-ϑ***) time series, from which parameters such as the maximum load carrying capacity (i.e., hereafter also referred to as "resistance") of the tree (M_{max}), and its corresponding rotation of the root-plate ($\vartheta(M_{max})$) can be directly extrapolated. The tree susceptibility to overturning is also analysed via evaluation of the secant stiffness (K_{root}) at a given rotation limit, which describes the amount of applied bending moment necessary to reach a specific rotation of the stem base. In this work, the rotation levels of 0.25° and

0.50° were chosen, as they normally refer to limits in which an elastic response of the root-plate system is assured, i.e., no irreversible damages and therefore rotations should occur (Lundström et al., 2007; Marchi et al., 2019; Peltola et al., 2000).

The post-processing data analysis was conducted in Matlab environment (Mathworks, 2020). The raw data from the two sensors at the tree base and the load cell were firstly synchronized via time stamps and the three accelerations were converted into corresponding biaxial rotation measurements with an estimated precision of 0.005°. The accuracy of these sensors was validated in a parallel study conducted on the real-time monitoring of natural anchors in cable logging (Marchi et al., 2020). Following those results, a digital infinite response filter was used to filter the signal and obtain a clear definition of the root-plate inclination. Due to technical issues occurring during the test of trees T7 and T12, the decreasing branch of the curves could not be derived in those two cases. However, a clear definition up to the peak point (M_{Max}, $\vartheta(M_{max})$) allowed the trees to be included in the dataset for the following analyses.

Subsequently to smoothing of the raw signals derived from the sensors, a locally weighted, quadratic, polynomial smoothing algorithm was used to obtain the general trend of each curve and analyse them in adimensional terms (M_0-ϑ_0 curves), i.e., M_0 is equal to M/M_{max} for the bending moment and ϑ_0 is equal to $\vartheta/\vartheta(M_{max})$ for the rotation. In this case a fixed window of 1% of the total data points was chosen (resulting in a time time frame of approximately 1s), apart from trees T7 and T12 which required a longer pulling time and a larger time window (5% of the datapoints) was used. The procedure was performed on both new and available data (previous tests on flat terrain) in order to provide consistent comparisons between the shapes of the M_0-ϑ_0 curves.

The main mechanical parameters describing the overturning resistance were calculated for each tree and the two stumps. The parameters were the failure load F (i.e., the maximum applied pulling force), the height of the lever arm h calculated according to Equation (6), the bending moment M_{max} and corresponding rotation of the root-plate $\vartheta(M_{max})$ at failure, and the secant stiffness k_{root} at both the 0.25° and 0.50° reference levels (Gardiner et al., 2000; Lundström et al., 2007).

To provide a deeper insight into the prediction of such a response with simple linear models, correlations of the peak bending moment and stiffness with respect to two well-known allometric predictors such as $DBH^2 \times H$ and stem mass were performed with data from this test campaign on sloped terrain and the previous one in a flat condition (Marchi et al., 2019). Regressions were all forced through the origin, to provide coherence with the physical condition that without mass the bending moment is equal to zero. Additionally, following the data analysis technique adopted by Lundström et al. (2007), the rotation $\vartheta(M_{max})$ was associated to the allometric parameter $DBH^2 \times H$ so as to identify the logarithmic correlation trend between the two variables.

Finally, the M_0-ϑ_0 curves were analysed according to the approach presented by Sagi et al. (2019) which adopted an analytical model based on a geotechnical engineering approach to describe the M_0-ϑ_0 relation for Norway spruce up to the failure point. The analytical model provided an interpolating equation modifying the formulation for shear failure of soils developed by Brinch-Hansen (1963) and expressed by Equation (7):

$$M_0 = \theta_0^n + \alpha \cdot \theta_0(1 - \theta_0^n) \quad (7)$$

where α and n are constants derived by experimental tests.

Most of the calculated parameters (e.g., the slope coefficient of the overturning resistance with respect to the tree size predictors) can be directly introduced as input parameters in existing mechanistic model's formulations. The secant stiffness K_{root} is also a valuable parameter which does not require specific manipulations and can be directly adopted as input if a higher level of complexity is pursued (e.g., the development of finite element models). Finally, the M_0-ϑ_0 parametrized relations can be used to test the suitability of advanced models in capturing the correct non-linear response of the overturning mechanism measured at the base of the tree.

4.3 Results

Overall behaviour

The twelve pulling tests on full standing trees included a tree that was found to be truncated at a height of 17.5 m (Tree T1), probably snapped by the Vaia storm, and was therefore excluded from the following statistical analyses. The eleven remaining trees had an average DBH of 0.50 ± 0.10 m, H equal to 31.5 ± 5.7 m and an estimated stem mass of 2.26 ± 1.0 t (Table 5). As a direct consequence of the specific pulling method, all the tested trees failed by uprooting, exhibiting the overturning mechanism typical of shallowly rooted trees. The roots on the leeward side, once fractured due to combined compression and bending, defined the position of the hinge; subsequently, windward roots failed due to tension leading to the tree overturn. The ground distance of the hinge on the leeward side l_h observed during the overturning phenomenon, extrapolated through the video analysis, was not exactly equivalent to the distance measured at the complete overturning d_2. This is due to the fact that normally the root-plate partially collapsed on its own weight during the final part of the overturning mechanism, thus underlining the importance of having a video camera in proximity to the tree base.
The suitability of the pulling system was confirmed by the test on the two tree stumps on sloped and flat terrain (Figure 21), S1 and S2 hereafter (Table 5), as they both failed due to uprooting. In these

cases, upon reaching the peak load, the force was released, and the stumps with the root-soil plate fell back onto their initial position.

Considering the soil type and tree species, the emerged root-plate was characterized by a very limited depth d_p, and the limestone bedrock often emerged below it. No signs of root decay were detected during the examination and measurements of the overturned root-plate. The measured width *w* listed in Table 5 refers to the maximum extension of the soil being pulled from the ground by the lateral roots, however in some cases the soil thickness in the farther areas was very limited (≤ 10 cm). In those circumstances, the shape of the pit caused by the root-plate overturning, i.e., the volume of soil involved in the turning mechanism, could be assimilated to a truncated cone. Dimensions were taken considering only the compacted soil attached to the plate neglecting some seldom protruding roots.

The time synchronization between values of force and rotations, allowed the characteristic M-ϑ curves to be derived from each pulling test (Figure 22a). Similarly, the secant stiffness vs. rotation curves were derived from the time series (Figure 22b). In general, large non-linearities start to develop from rotations above 0.10°. It emerges how defining specific thresholds to those rotations such as the common value of 0.25° or 0.50°, may substantially change the theoretical stiffness value, which would directly affect the response of the mechanistic models.

Table 5. Main allometric parameters of each tested tree; DBH = diameter at breast height; H = height; m = stem mass; d_1 = dimensions of the overturned root-plate on the leeward side; d_2 = dimensions of the overturned root-plate on the windward side; w = width of the pit; d_p = depot of the pit.

Tree	***DBH*** **[m]**	***H*** **[m]**	***m*** **[t]**	d_1 **[m]**	d_2 **[m]**	***w*** **[m]**	d_p **[m]**
T1	0.51	17.5[1)]	2.35	2.6	3.1	4.4	0.50
T2	0.57	31.0	3.42	2.8	3.3	4.7	0.60
T3	0.63	30.0	3.25	2.2	2.7	5.8	0.50
T4	0.61	37.9	3.60	3.3	3.8	6.9	0.65
T5	0.38	29.5	1.25	1.3	1.8	3.4	0.50
T6	0.43	30.0	1.55	2.1	2.6	5.3	0.55
T7	0.65	38.0	3.94	3.4	3.9	7.2	0.70
T8	0.35	29.4	1.25	1.2	1.7	2.2	0.50
T9	0.42	32.0	1.51	1.8	2.3	3.1	0.50
T10	0.57	37.6	3.37	2.0	2.5	5.0	0.60
T11	0.47	33.1	2.17	2.2	2.7	4.5	0.50
T12	0.44	36.5	2.12	1.5	2.0	4.2	0.50
S1[2)]	0.63	38.0[3)]	-	2.8	1.9	2.1	0.50
S2[2)]	0.43	31.0[3)]	-	0.0	0.0	0.0	0.00

[1)] height of the truncated stem; [2)] stump; [3)] values referred to the original standing tree.

Figure 20. Pulling test of the Stump S1.

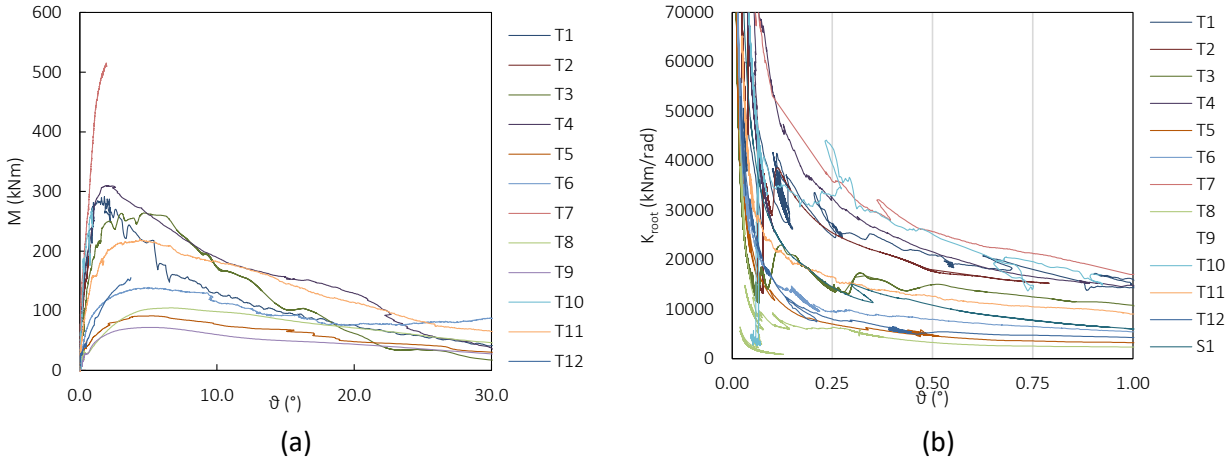

Figure 21. M vs. ϑ (a) and K_{root} vs. ϑ (b) curves extrapolated for the tests.

Main mechanical parameters

Table 6 and Table 7 report the main mechanical parameters describing the overturning resistance for trees and stumps respectively. Despite the considerably high magnitude of the applied forces, the pulling system was capable of overturning a particularly large tree in the set (Tree T7 with DBH = 0.65 m) through the application of a load *F* equal to 351kN near its base. In this occasion, a peak bending moment of 516 kNm was applied to the tree; the same tree also exhibited the lowest value of rotation at failure $\vartheta(M_{max})$, i.e., 1.94°. On the contrary, the lowest value of M_{max}, 77 kNm, was obtained on the second smallest tree in the set, Tree T8. The maximum value of $\vartheta(M_{max})$, 6.2°, was registered for the smallest tree (Tree T9 with a DBH equal to 0.35 m).

Unexpectedly, stump S1 returned a M_{max} of 92kNm, more than 40kNm lower than stump S2, although the stem size of the originating tree (Table 5) would suggest quite the opposite. Comparing the response of Stump S1 to that of pulled trees having a similar stem mass (T4 and T7, if the full stem of a felled tree is considered), it emerges that the peak resistance M_{max} was about one third and one fifth of the one manifested by the whole trees.

The calculated secant stiffness varied considerably (nearly one order of magnitude) at both 0.25° and 0.50° reference levels. The lower and upper bounds were registered by the smallest and largest tree in the set respectively. The calculated secant stiffness at 0.50° was reduced on average by 27% with respect to the values registered at 0.25°, with the exception of tree T3 that showed an already highly non-linear response and similar stiffness at both reference levels.

Table 6. Main parameters obtained for the standing trees; F_{max} = maximum applied force; h' = height of the lever arm; M_{max} = maximum bending moment; $\vartheta(M_{max})$ = rotation corresponding to M_{max}; K_{root} = rotational stiffness of the root-plate.

Tree no.	F_{max} (kN)	h' (m)	M_{max} (kNm)	$\vartheta(M_{max})$ (°)	k_{root} ϑ=0.25° (kNm/rad)	k_{root} ϑ=0.50° (kNm/rad)
T1	228	1.46	295	1.95	32086	22918
T2	210	1.45	269	2.40	28648	19939
T3	189	1.40	233	2.89	18344	16043
T4	227	1.35	270	2.07	32086	21199
T5	93	1.10	91	3.53	6875	4698
T6	101	1.55	144	4.98	10542	8824
T7	351	1.60	516	1.94	43545	30367
T8	101	1.20	106	6.20	6875	3782
T9	93	0.97	77	4.87	7105	3896
T10	195	1.80	315	2.10	33232	25783
T11	193	1.30	220	4.38	18105	14324
T12	131	1.31	151	4.88	3209	5157
Mean	177	1.27	224	3.88	17677	13026
Median	193	1.25	220	4.39	14209	12605
SD	83	0.23	130	1.54	11880	8680

Table 7. Main parameters obtained for the two stumps; F_{max} = maximum applied force; h' = height of the lever arm; M_{max} = maximum bending moment; $\vartheta(M_{max})$ = rotation corresponding to M_{max}; K_{root} = rotational stiffness of the root-plate.

Tree no.	F_{max} (kN)	h' (m)	M_{max} (kNm)	$\vartheta(M_{max})$ (°)	k_{root} ϑ=0.25° (kNm/rad)	k_{root} ϑ=0.50° (kNm/rad)
S1 (slope)	151	0.40	92	6.85	11746	8980
S2 (flat)	157	0.90	138	4.58	36669	21772

Correlation with allometric parameters

For both the peak bending moment and root-plate stiffness a positive correlation was found with the explanatory variables employed (Table 8). The slope of all models resulted significant (P<0.001) and the coefficient of determination provided all values above 0.87. Considering the regression of M_{max} over m (Figure 23a) and $DBH^2 \times H$ (Figure 23b), the slope coefficient obtained in these tests showed an important increment if compared to the tests conducted on flat terrain, resulting in +50.6% and 33.8%

respectively. Referring to the regressions of secant stiffness (Figure 24), it can be noticed that the results obtained on flat terrain could also be extended to a sloped condition (-1.8% of relative difference) assuming a reference rotation of 0.50°, whilst calculated at 0.25° a higher decrease is observed (-14.3%). Considering the correlation between $\vartheta(M_{max})$ and $DBH^2 \times H$ (Figure 25), the latest tests on sloped terrain confirmed that in the range between 3.5 to 16.0 m³ of $DBH^2 \times H$, a comparable negative exponential trend was extrapolated (Table 4) and an estimated average increase of 0.4° of $\vartheta(M_{max})$ was observed between the two terrain conditions.

Table 8. Linear regression parameters for plain and sloped terrain; b = slope of the regression; SE(b) = standard error of the slope; R^2 = coefficient of determination.

Parameter (units)	**Site**	**b**	**SE(b)**	**F-value**	**R^2**
M_{max}					
m (t)	Plain	62.00	4.03	237	0.91
	Slope	92.72	6.94	179	0.94
$DBH^2 \cdot H$ (m^3)	Plain	19.37	1.17	276	0.92
	Slope	25.86	2.29	128	0.92
k_{root} *(0.25°)*					
m (t)	Plain	7802	442	312	0.93
	Slope	8533	831	105	0.91
$DBH^2 \cdot H$ (m^3)	Plain	2437	126	377	0.94
	Slope	2365	271	76	0.87
k_{root} *(0.50°)*					
m (t)	Plain	5020	282	317	0.93
	Slope	6251	536	136	0.93
$DBH^2 \cdot H$ (m^3)	Plain	1571	78	409	0.94
	Slope	1731	182	90	0.89

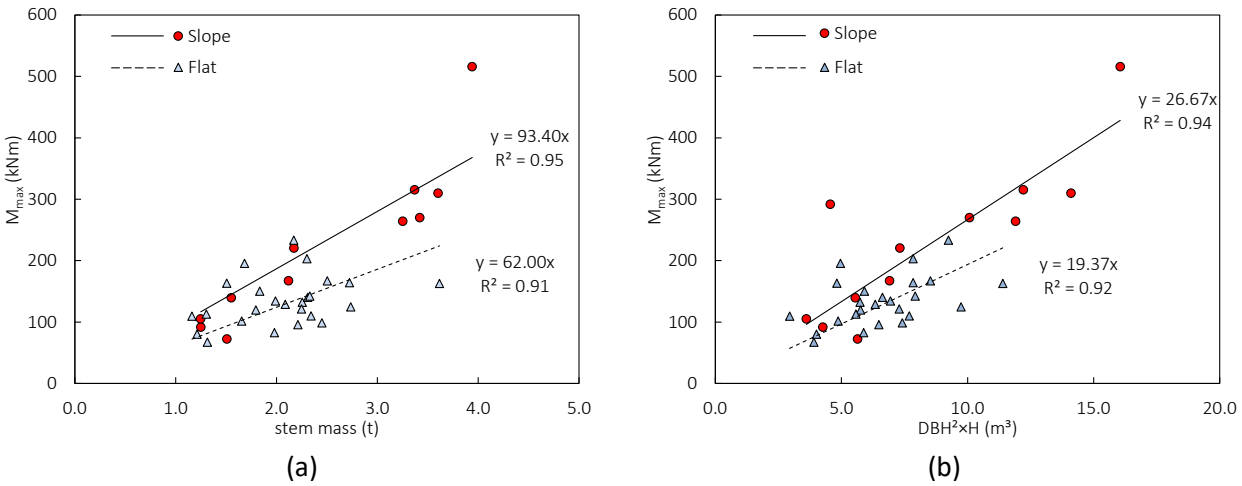

Figure 22. Linear regressions of the maximum resisting bending moment over the stem mass (a) and DBH^2xH (b); regression lines are fitted through zero.

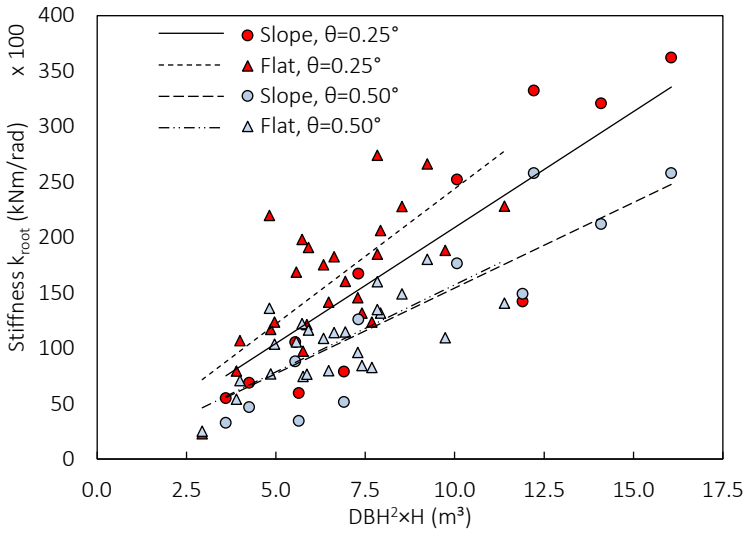

Figure 23. Linear regressions of the secant stiffness vs. DBH²xH at 0.25° and 0.50°; regression lines are fitted through zero.

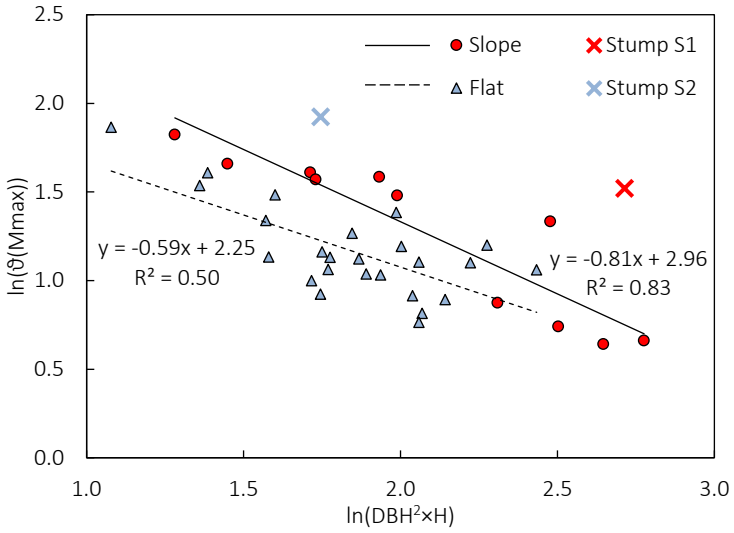

Figure 24. Prediction of $\vartheta(M_{max})$ from DBH²H extrapolated from the two datasets. Results from stumps are plotted for reference only.

Adimensional curves

Adimensional M_0-ϑ_0 curves are an essential parameter in the development of models that seek to describe the response of the roots-soil system. Comparing the shapes of the curves obtained, it emerges how the average shape of the curves appears to be different between the two soil inclinations (Figure 26). Assuming the parameters declared by Sagi et al. (2019), n = 0.68 and α = 1 return a conservative interpolation of the curves obtained in this study (Figure 26a). In our study, the average curve could be better fitted adopting n = 0.50, whereas n = 0.40 would define an upper bound condition of the performed tests. Superimposing those analytical predictions to the test on flat terrain (Figure 26b) the different shape of the adimensional curves emerges. In this case the n = 0.40 and α = 1 would define not the average but a lower bound condition. Differences between Figure 27a and Figure 27b are the result of two concurring facts: a) a lower initial stiffness (measured at low degrees

of rotations) of trees standing on slopes; b) a higher maximum bending moment M_{max}. It must be emphasized that both soil conditions and seasonality did not change between the two experiments. The M_0-ϑ_0 curves of the two stumps (Figure 25a), compared to full standing tree specimens having comparable stem sizes and grown in the same terrain conditions, suggest a "rigid-plastic" behaviour for the large stump S1, while stump S2 averages well with the characteristic curve observed with the full trees. In detail, S1 provided a "stiffer" characteristic curve: it appears that the roots on the leeward side did not break due to bending as within full standing trees enabling a fully rigid body motion of the stem base / root system assembly. Additionally, upon reaching about 75% of the peak bending moment, the corresponding rotation was limited to nearly 10% of the rotation at the peak point. For flat terrain, Stump S2 provides a more similar trend with three trees selected from the previous campaign (DBH²xH equal to 5.73, 5.76 and 5.87 m³) (Figure 25b).

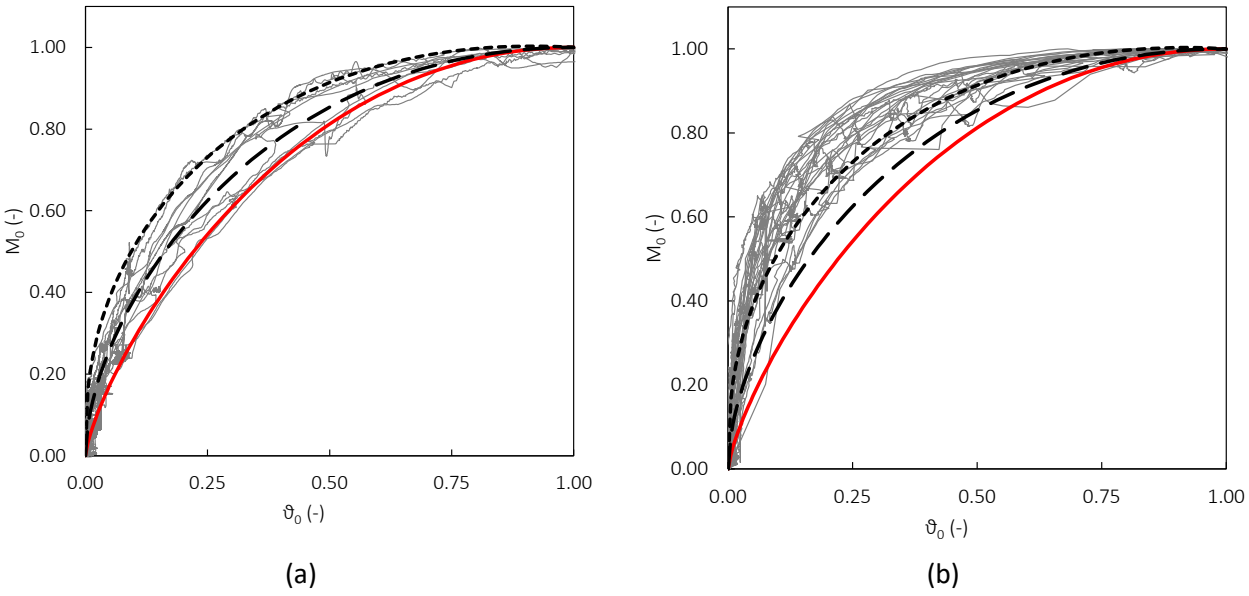

Figure 25. Normalized M_0-ϑ_0 curves obtained from tests on sloped (a) and flat (b) terrain. Thick lines represent analytical expression according to Eq. (4): continuous line for n=0.68, dashed line for n=0.50 and dotted line for n=0.35.

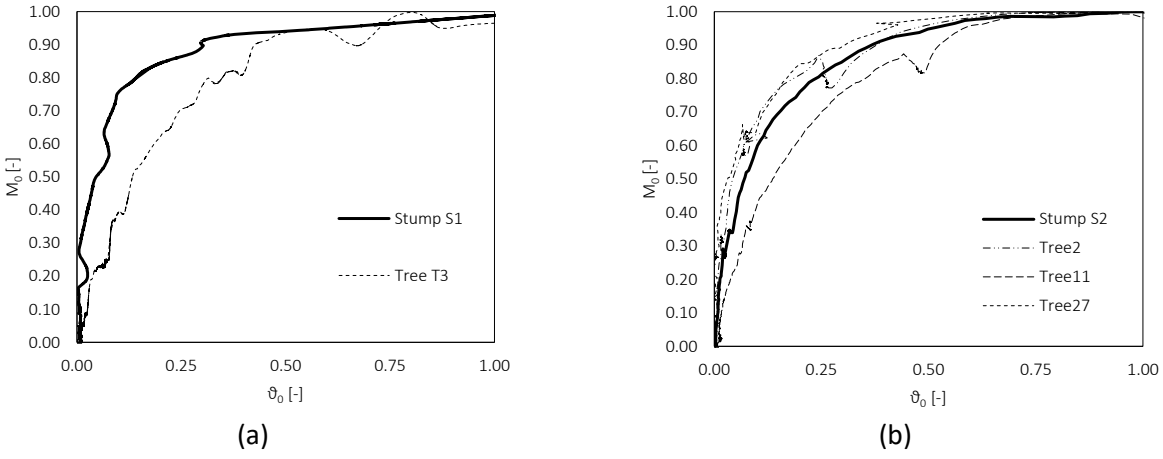

Figure 26. Normalized M_0-ϑ_0 curves for stump on sloped terrain (a) and stump on plain terrain (b). Data for Trees 2,11 and 27 are extrapolated from (Marchi et al., 2019).

4.4 Discussions

Fourteen pulling tests including twelve trees and two stumps were conducted in the Cansiglio Forest, in the north-eastern Italian Alps. A high load capacity pulley was designed and used to perform tests on Norway spruce trees, with average DBH equal to 0.50 m, by applying the pulling force at the base, thus neglecting the influence of the stem deflection-related issues typical of more traditional pulling techniques. Compared to a previous work conducted in the same area (Marchi et al., 2019) and to the data available in the scientific literature, this study aimed to extend the coverage of tree size in terms of $DBH^2 \cdot H$ (Figure 23) and stem mass (Figure 24) parameters and to increase knowledge on the effect of sloped terrain on the overturning resistance of coniferous trees with superficial root development.

Failure mechanism and peak point parameters

All fourteen tests ended in failure due to overturning typical of shallowly rooted trees (Achim and Nicoll, 2009; Blackwell et al., 1990). Although no specific instruments were set at soil level, the video analysis confirmed the pattern reconstructed by Lundström et al. (2007) and Sagi et al. (2019) with a development of the rotational hinge point at a distance between one to two times the DBH. However, the shape of the root–soil plate was likely more a truncated cone rather than an elliptical cross-section (Lundstrom et al., 2007). Even large DBH specimens provided with some massive lateral roots, mobilized a relatively small amount of soil during overturning. This shows their unsuitable root morphology in delivering high resistance to overturning.

The synchronization of the time series obtained by the sensors allowed M-ϑ curves to be extrapolated and identify the peak point values (M_{max}; $\vartheta(M_{max})$) for each test. The magnitude of the peak applied force (and bending moment) values were found to be comparable to those observed on flat terrain (Marchi et al., 2019) with the highest peak measuring over 350kN, which resulted in the application of a maximum bending moment of 516kNm for a tree with a DBH of 0.65 m. The rotations $\vartheta(M_{max})$ ranged between 1.94° and 6.20° appearing in line not only with the above-mentioned tests conducted two years before in the absence of slope but also with other studies available in the literature on Norway spruce (Lundström et al., 2007; Sagi et al., 2019) or other coniferous trees with similar shallow root systems such as the Western hemlock (*Tsuga heterophylla*) (Byrne and Mitchell, 2007).

Effects of tree size on overturning risk

Excluding the tests on the two stumps and wind-snapped tree, allometric predictors such as stem mass and $DBH^2 \times H$ were positively correlated with the calculated M_{max} and secant stiffness at 0.25° and 0.50° rotation reference levels. Regressions confirmed that large-size trees tend to provide a stiffer but "more fragile" response at failure, as the peak resistance is observed at lower rotation levels. Considering that large trees are normally tall trees, the susceptibility to be windthrown greatly

increases since the leverage effect on the wind load raises the resulting torque (Stathers et al., 1994). This highlights the need to adapt the models included in available decision-making tools, originally developed for forest plantations that are clearly different from the case of semi-natural or more heterogeneous managed forest stands characterized by longer harvesting rotations. It is also worth noting that the truncated tree returned the third highest overturning resistance, confirming, from a forest management point of view, the valuable contribution of windthrown elements in maintaining slope stability and increasing slope roughness. This is valid until the decay process does not reduce root strength and mechanical resistance of deadwood (Costa et al., 2021; Sidle, 2005).

Effects of slope on the peak bending moment

Effect of the slope among the linear regressions shows an increment of 50.6% and 33.8% if stem mass and $DBH^2 \times H$ respectively are taken as explanatory variables. A possible explanation may be related to a different water depth, which is known to be a key point affecting the stability of conifers (Gardiner, 2021).

Comparative tests performed by Nicoll et al. (2005) on Sitka spruce did not show any differences between flat and sloped terrain but were performed only on relatively small trees with average DBH < 0.25 m, thus the root-system of mature trees may provide a greater level of acclimatization. Several studies have been conducted in plantations with relatively short rotations compared to silvicultural systems applied in the Alps on semi-natural forests. This led to considering generally small-size trees with lower resistance (i.e., wider tree rings) compared to the characteristics of mountain stands, like the forests affected by storm Vaia.

Furthermore, the obtained slope coefficients are comparable to the one determined by Lundström et al. (2007) for Norway spruce on sloped terrain, even if values in that study also included the contribution of the overhanging mass, which was calculated to be between 10 and 25%, respectively in the range between 0.69 and 0.20 m of DBH. Therefore, the actual difference between our and the Swiss study may set in the range 11%-26% or 8%-23% if stem mass or $DBH^2 \times H$ are taken as reference predictors respectively.

On the contrary, the slope of the regressions between M_{max} over stem mass or DBH^2xH found in the literature and contemplating trees with DBH < 0.20 m and H/DBH ratio of ≈ 100 on flat terrain (Nicoll et al., 2006; Peltola et al., 2000; Sagi et al., 2019), appears rather different from this study. A hypothesis may arise on this evidence, that is, whether these trees did not collapse during the Vaia storm due to an inherently greater resistance to overturning. Nevertheless, no indication of a possibly different acclimatization process to wind could be found and perhaps a simpler conclusion is that the area of the test site was not directly affected by the wind gusts that struck nearby trees. Finally, the lack of

tests in other directions does not allow to understand if the resistance measured in these tests is the actual maximum or can be even greater, for example in the upslope direction (Nicoll et al. 2005).

Effects of the slope on the root-plate stiffness

The stem-base rotational stiffness K_{root} was calculated at the two reference levels of inclination, namely 0.25° and 0.50°. The first level (K_{root} at 0.25°) appears to be lower on sloped terrain, suggesting a higher propensity of the root-plate to rotate, i.e., about 15% less of bending moment is required to obtain a given rotation within the 0.25° limit. Contrarily, the second level (K_{root} at 0.50°), shows overlapping values, implying that the later response on sloped terrain (between 0.25° and 0.50°) is more rigid than in flat conditions.

Bringing together these outcomes with the previous ones about the resistance it appears that the tree behaves similarly on both sloped and flat terrain, whereas the higher anchorage capacity of the root systems provides a higher reserve of resistance when sloped terrain is considered. Such a different "pattern" of the tree motion before reaching its peak strength was clarified through the adimensional curves (M_0-ϑ_0). The simple formulation proposed by Sagi et al. (2019) to define M_0-ϑ_0 response of Norway spruce returned a quite conservative, but still satisfactory response according to the pulling tests on sloped terrain, whereas only a much lower exponent parameter could explain the much more distinct elasto-plastic pattern observed for the tests on flat terrain.

Effects of the tree self-weight

Lastly, this study provided novel experimental evidence about the effect of the tree self-weight through the determination of the resistance of stumps with respect to standing trees in terms of ϑ_f *vs.* DBH^2xH relationship. It resulted that the absence of the tree self-weight seems to affect quite strongly the overturning moment required to overturn the tree as well as the M-ϑ curves.

Stump S1 showed a clear two-phase behaviour (Coutts, 1986) as a result of the breakage of the soil occurring at very small rotations and developing the remaining strength to the weight of the root-plate system. Concerning the stump on flat terrain, Stump S2, the decrease of resistance with respect to the one determined by regression over the original full stem mass was limited to 25%. Such outcomes suggests that the contribution of stem weight to the total anchoring capacity is predominant for large trees, while the anchoring capacity of smaller trees relies more on the root-soil interaction and self-weight.

By analysing the stump response in terms of root-soil plate rotation, a much higher rotation value at the peak load ϑ_f was observed in both cases. Comparing them to the logarithmic regression of ϑ_f valid for the full standing tree, the stump on plain terrain showed values of 6.85° instead of the 3.82° predicted; the one on the slope of 4.58° in place of 2.22°. These tests confirm the great stiffening contribution of tree weight to the root-plate stability. How long this resistance is maintained in stumps

or eventually standing dead trees, is an important parameter to investigate, both concerning root reinforcement (i.e., for slope stability (Cislaghi et al., 2021) and wood decay processes (i.e., potential kinetic energy dissipation in rockfalls) (Olmedo et al., 2018).

Limitations and future studies

Considering slope as a variable allows tree stability to be better investigated according to growing site, either on flat or steep terrain, introducing a higher accuracy that may be relevant for forest management. Slope may influence wind risk susceptibility of trees and it has not been sufficiently investigated as a relevant variable (Gardiner, 2021), thus adding this variable to already existing models may help providing a better spatialisation of exposed areas.

More precisely, the outcomes of this work can be used to parameterise existing predictive models for wind risk in order to assess the effect of the slope on the critical wind speed of trees (i.e. the minimum wind speed that can cause structural damage to trees), as was done previously with the ForestGALES model using pulling tests carried out in the field (Locatelli et al., 2016). For instance, we can easily include the slope effect in these models by modifying the overturning coefficient for trees growing in steeply sloping conditions.

A deeper knowledge on slope's influence on stability may also help to enhance the accuracy of the expected interaction of trees with natural hazards, such as rockfall, avalanches or shallow landslides. It is worth noting that this study included tests only with a downslope pulling direction and a lack of information still exists about the effects on the pulling direction for large diameter trees standing on slopes, for example by pulling the trees upslope or across slope as already done for small DBH trees.

4.5 Conclusions

The overturning risk of large DBH shallowly rooted trees in sloped terrain was found to be considerably lower with respect to flat terrain conditions (evidenced through a higher mechanical resistance of the root-plate system in the first case). On the contrary, the root-plate stiffness appears to be less dependent by the terrain inclination. The combination of these two concurring outcomes is responsible for a different pattern of the non-linear bending moment vs. rotation relations (explained via adimensional M_0-ϑ_0 curves), thus requiring a more precise adaptation of actual semi-mechanistic models used in decision-making risk tools which can be pursued with the data presented in this work. It's also been proven by specific pulling test of stumps, that the tree self-weight (i.e., crown and stem weight) provides a great contribution to the tree stability especially for large diameter trees. In order to confirm our findings, further research should be conducted for different soil types and tree species, trying to always include different tree sizes and slope conditions.

4.6 References

Achim, A., Nicoll, B.C., 2009. Modelling the anchorage of shallow-rooted trees. Forestry 82, 273–284. https://doi.org/10.1093/forestry/cpp004

Achim, A., Nicoll, B.C., Mochan, S., Gardiner, B.A., 2003. Wind Stability of Trees on Slopes, in: International Conference 'Wind Effects on Trees' September 16-18, 2003. Karlsruhe, Germany.

Blackwell, P.G., Rennolls, K., Coutts, M.P., 1990. A root anchorage model for shallowly rooted sitka spruce. Forestry 63, 73–91. https://doi.org/10.1093/forestry/63.1.73

Brang, P., Schönenberger, W., Frehner, M., Schwitter, R., Thormann, J.J., Wasser, B., 2006. Management of protection forests in the European Alps: An overview. Forest Snow and Landscape Research 80, 23–44.

Brinch-Hansen, J., 1963. Diskussionsbeitrag zu Zweck/Dietrich. Modellversuche mit steifen Dalben in bindigen Böden bei plötzlicher Belastung.

Byrne, K.E., Mitchell, S.J., 2007. Overturning resistance of western redcedar and western hemlock in mixed-species stands in coastal British Columbia. Canadian Journal of Forest Research 37, 931–939. https://doi.org/10.1139/X06-291

Caudullo, G., Tinner, W., Rigo, D. de, 2016. Picea abies in Europe: distribution, habitat, usage and threats., in: San-Miguel-Ayanz, J., de Rigo, D., Caudullo, G., Houston Durrant, T., Mauri, A. (Ed.), European Atlas of Forest Tree Species. Publ. Off. EU, Luxembourg, pp. 114–116.

Chiatante, D., Scippa, S.G., di Iorio, A., Sarnataro, M., 2002. The Influence of Steep Slopes on Root System Development. J Plant Growth Regul 21, 247–260. https://doi.org/10.1007/s00344-003-0012-0

Cislaghi, A., Alterio, E., Fogliata, P., Rizzi, A., Lingua, E., Vacchiano, G., Bischetti, G.B., Sitzia, T., 2021. Effects of tree spacing and thinning on root reinforcement in mountain forests of the European Southern Alps. For Ecol Manage 482, 118873. https://doi.org/10.1016/j.foreco.2020.118873

Costa, M., Marchi, N., Bettella, F., Bolzon, P., Berger, F., Lingua, E., 2021. Biological Legacies and Rockfall: The Protective Effect of a Windthrown Forest. Forests 2021, Vol. 12, Page 1141 12, 1141. https://doi.org/10.3390/F12091141

Coutts, M.P., 1986. Components of tree stability in sitka spruce on peaty gley soil. Forestry 59, 173–197. https://doi.org/10.1093/forestry/59.2.173

Dorren, L.K.A., Berger, F., 2006. Stem breakage of trees and energy dissipation during rockfall impacts. Tree Physiol 26, 63–71. https://doi.org/10.1093/treephys/26.1.63

Dupuy, L., Fourcaud, T., Stokes, A., 2005. A Numerical Investigation into the Influence of Soil Type and Root Architecture on Tree Anchorage. Plant Soil 278, 119–134. https://doi.org/10.1007/s11104-005-7577-2

Forzieri, G., Girardello, M., Ceccherini, G., Spinoni, J., Feyen, L., Hartmann, H., Beck, P.S.A., Camps-Valls, G., Chirici, G., Mauri, A., Cescatti, A., 2021. Emergent vulnerability to climate-driven disturbances in European forests. Nat Commun 12. https://doi.org/10.1038/s41467-021-21399-7

Fourcaud, T., Ji, J.N., Zhang, Z.Q., Stokes, A., 2008. Understanding the impact of root morphology on overturning mechanisms: A modelling approach. Ann Bot 101, 1267–1280. https://doi.org/10.1093/aob/mcm245

Fourcaud, T., Lac, P., Stokes, A., Dupuy, L., 2007. Integrating Soil Mechanics and Real Root System. Journal of Forest Research 94, 1506–1514.

Gardiner, B.A., 2021. Wind damage to forests and trees: a review with an emphasis on planted and managed forests. Journal of Forest Research 26, 248–266. https://doi.org/10.1080/13416979.2021.1940665

Gardiner, B.A., Achim, A., Nicoll, B., Ruel, J.-C., 2019. Understanding the interactions between wind and trees: an introduction to the IUFRO 8th Wind and Trees Conference (2017). Forestry: An International Journal of Forest Research 92, 375–380. https://doi.org/10.1093/forestry/cpz044

Gardiner, B.A., Berry, P., Moulia, B., 2016. Review: Wind impacts on plant growth, mechanics and damage. Plant Science 245, 94–118. https://doi.org/10.1016/J.PLANTSCI.2016.01.006

Gardiner, B.A., Peltola, H., Kellomäki, S., 2000. Comparison of two models for predicting the critical wind speeds required to damage coniferous trees. Ecol Modell 129, 1–23. https://doi.org/10.1016/S0304-3800(00)00220-9

Gardiner, B.A., Quine, C.P., 2000. Management of forests to reduce the risk of abiotic damage - A review with particular reference to the effects of strong winds, in: Forest Ecology and Management. Elsevier, pp. 261–277. https://doi.org/10.1016/S0378-1127(00)00285-1

Garlato, A., 2016. I suoli del SIC-ZPS IT3230077 “Foresta del Cansiglio” (NE-Italia). Lavori Soc. Ven. Sc. Na 41, 115–120.

Hale, S.A., Gardiner, B.A., Peace, A., Nicoll, B., Taylor, P., Pizzirani, S., 2015. Comparison and validation of three versions of a forest wind risk model. Environmental Modelling and Software 68, 27–41. https://doi.org/10.1016/j.envsoft.2015.01.016

Irauschek, F., Rammer, W., Lexer, M.J., 2017. Evaluating multifunctionality and adaptive capacity of mountain forest management alternatives under climate change in the Eastern Alps. Eur J For Res 136, 1051–1069. https://doi.org/10.1007/s10342-017-1051-6

James, K.R., Dahle, G.A.G.A., Grabosky, J., Kane, B., Detter, A., 2014. Tree biomechanics literature review: Dynamics. Arboric Urban For 40, 1–15. https://doi.org/10.13140/RG.2.1.1089.1765

James, K.R., Hallam, C., Spencer, C., 2013. Measuring tilt of tree structural root zones under static and wind loading. Agric For Meteorol 168, 160–167. https://doi.org/10.1016/j.agrformet.2012.09.009

Jonsson, M.J., Foetzki, A., Kalberer, M., Lundström, T., Ammann, W., Stöckli, V., 2006. Root-soil rotation stiffness of Norway spruce (Picea abies (L.) Karst) growing on subalpine forested slopes. Plant Soil 285, 267–277. https://doi.org/10.1007/s11104-006-9013-7

Leverkus, A.B., Buma, B., Wagenbrenner, J., Burton, P.J., Lingua, E., Marzano, R., Thorn, S., 2021. Tamm review: Does salvage logging mitigate subsequent forest disturbances? For Ecol Manage 481, 118721. https://doi.org/10.1016/J.FORECO.2020.118721

Lingua, E., Bettella, F., Pividori, M., Marzano, R., Garbarino, M., Piras, M., Kobal, M., Berger, F., 2020. The Protective Role of Forests to Reduce Rockfall Risks and Impacts in the Alps Under a Climate Change Perspective, in: Climate Change Management. Springer, pp. 333–347. https://doi.org/10.1007/978-3-030-37425-9_18

Locatelli, T., Gardiner, B., Tarantola, S., Nicoll, B., Bonnefond, J.-M., Garrigou, D., Kamimura, K., Patenaude, G., 2016. Modelling wind risk to Eucalyptus globulus (Labill.) stands. For Ecol Manage 365, 159–173. https://doi.org/10.1016/j.foreco.2015.12.035

Locatelli, T., Tarantola, S., Gardiner, B.A., Patenaude, G., 2017. Variance-based sensitivity analysis of a wind risk model - Model behaviour and lessons for forest modelling. Environmental Modelling and Software 87, 84–109. https://doi.org/10.1016/j.envsoft.2016.10.010

Lundstrom, T., Jonas, T., Stockli, V., Ammann, W., 2007. Anchorage of mature conifers: resistive turning moment, root-soil plate geometry and root growth orientation. Tree Physiol 27, 1217–1227. https://doi.org/10.1093/treephys/27.9.1217

Lundström, T., Jonsson, M.J., Kalberer, M., 2007. The root-soil system of Norway spruce subjected to turning moment: Resistance as a function of rotation. Plant Soil 300, 35–49. https://doi.org/10.1007/s11104-007-9386-2

Marangon, D., Marchi, N., Lingua, E., 2022. Windthrown elements: a key point improving microsite amelioration and browsing protection to transplanted seedlings. For Ecol Manage 508, 120050. https://doi.org/10.1016/J.FORECO.2022.120050

Marchi, L., Grigolato, S., Mologni, O., Scotta, R., Cavalli, R., Montecchio, L., 2018. State of the Art on the Use of Trees as Supports and Anchors in Forest Operations. Forests 9, 467. https://doi.org/10.3390/f9080467

Marchi, L., Mologni, O., Grigolato, S., Cavalli, R., 2020. Evaluation on the Stability of Tree Used as Anchors in Cable Yarding Operations: A Preliminary Test Based on Low-Cost MEMS Sensors, Lecture Notes in Civil Engineering. https://doi.org/10.1007/978-3-030-39299-4_53

Marchi, L., Mologni, O., Trutalli, D., Scotta, R., Cavalli, R., Montecchio, L., Grigolato, S., 2019. Safety assessment of trees used as anchors in cable-supported tree harvesting based on experimental observations. Biosyst Eng 186, 71–82. https://doi.org/10.1016/j.biosystemseng.2019.06.022

Marchi, L., Trutalli, D., Mologni, O., Gallo, R., Roeser, D., Cavalli, R., Grigolato, S., 2021. Mechanical response of natural anchors in cable logging. International Journal of Forest Engineering 32, 29–42. https://doi.org/10.1080/14942119.2021.1826882

Mathworks, T., 2020. MATLAB 2020a.

Moore, J.R., 2000. Differences in maximum resistive bending moments of Pinus radiata trees grown on a range of soil types. For Ecol Manage 135, 63–71. https://doi.org/10.1016/S0378-1127(00)00298-X

Moos, C., Dorren, L., Stoffel, M., 2017. Quantifying the effect of forests on frequency and intensity of rockfalls. Natural Hazards and Earth System Sciences 17, 291–304. https://doi.org/10.5194/nhess-17-291-2017

Neild, S.A., Wood, C.J., 1999. Estimating stem and root-anchorage flexibility in trees. Tree Physiol 19, 141–151. https://doi.org/10.1093/treephys/19.3.141

Nicoll, B.C., Achim, A., Mochan, S., Gardiner, B.A., 2005. Does steep terrain influence tree stability? A field investigation. Canadian Journal of Forest Research 35, 2360–2367. https://doi.org/10.1139/x05-157

Nicoll, B.C., Gardiner, B.A., Rayner, B., Peace, A.J., 2006. Anchorage of coniferous trees in relation to species, soil type, and rooting depth. Canadian Journal of Forest Research 36, 1871–1883. https://doi.org/10.1139/x06-072

Olmedo, I., Bourrier, F., Bertrand, D., Berger, F., Limam, A., 2018. Dynamic analysis of wooden rockfall protection structures subjected to impact loading using a discrete element model. https://doi.org/10.1080/19648189.2018.1472042 24, 1430–1449.

Peltola, H.M., Kellomäki, S., Hassinen, A., Granander, M., 2000. Mechanical stability of Scots pine, Norway spruce and birch: An analysis of tree-pulling experiments in Finland. For Ecol Manage 135, 143–153. https://doi.org/10.1016/S0378-1127(00)00306-6

Peltola, H.M., Kellomäki, S., Väisänen, H., Ikonen, V.-P., 1999. A mechanistic model for assessing the risk of wind and snow damage to single trees and stands of Scots pine, Norway spruce, and birch. Canadian Journal of Forest Research 29, 647–661. https://doi.org/10.1139/cjfr-29-6-647

Sagi, P., Newson, T., Miller, C., Mitchell, S., 2019. Stem and root system response of a Norway spruce tree (Picea abies L.) under static loading. Forestry: An International Journal of Forest Research 92, 460–472. https://doi.org/10.1093/forestry/cpz042

Schönenberger, W., Noack, A., Thee, P., 2005. Effect of timber removal from windthrow slopes on the risk of snow avalanches and rockfall. For Ecol Manage 213, 197–208. https://doi.org/10.1016/j.foreco.2005.03.062

Schütz, J.P., Götz, M., Schmid, W., Mandallaz, D., 2006. Vulnerability of spruce (Picea abies) and beech (Fagus sylvatica) forest stands to storms and consequences for silviculture. Eur J For Res 125, 291–302. https://doi.org/10.1007/s10342-006-0111-0

Seidl, R., Rammer, W., Spies, T.A., 2014. Disturbance legacies increase the resilience of forest ecosystem structure, composition, and functioning. Ecological Applications 24, 2063–2077. https://doi.org/10.1890/14-0255.1

Seidl, R., Thom, D., Kautz, M., Martin-Benito, D., Peltoniemi, M., Vacchiano, G., Wild, J., Ascoli, D., Petr, M., Honkaniemi, J., Lexer, M.J., Trotsiuk, V., Mairota, P., Svoboda, M., Fabrika, M., Nagel, T.A., Reyer, C.P.O., 2017. Forest disturbances under climate change. Nat Clim Chang. https://doi.org/10.1038/nclimate3303

Sidle, R.C., 2005. Influence of forest harvesting activities on debris avalanches and flows. Debris-flow Hazards and Related Phenomena 387–409. https://doi.org/10.1007/3-540-27129-5_16

Stathers, R., Rollerson, T., Mitchell, S., 1994. Windthrow handbook for British Columbia forests. Research program working paper No. 9401.

Sun, H.L., Li, S.C., Xiong, W.L., Yang, Z.R., Cui, B.S., Tao-Yang, 2008. Influence of slope on root system anchorage of Pinus yunnanensis. Ecol Eng 32, 60–67. https://doi.org/10.1016/j.ecoleng.2007.09.002

Vergani, C., Chiaradia, E.A., Bischetti, G.B., 2012. Variability in the tensile resistance of roots in Alpine forest tree species. Ecol Eng 46, 43–56. https://doi.org/10.1016/j.ecoleng.2012.04.036

Wohlgemuth, T., Schwitter, R., Bebi, P., Sutter, F., Brang, P., 2017. Post-windthrow management in protection forests of the Swiss Alps. Eur J For Res 136, 1029–1040. https://doi.org/10.1007/s10342-017-1031-x

5. Evaluating wind vulnerability: a new parametrisation for the Alps

Based on **Costa M.**; Gardiner B.; Locatelli T.; Marchi L.; Marchi N.; Lingua, E.

Evaluating wind susceptibility in the Alps: a new wind risk parametrization

(Ready to be submitted)

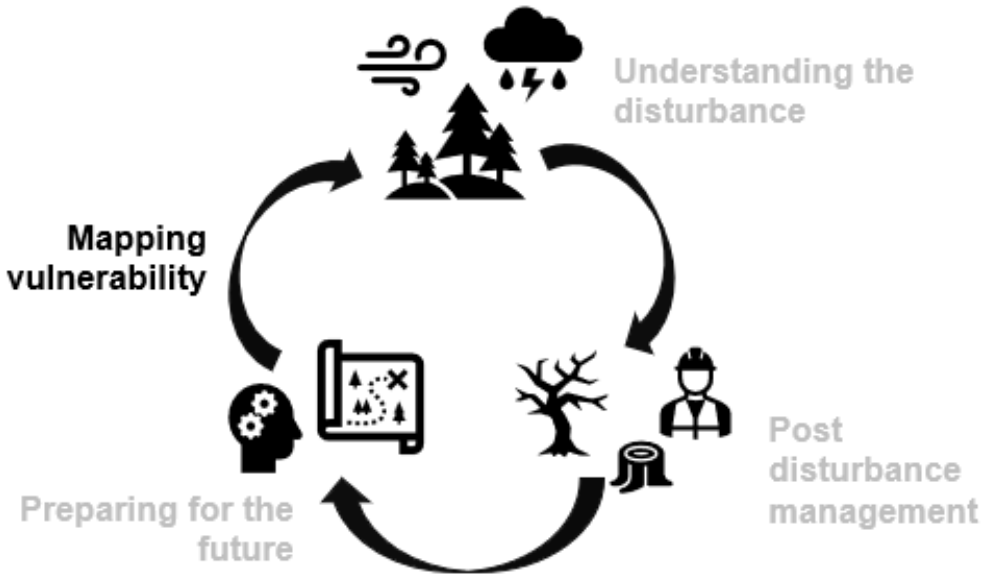

The risk of wind damage to European forests is expected to increase due to the changed climate. Research efforts in forestry have been focussing on the development of analytical and modelling tools to aid with the evaluation and the prediction of forests' vulnerability to wind damage, and ultimately to inform forest management decisions aimed at promoting wind-resistance in forest stands. Recent catastrophic wind damage to European forests has shown that wind damage risk applies also to montane forests. These are of particular importance for the various ecosystem services they provide, including protection from gravitational hazards and defence against soil erosion. At present, the available forest wind risk models have been tested and used mainly on production or planted forests in different countries, but never in the complexity of mountainous terrains. The aim of this chapter is to introduce a methodology for the validation of a new parametrisation of ForestGALES wind risk model, specifically designed for the alpine scenario. To do so, we used parameters from pulling tests in the field (previous chapter), and laboratory mechanical tests. We also developed a workflow that, starting from data obtained by LiDAR, aims at producing wind damage vulnerability maps. After validating this new parameterisation, we investigated the variations in wind vulnerability for a case study in the Italian Alps by introducing the Difference of Vulnerability (DoV) raster. Our main results show how the use of DoV can help in the identification of silvicultural practices to increase the stability of forest stands against wind damage.

5.1 Introduction

Natural disturbances such as windstorms, wildfires, droughts, ice storms, and insect outbreaks, are increasingly impacting European forests (Forzieri et al., 2021). Moreover, the frequency and the magnitude of these disturbances are expected to increase all over Europe due to the changed climate (Machado Nunes Romeiro et al., 2022; Seidl et al., 2017). Among the different types of disturbances, to date windstorms have had the highest impact on European forests in terms of damaged timber, and it is expected that their dominance over damage patterns will remain for the foreseeable future (Forzieri et al., 2021, 2020; Patacca et al., 2022; Seidl et al., 2014). Scientific research has focused on topics related to wind-tree interactions in different scenarios, starting from single tree level (Jackson et al., 2021; Kamimura et al., 2022; Marchi et al., 2022; Sagi et al., 2019) to stand-level (Kamimura et al., 2022; Seidl et al., 2014; Seidl and Blennow, 2012), with studies in both planted and natural forests (Gardiner, 2021). Different models have been developed through time to better investigate wind risk in forest management. Some models are mechanistic or semi mechanistic, such as HWind (Peltola et al., 1999), ForestGALES (Gardiner and Quine, 2000; Quine et al., 2021), and FOREOLE (Ancelin et al., 2004). Moreover, it is possible to find combinations of different models (Blennow and Olofsson, 2008). Some authors coupled mechanistic models with dynamic models to better observe the evolution of wind vulnerability in future scenarios (Ancelin et al., 2004; Rau et al., 2022), while others adopted machine learning techniques to improve the performance of mechanistic models (Hart et al., 2019). Models have also been used to observe and study the effect of different management strategies, for instance the different outcomes of thinning (Duperat et al., 2021; Kamimura et al., 2022; Seidl et al., 2014) or the effect of new openings, or gaps, on the stability of tree edges (Talkkari et al., 2000; Zeng et al., 2004). However, there is still a gap in the literature about testing and applying these models in a mountainous scenario. In this context, it is known that wind disturbances are an actual problem in the Alps (Bebi et al., 2017) and that windstorms can heavily affect the multifunctionality of forests and compromise the ecosystem services that these provide (Fleischer et al., 2017). A clear example is the protective role of forest stands against natural hazards such as rockfall or avalanches (Brang et al., 2006): even if a wind-damaged stand can still provide protection against gravitative hazards (Costa et al., 2021; Schönenberger et al., 2005; Wohlgemuth et al., 2017) the primary aim of forest managers should be to improve the resistance, rather than the resilience, of multifunctional forests against wind damage. The aims of the present work are: (i) to introduce a new parametrisation for the ForestGALES model adapted to the mountain/Alpine scenario; (ii) to provide a common methodology to improve the performance of the ForestGALES model when used in new scenarios, and (iii) to produce a wind vulnerability map, a new tool for the alpine context. Towards (i), our approach considers some of the main features of the mountain environments, such as slope influence on tree stability, and it

focusses on trees with a relatively large Diameter at Breast Height (DBH) (Marchi et al., 2022). For (ii), we present a methodology for performing and validating this novel parametrisation, based on both field activities (e.g., tree pulling tests), laboratory tests of mechanical properties of wood, and data analysis, to improve the overall performance of the model. Lastly, the development of (iii) is intended to help identify the best strategies for enhancing forest management against wind damage.

5.2 Materials and methods

Wind risk model – fgr

Wind-tree interactions are widely studied at many scales, from the single tree level up to the landscape level. This wide breadth of research has led to the development of many predictive models to assess the vulnerability of forest stands to damaging wind forcing. For this work we adopted the hybrid empirical/mechanistic risk model ForestGALES (Hale et al., 2015) since it is widely used in research and operationally (e.g., in the UK and several other European countries), and it has been parametrized for different tree species and different soil types. ForestGALES was initially developed in the United Kingdom as a decision support tool to assess the vulnerability of planted forest stands to windstorm damage (Hale et al., 2015; Kamimura et al., 2016). This process-based wind risk model has since been improved and used in other contexts, both European and non-European (Anyomi et al., 2016; Duperat et al., 2021; Elie and Ruel, 2005; Locatelli et al., 2016). The initial ForestGALES model was developed to operate at the stand level, but it has since been expanded to include a methodology that allows for vulnerability and risk calculations for individual trees within a stand (Hale et al., 2012; Locatelli et al., 2022). The main inputs required to run the model to calculate the wind vulnerability and risk are listed in order of importance (defined as the sensitivity of model outputs to individual inputs and inputs combinations, Locatelli et al., 2017) in Table 9 together with the main outputs.

Table 9. Main inputs and outputs of the ForestGALES (fgr) model. The main inputs are listed in order of importance (Locatelli et al., 2017).

MAIN INPUTS	MAIN OUTPUTS
Tree data (DBH, height, tree density)	Minimum Critical Wind Speed (CWS)
Soil type and rooting depth	Critical Wind Speed for overturning
Species morphology parameters	Critical Wind Speed for breakage
Wood characteristics (MOE, MOR, density of green wood)	

Main inputs include tree characteristics, such as DBH and tree height, stand properties such as mean tree spacing (or stems per hectare), soil type and rooting depth, and species-specific parameters related to tree morphology: some of them are crown depth, crown width, canopy density, etc. For further information see Locatelli et al. (2022). Some wood parameters that are characteristic of the different species are needed: the Modulus of Elasticity (MOE), the Modulus of Rupture (MOR), and the density of green wood. The main output of the model is the minimum Critical Wind Speed (CWS), i.e. the minimum wind speed that is predicted to cause damage to the forest stand. This minimum CWS is the lowest of the CWS values for overturning and for stem breakage. Lastly, if data about the mean wind regime for the area of interest are available, the model can calculate the risk of damage (for both overturning and stem breakage). The risks of overturning and stem breakage are expressed as the annual probabilities of exceeding the respective CWS and are calculated from a Weibull distribution of mean wind speeds linked to a Fisher-Tippett Type I extreme value distribution (Locatelli et al., 2022; Quine, 2000). Recently, ForestGALES has been updated and the latest version developed and released in the R framework (package "*fgr*"), to be easily applicable to different scenarios and to allow users to modify parameters according to their needs (www.forestresearch.gov.uk/tools-and-resources/fthr/forestgales/fgr-the-forestgales-r-package/). This new version of the model can calculate the Critical Wind Speed (CWS) with two different methods: the Roughness (ROU, for stand-level calculations) method and the Turning Moment Coefficient (TMC, for individual trees within a stand) method. The main formulas that are used to calculate the CWS with the two methods are reported below. For the ROU method the formulas for CWS breakage and CWS overturning are shown in Equation 8 and Equation 9 respectively:

$$ROU\ CWS_{breakage} = \frac{1}{D}\sqrt{\frac{\pi * MOR * dbh^3 * f_{knot}}{32\rho f_{EdgeGapGust}(d-1.3) * DLF}} * \gamma \quad (8)$$

$$ROU\ CWS_{overturning} = \frac{1}{D}\sqrt{\frac{C_{reg} * SW}{\rho d * f_{EdgeGapGust} * DLF}} * \gamma \quad (9)$$

Where π: pi mathematical constant; *D*: average spacing between trees; *MOR*: modulus of rupture (MPa); *dbh*: diameter at breast height; f_{knot}: a species-specific factor that accounts for wood knots; *ρ*: air density (kg/m^3); $f_{EdgeGapGust}$: an improvement of the gust factor including edge and gap size effects (Quine et al., 2021); *DLF*: deflection loading factor (Gardiner 1992); *d*: zero-plane displacement; *γ*: gamma function, the ratio between wind speed at canopy top and the friction velocity (i.e., the square root of the ratio of shear stress on the canopy surface and the air density) that incorporates the effect of the aerodynamic roughness (Raupach, 1992; Raupach et al., 1994); C_{reg}: overturning coefficient, a species-specific empirical measure of root anchorage calculated for different soil and rooting depth

combinations (Nm/kg); *SW*: stem weight (kg). For the TMC method the formulas for CWS breakage and CWS overturning are shown in Equation 10 and Equation 11 respectively:

$$TMC\ CWS_{breakage} = \sqrt{\frac{\pi * MOR * d_{(0)}^{3} * f_{knot}}{32 T_C * TMC_{ratio} * f_{EdgeGap} * DLF}} \quad (10)$$

$$TMC\ CWS_{overturning} = \sqrt{\frac{C_{reg} * SW}{T_C * TMC_{ratio} * f_{EdgeGap} * DLF}} \quad (11)$$

Using $d_{(0)}$ according to Quine et al. (2021) to ensure that the surface stress is the same as at DBH and where T_C: turning moment coefficient (Quine et al., 2021); TMC_{ratio}: turning moment ratio (Quine et al., 2021); $f_{EdgeGap}$: the combined effect of tree position relative to the upwind stand edge and the upwind gap size. For both methods the final value of minimum CWS is the lower between the CWS for breakage and CWS for overturning. Further information on these calculations is available in Quine et al. (2021). For an in-depth description of the fgr model, see Locatelli et al. (2022).

The original ForestGALES tree-pulling database used to derive the empirical coefficients of tree anchorage is limited to relatively flat areas (slopes usually ≤ 20°) and small-to-medium sized trees (DBH ≤ 30 cm) (Nicoll et al., 2006). On the contrary, the alpine forests that have been affected by recent storms were often composed of trees with larger diameters, and most of the damaged stands were in sloped terrains. In this context, recent tree pulling experiments were able to identify the different coefficients of overturning between trees in alpine environments both on a slope or on flat terrain (Marchi et al., 2022). The aim of the present work is to validate these new parameters so that the model can be used with a higher accuracy in alpine environments, and to provide an appropriate modelling workflow that can be applied in other mountainous contexts.

We applied the new parameters to large diameter trees and to trees growing on steep terrain (slope > 20°), as summarised in Table 10. To represent the difference observed in Marchi et al. (2022) for plants with large DBH between flat and sloped terrains (i.e., an approximately +50% higher overturning coefficient for trees growing on slopes), a correction factor was applied to the default parameters (i.e., those calculated for small diameter trees growing in flat terrain) to describe anchorage on steep terrain (Marchi et al., 2022).

Table 10. Tree anchorage parameters according to tree dimensions and steepness of the growing site.

Condition	Parameters	C_{reg} value
Norway spruce, DBH < 40cm	*fgr* default parameters	126.0
Norway spruce, DBH <40 cm + steep terrain	*fgr* default parameters adjusted	187.7
Norway spruce, DBH > 40 cm	New parameters	62.0*
Norway spruce, DBH > 40 cm + steep terrain	New parameters	92.4*

* Parameters derived from pulling tests (Marchi et al. 2022).

The parameters in Table 10 were added to a customised Norway spruce (*Picea abies* (L.) Karst.) parametrisation in *fgr*. Because of the particular tree pulling protocol used in Marchi et al. (2022) to derive their Creg values (i.e., the additional moment contribution of the overhanging crown and stem was not calculated), in our new parametrisation for trees with DBH > 40 cm we set the Deflecting Loading Factor (DLF) is set equal to 1. This is because the influence of the overhanging crown and stem is already implicitly incorporated in the Marchi et al. (2022) C_{reg} values, and therefore we do not want to add their contribution again.

MOE and MOR of Alpine Norway spruce

We adopted the protocol applied by Locatelli et al. (2016) to add custom values of the Modulus of Elasticity (MOE) and the Modulus of Rupture (MOR) to our Norway spruce parametrisation. MOE and MOR were derived experimentally by testing wood samples collected from Norway spruce trees grown in the Alps. We extracted 1-metre-long sample logs from five different trees that had been pulled to failure in the work of Marchi et al. (2021, 2022). The green logs were cut lengthwise in boards, transported to the testing lab, conditioned to reach 12% Moisture Content (MC) before wood clears were extracted from each log; the dimensions of the wood clears were 40cm x 2cm x 2cm. During the cutting process, we took note of the relative distance of each sample from the pith of the tree that it was extracted from. We obtained 145 samples, these samples were tested using a universal testing machine equipped with a bench to perform 3-point bending tests to obtain values of MOE and MOR; we also measured the MC % of the samples during the test. These values were used to extrapolate the new values of MOE and MOR for greenwood, as required for new *fgr* parametrisations.. As done in Locatelli et al. (2016) we followed the method of Unterwieser and Schickhofer (2011) to calculate the MOE and MOR of green wood, for which formulas are shown in Equation 12 and Equation 13:

$$MOE_{green\ wood} = \frac{MOE_{MC\%_{test}}}{1 - 0.00825 * (MC\%_{test} - FSP)} \quad (12)$$

$$MOR_{green\ wood} = MOR_{MC\%_{test}} - \left(MOR_{MC\%_{test}} * \frac{FSP - MC\%_{test}}{100} \right) \quad (13)$$

where FSP is the Fibre Saturation Point that corresponds approximately to 28% (Unterwieser and Schifofer 2011). The values that were obtained through this procedure were used for the new *fgr* parametrisation customized for Norway spruce grown in an alpine environment. These values of MOE and MOR are reported as preliminary results in Table 3.

Table 11. New values of MOE and MOR for Norway spruce grown on the Italian Alps. Values were obtained by mechanical testing of 145 samples.

Alpine Norway spruce MOE (MPa)	1.46e10
Alpine Norway spruce MOR (MPa)	7.99e07

Modelling framework and vulnerability mapping

To map vulnerability to wind damage, we selected to map the minimum CWS output. By default, the model returns the CWS output calculated at ten metres above the ground; this default can be modified if needed and we chose to run the model also to return the CWS output at five meters above the ground. The workflow used in our work is represented in Figure 28. Starting from Light Detection and Ranging (LiDAR) data, we produced a Canopy Height Model (CHM) and a Digital Terrain Model (DTM) of the Agordino valley in the Italian Alps, the valley where the study area is located. Both CHM and DTM have 0.5 meters horizontal resolution. By applying the FINT V1 software (ecorisq.com) to the CHM, we derived the position of each tree together with its DBH and height (H) using formulas based on previously collected field data. The FINT V1 software uses an inverted hypsometric curve to derive diameter values from heights. We used a hypsometric curve calculated from data gathered from approximately 90 sample plots, where more than 1500 Norway spruce trees had been measured; all these sample plots were located in the Agordino valley within 20 km range from the study area. We derived slope data for the position of each tree from the DTM. We created an input 'Tree file' for the R programming language (R Core Team, 2022) with all the data required to execute the model, including the new parameters (overturning coefficient, MOE and MOR) which were assigned to each tree on the basis of their size and location. We selected the minimum CWS from the list of the model outputs and linked it to the spatial information contained in the Tree File input to produce a map of wind damage vulnerability.

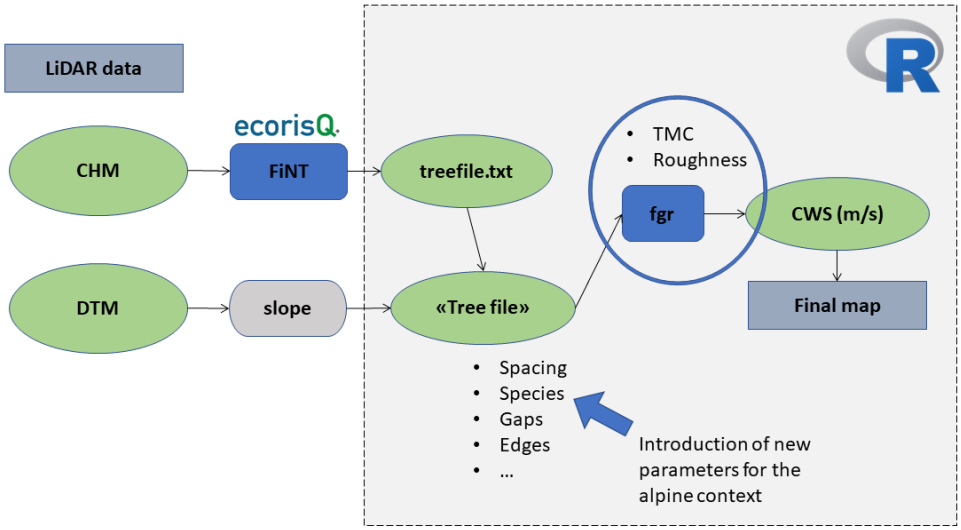

Figure 28. Workflow for wind vulnerability mapping. Starting from LiDAR-derived spatial data, a CHM and a DTM, and a tree file were created. The fgr model was run with the tree file as an input. The CWS output was used to produce a map of wind vulnerability.

Case study: the storm Vaia

Storm Vaia was an intense cyclone that generated in the Mediterranean Sea and hit the northeast regions of Italy between 27 and 30 October 2018, causing widespread damage due to floods and landslides (Davolio et al., 2020). Vaia hit the forests of the Italian Alps with strong winds causing catastrophic damage to more than 40'000 ha of forests and the loss of at least 10 million m^3 of timber (Piragnolo et al., 2021; Udali et al., 2021). The study area selected for the validation of the *fgr* model is the municipality of Rocca Pietore, situated in the eastern Dolomites, in the Italian Alps (Figure 29). The total area of the municipality is 7400 ha, 3700 ha of which are classified as forest area. Storm Vaia affected with high severity 730 ha, i.e., almost 20% of the forested area of the municipality. These data were elaborated starting from an acquisition from the Italian Ministry of the Environment, Land and Sea (MATTM). Municipality forests are mainly composed of Norway spruce (> 40% of area cover), and larch (*Larix decidua* Mill.) (~30% of area cover), on north-exposed slopes and close to the treeline. At lower altitudes It is possible to find beech (*Fagus sylvatica* L.) (~ 5% of area cover) and other broadleaves (~25% of area cover). The windthrown areas were mainly in Norway spruce stands.

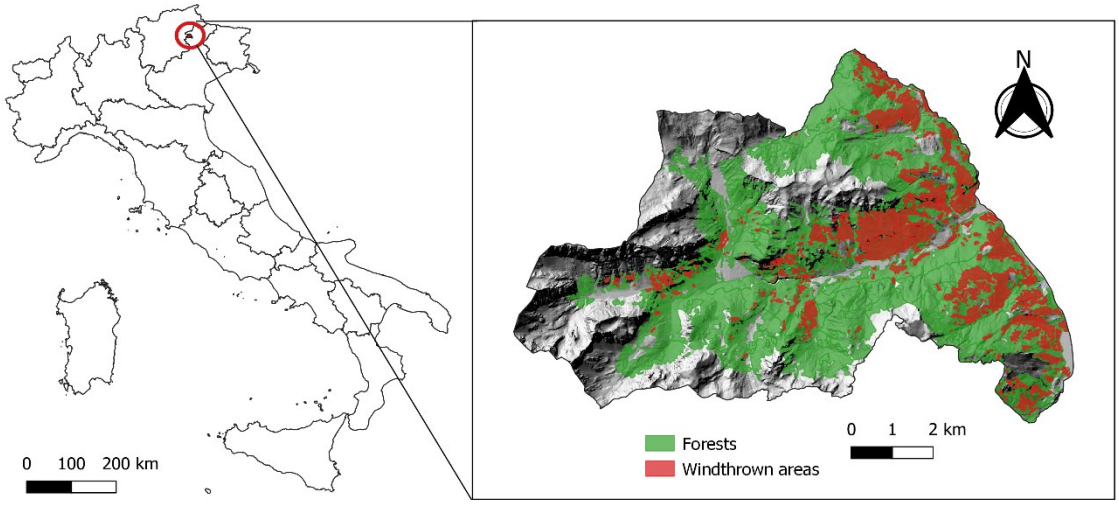

Figure 29. Study area outline. Municipality of Rocca Pietore in the Italian Alps, province of Belluno. The figure also shows the forest area of the municipality and the area damaged by storm Vaia in October 2018

The lithological types mainly present in the area are portions of limestones and dolomites. Some volcanic sandstones and breccias in the area at higher altitudes can be found, as well as sandstones and conglomerates in the lower valleys. Finally, alongside the main stream, there is presence of gravels, sands, silts and clays. This study area was selected because the forests are growing both on steep and flat terrain to fully test the capability of the new fgr parametrisation.

In the municipality there are two weather stations recording wind data, one on the Marmolada massif (this instrument was destroyed during the windstorm event), and one close to the village of Caprile. This weather station registered the highest wind speeds during the evening of the 29th of October, with a maximum wind gust equal to 31.6 m/s at 21.20 (data from the Veneto Regional Agency for the Environmental Prevention and Protection, https://wwwold.arpa.veneto.it).

Pre storm scenario

The first scenario designed for model validation is a pre-storm scenario. The processing of the 'Tree file' was based on a CHM and DTM obtained from LiDAR data acquired in 2015, as these were the most recent available data prior to the year of the storm for the Rocca Pietore municipality.

The model was run 4 times using the new parametrisation:

- using the TMC method, with the output CWS set at 10 m above the zero-plane displacement height;
- using the TMC method, with the output CWS set at 5 m above the zero-plane displacement height;

- using the ROU method, with the output CWS set at 10 m above from the zero-plane displacement height;
- using the ROU method, with the output CWS set at 5 m above from the zero-plane displacement height.

The output CWS of each scenario were used to create a wind vulnerability map that was used for the validation of the new parametrisation of the *fgr* model developed in this study against recorded storm Vaia damage.

Post-storm scenario

A second, post-storm scenario was run with fgr after the model had been validated. This scenario seeks to represent the post-storm vulnerability to future wind damage. The 'Tree file' for this scenario was obtained using the most recent post-Vaia available data, i.e., LiDAR data from a flight that occurred in July 2019.

For this scenario we also considered the influence of newly created gaps within the forest caused by storm Vaia, and therefore the lower stability of brown edges. In the TMC method, fgr can simulate the influence of new gaps by simply modifying the parameter 'distance from the edge' of each tree. In order to assign this parameter to each tree we created a raster in which each cell has the value of the distance from the new, closer edge, and we assigned this value to the trees that were located within that cell. In this case, the model was run only with the TMC method. TMC method was introduced to better evaluate single trees vulnerability to wind, so we decided to use it because we found it more suitable than the roughness method for assessing the influence of new edges on the stability of forest stands damaged by the 2018 storm (Hale et al., 2015, 2012).

The outputs of the model were also used to generate a new raster to detect changes in vulnerability to wind damage in the surviving stands between pre- and post-storm conditions. We called this raster 'Difference of Vulnerability' (DoV). It was obtained by subtracting pre-storm CWS from post-storm CWS, as shown in Equation 14.

$$DoV = CWS\ (2019) - CWS\ (2015) \tag{14}$$

The changes in vulnerability shown in the DoV raster can either indicate higher vulnerability (where CWS values decrease over time, from 2015 to 2019) or lower vulnerability (where CWS values increase over this time period).

Modelled damage

The validation of the new fgr parametrisation developed in this study was performed through the spatial identification of forest areas where the model calculated wind damage to have occurred because of storm Vaia. That is, the areas where the mean wind speed during storm Vaia exceed the CWS calculated by fgr. However, for our case study area, wind data during the storm were only available from a few weather stations which are also not homogeneously distributed within the municipality area. To overcome this issue, we adopted two different approaches for mapping wind speed differences between the storm and the modelled CWS: WAsP model simulations and TOPEX indices.

The WAsP method

The Wind Atlas Analysis and Application Program, hereafter WAsP (Mortensen et al., 2004) is an airflow model that can extrapolate wind speeds and their spatialization knowing at least two locations (where wind speed was measured) and the surrounding topography (through a DTM). The model considers the influence of local topography, changes in aerodynamic roughness across the landscape, and the presence of obstacles. The model works on the assumption that all the considered locations are within the same weather system, i.e., the same wind regime. For this study, the wind data used as input for WAsP were based on 5-minutes average wind speed data collected at the peak of storm Vaia from the weather stations of Caprile (1005 m a.s.l.), Arabba (1642 m a.s.l.) and Monti Alti di Ornella (2227 m a.s.l.), all located within a 10 km radius from the case study area. The DTM was derived from LiDAR data, as used for the pre-storm scenario. The output of the WAsP model is a raster with wind speed spatialized on the overall study area. For the purpose of validating our fgr parametrisation, the predicted damaged areas were identified as those where WAsP values of wind speed were higher than the CWS calculated for the pre-storm scenario. After calculating the wind speeds with the WAsP model, we created a new raster where each cell contained only one of two values: damage and no damage (Equations 15 and 16).

$$WAsP\ wind\ speed > Critical\ Wind\ Speed = damage \quad (15)$$

$$WAsP\ wind\ speed < Critical\ Wind\ Speed = no\ damage \quad (16)$$

The values of wind speed for each weather station that were used for modelling with WAsP are reported in Table 12.

Table 12. Average 5 minutes wind speed measured at 5 m, during the peak of storm Vaia, for each weather station. Distance is referred from the centre of the municipality of Rocca Pietore, the case study area.

Weather station	Wind speed (m/s) at 5m	Distance (km)	Altitude (m asl)
Arabba	8.8	9	1642
Caprile	9	3	1005
Monti Alti di Ornella	16.8	6	2227
Passo Pordoi	12.4	10	2239

The TOPEX index method

The TOPographic EXposure index, hereafter TOPEX (Chapman, 2000) is a parameter that describes wind exposure using only a quantitative assessment of the horizontal inclination of the terrain over a fixed distance from each calculation point. Despite being simply based on topography this index proves to be effective and a good approximation of exposure in difficult terrains such as in Alpine environments. The biggest advantage of TOPEX is that it is easy to compute since only a DTM is needed. To compute the TOPEX index we used a DTM and the R package *Horizon Search Algorithm* (https://rdrr.io/cran/horizon). The two main variables for computing the TOPEX index are the distance from the horizon and the direction of the wind. Usually, TOPEX is calculated combining all eight cardinal directions, but we also computed the indices for specific combinations (e.g., S+SE+E) to investigate whether focussing on the main direction of the wind during storm Vaia (i.e., south + south/east + east) would improve the performance of the *fgr* model. After calculating the TOPEX index, we applied a simple ratio to derive the probability that the CWS calculated with fgr were exceeded during the storm (Equation 17). We applied a simple ratio based on the assumption that the wind speed reached at a specific point (the weather station) with its associated TOPEX value would be higher for higher values of TOPEX. This simplification seeks to help identify correctly the damage areas modelled with fgr in a complex terrain where the precision of other models (e.g., WAsP) is uncertain (Suárez et al., 1999). As done for the WAsP method, once the wind speeds were estimated for each cell of the raster, we created a new binary raster with only one of two values: damage and no damage (Equations 19 and 20). The weather stations reported the 5-minutes average wind speed every 5 minutes at a height of 5 m from the ground. Therefore, to compare these values with the modelled CWS's, the output of the model was coherently set at 5m above the ground instead of the default value (10m).

$$Estimated\ wind\ speed = \left(\frac{(1+topex\ weather\ station) * wind\ speed\ weather\ station}{1+topex}\right) \quad (17)$$

This formula was applied to each raster cell and for each weather station, and the final raster was obtained calculating the average of the results obtained, see Equation 18.

$$Estimated\ wind\ speed_{total} = \frac{\sum estimated\ wind\ speed\ derived\ for\ each\ weather\ station}{n\ of\ meteostations} \quad (18)$$

$$Estimated\ wind\ speed\ total > Critical\ Wind\ Speed\ at\ 5\ m = damage \quad (19)$$

$$Estimated\ wind\ speed\ total < Critical\ Wind\ Speed\ at\ 5m = no\ damage \quad (20)$$

We applied the TOPEX index approach modifying the wind direction data to observe changes in the final performance of the model. The different TOPEX that we used are reported in the list below:

- TOPEX from all cardinal directions
- TOPEX from South (S)
- TOPEX from South + Southeast + East (S + SE + E)
- TOPEX from West + Southwest + South + Southeast + East (W + SW + S + SE + E)

The performance of the model was tested for all the indices with different distances of each raster cell from the horizon: 1000 m, 500 m, 250 m, and 100 m.

Validation process

To validate the model, we followed a similar process to that of Hale et al. (2015). We started from two rasters: the observed damage, obtained using the official layer provided by the Italian Ministry of the Environment, Land and Sea (MATTM) and the modelled damage. The latter was obtained from either one of the two different approaches detailed in the previous section. We used these rasters to compute a confusion matrix, or contingency table (Bennett et al., 2013). This table counts (i) the number of cases in which the model correctly predicts damage or no damage (*hits* and *correct negatives*), and (ii) the number of cases in which the model failed its predictions (*false alarms* and *misses*). The structure of the matrix is reported in Table 13.

Table 13. Confusion matrix structure, based on Bennett et al. 2013

	Modelled damage	**Modelled no damage**
Observed damage	Hits	Misses
Observed no damage	False alarms	Correct negatives

We varied the model probability threshold (the CWS) from 0 to 100% by increments of 10% and for each variation we computed a new confusion matrix, similarly to the approach in Hale et al. (2015).

For each method (WAsP vs TOPEX) we used each incremental confusion matrix to compute a performance index for each scenario: the Success Index (SI) is an index that evaluates the performance of a model by assessing its effectiveness in correctly identifying occurrence or non-occurrence of events (Bennett et al., 2013). The same index was used in previous works for the evaluation of the performance of ForestGALES and for calculating the Profit Score (PS) for the model (Hale et al., 2015).

The formula for the calculation of the SI and of the PS are based on the results of the confusion matrix (Equation 21 and Equation 22):

$$Success\ Index = \frac{1}{2}(Sensitivity + Specificity) = \frac{1}{2}\left(\frac{hits}{hits+misses} + \frac{correct\ negatives}{observed\ no}\right) \quad (21)$$

$$Profit\ Score = Success\ Index * 2 \quad (22)$$

The perfect value of the Success Index is 1, i.e., the closer the SI value is to 1 the better is the performance of the model. We decided to consider the model validated with the new parameters if the SI value was over 0.7, a threshold similar to that adopted in the Area Under the Curve (AUC) value approach (Hale et al., 2015). For each scenario we observed the values of SI for each 10% increment, observing if the model could be validated and with which correction. Usually, the higher value of SI is reached when sensitivity is equal to specificity (Bennett et al., 2013). This point is defined as cutpoint (Hale et al., 2015). The validation process is represented in Figure 30.

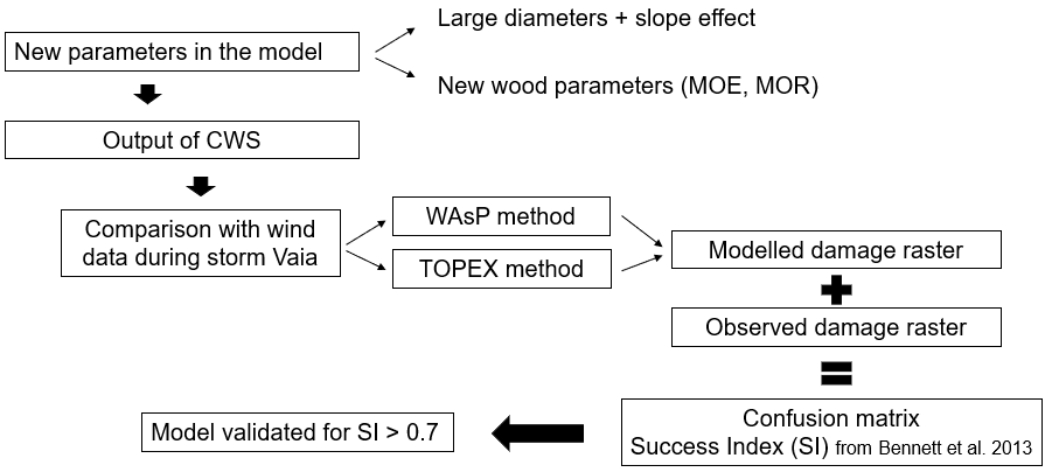

Figure 30. Workflow for the validation of the fgr *model with the new parameters*

All statistical elaborations and model validation were done within Rstudio (www.rstudio.com) and the R packages of the tidyverse (www.tidyverse.org/).

5.3 Results

Pre storm scenario and model validation

The workflow based on the new fgr parametrisation was entirely developed in the R environment to produce a vulnerability map (Figure 4). The map is based on the CHM that was obtained from LiDAR data from 2015 and it shows the different CWS in the Rocca Pietore (BL) municipality. Figure 31 reports the results of the *fgr* model run in TMC mode; the CWS are divided into vulnerability classes where red corresponds to the highest vulnerability, (i.e., lowest values of CWSs), and blue to the lowest vulnerability, (i.e., higher values of CWSs).

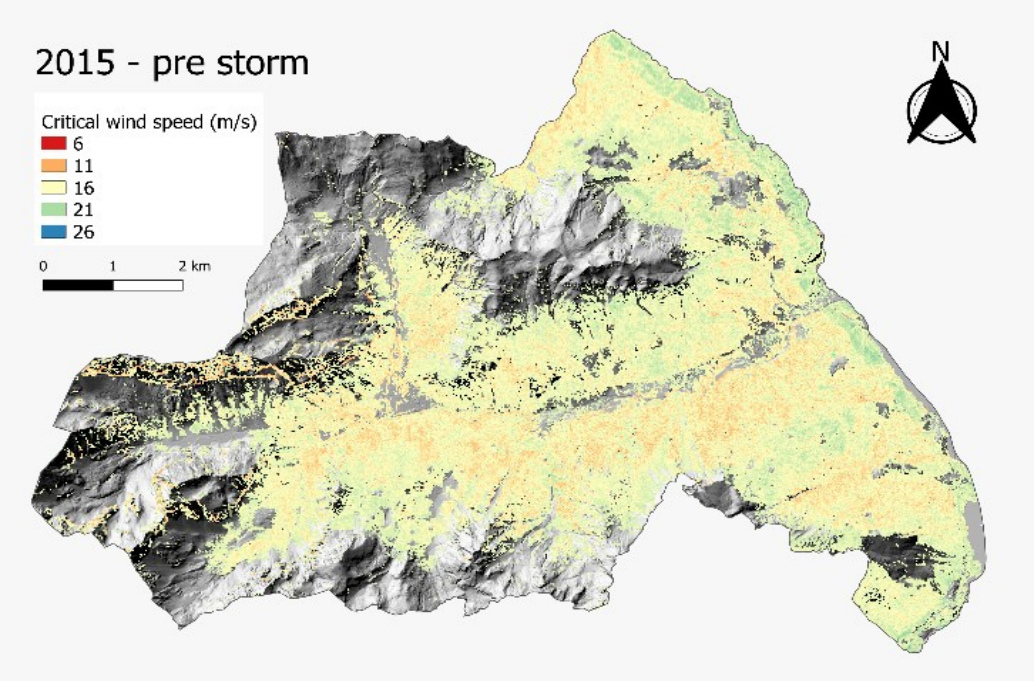

Figure 31. Wind vulnerability map for Rocca Pietore municipality, Italian Alps. Vulnerability calculated with the fgr model using the TMC method. Input data derived from a LiDAR flight from 2015.

The average CWS calculated for the 2015 pre-storm scenario is ~17 m/s, the lowest value is 13 m/s, and the highest value is ~21 m/s. This vulnerability map was used as the base layer for model validation, to compute the damage and no damage raster on the basis of the storm Vaia wind speeds calculated with the WAsP model and the TOPEX index approach. Table 14 summarises the results of the validation of fgr with the new parametrisation as performed with WAsP. The Success Index values from the validation with WAsP are 0.53 for the TMC method and 0.51 for the ROU method, i.e., both below the SI threshold of 0.7 that was set for the validation.

Table 14. Results of model validation with WAsP model

fgr mode	SI no multipliers	SI at cutpoint	PS at cutpoint	Multiplier at cutpoint
TMC	0.53	0.57	1.14	0.5
ROU	0.51	0.55	1.10	0.5

For TOPEX, in this section we only report the significant results for the main wind directions during storm Vaia, i.e., S + SE + E. The values of TOPEX and wind speed that were used to compute the modelled damage raster are reported in Table 15.

Table 15. Meteo stations and data that were used to compute the estimated wind speeds for model validation. Wind speeds represent the peak of storm Vaia. Only the S + SE + E TOPEX direction is shown here.

Weather station	TOPEX	Wind speed (m/s) at 5 m
Arabba	0	8.8
Caprile	18	9
Monti Alti di Ornella	18.4	16.8
Passo Pordoi	12.1	12.4

Table 16 shows the results of the validation of fgr with our new parametrisation when compared with TOPEX-adjusted wind speed maps. The best results were achieved with a TOPEX distance of 1000m and TOPEX direction S + SE + E, which had a SI at cutpoint equal to 0.74. The relative Receiver Operating Characteristic (ROC) curve is shown in Figure 32. Only the results of TMC simulations are shown in Table 8.

Table 16. Results of model validation. SI is success index; PS is Profit Score. The ROC curve for the highlighted line is shown in Figure 5. Only the S + SE + E TOPEX direction is shown here.

fgr mode	Topex distance	SI no multipliers	SI at cutpoint	PS at cutpoint	Multiplier at cutpoint
TMC 5 m	1000	0.68	0.74	1.46	0.5
TMC 5 m	500	0.68	0.73	1.46	0.5
TMC 5 m	250	0.67	0.72	1.44	0.5
TMC 5 m	100	0.67	0.71	1.42	0.5

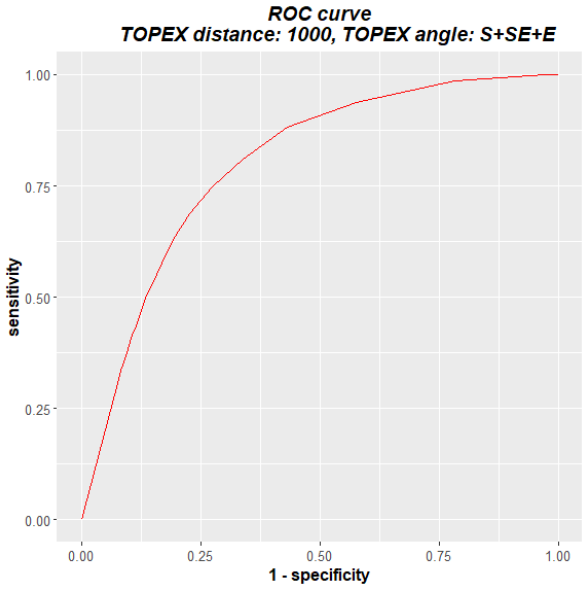

Figure 32. ROC curve for fgr simulation, TMC method with an output at 5m above the ground. TOPEX distance = 1000m and TOPEX angle: S+SE+E.

Post storm scenario and DoV

The workflow adopted for the pre storm scenario was repeated using data derived from a LiDAR flight from 2019. This generated a vulnerability map for the 2019 scenario, i.e., a post storm scenario, for the Rocca Pietore municipality. Figure 33 shows the results of our new parametrisation of the *fgr* model run in the TMC mode. As for Figure 31, CWS are divided into vulnerability classes where red indicates the highest vulnerability (i.e., lowest values of CWSs), and blue the lowest vulnerability (i.e., higher values of CWSs).

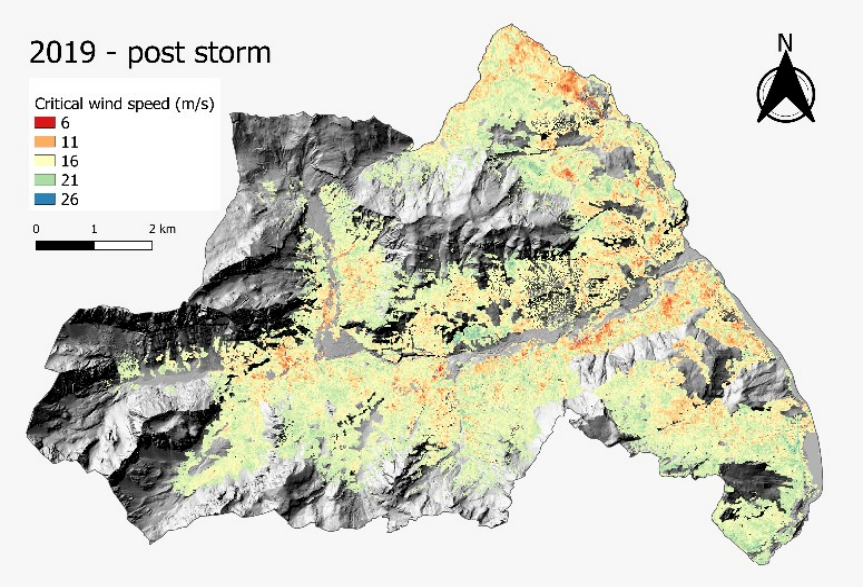

Figure 33. Wind vulnerability map for Rocca Pietore municipality, Italian Alps. Vulnerability calculated with the fgr model using the TMC method. Input data derived from a LiDAR flight from 2019.

The average CWS calculated for the post-storm scenario is ~17 m/s, the lowest value is 9 m/s, the highest value is >21 m/s. The areas with the lowest CWS values are situated close to Vaia-damaged areas, where brown edges have been created by the storm, and close to the bottom of the main valleys. The areas with the highest CWS values are situated at the higher altitudes. We combined the pre-and post-storm vulnerability maps shown in Figures 31 and 33, to produce the DoV map shown in Figure 34.

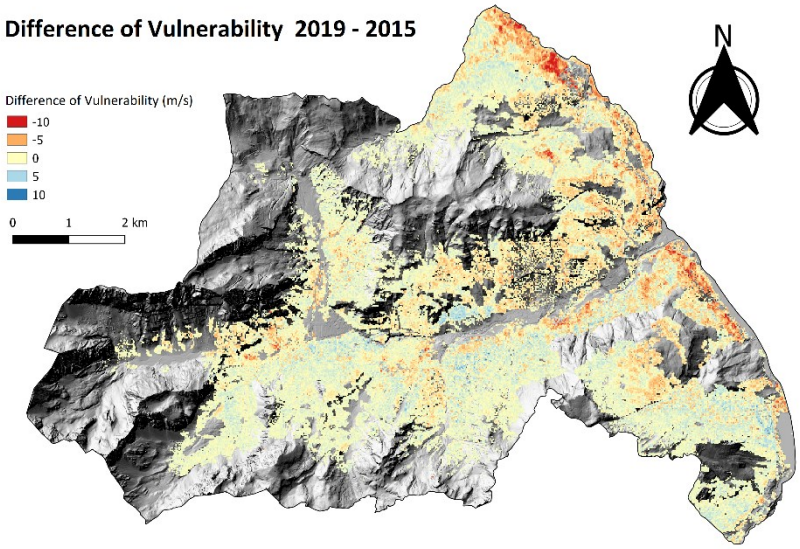

Figure 34. DoV raster of Rocca Pietore municipality. Red areas indicate negative CWS differences, indicating higher vulnerability to wind damage. Blue areas have higher values of CWS difference indicating lower vulnerability to wind damage.

The DoV map shows areas where the CWS have decreased by up to 10 m/s (in red), i.e., areas where the vulnerability to wind damage has increased significantly. In other areas however the post-storm CWS have increased up to 10 m/s, i.e., in these areas the vulnerability has decreased significantly. The areas where the CWS decreased more consistently are those close to Vaia-damaged areas at the bottom of the main valleys, while areas with a major increase of CWS are located at higher altitudes.

5.4 Discussion

Pre storm and model validation

Our LiDAR-centred workflow produced interesting and useful results. Airborne LiDAR data have already been used with the ForestGALES model (Suarez et al., 2008) and other wind risk models (Gopalakrishnan et al., 2020). The suitability and advantages of LiDAR-derived datasets for wind risk modelling had already been recognised and suggested especially for complex forests such montane forests (Hale et al., 2015). The high accuracy of the spatialization of forest data, achieved through a CHM with a high resolution, and the use of an algorithm to extract data (height and DBH) for single trees, can significantly improve the quality of input data for the *fgr* model. The resolution of the

output, i.e. the CWS spatialisation, can likewise be high, e.g., in our case the final raster has a resolution of 20x20m. We found of key importance the pulling tests that were performed on Norway spruce in steep conditions (Marchi et al., 2022). They allowed us to understand the different response of trees grown on flat as opposed to steep terrain, which allowed us to incorporate this new variable in our modelling workflow and therefore to use a more accurate parametrisation of the model by modifying the overturning coefficient of Norway spruce according to DBH and terrain steepness. The validation process of the new parametrisation was unsuccessful using the WASP model approach. The final values of the Success Index were always under the selected threshold. This can be explained by the high orographic complexity of mountainous scenarios. The WAsP model was developed for situations with much less complex terrain (Rau et al., 2022; Venäläinen et al., 2004) and it is to be expected that the uncertainties of the WAsP outputs for very complex terrain, like mountains and steep slopes, would increase over short horizontal distances (Suárez et al., 1999). In our validation process these uncertainties have likely propagated to affect the correct identification of the modelled wind damaged areas: when combined with the *fgr* vulnerability output, the output of the WAsP model (the peak mean wind speeds in our study) will lead to a decrease in the performance of the overall modelling framework, as reflected in the low SI values related to the WAsP approach in our study. Even if both cases ended with nonsignificant results (SI < 0.7), in our study using *fgr* with the TMC method yielded better results. This might be because TMC method operates at the individual tree level and can also consider the effect of competition with other trees (Hale et al., 2012). We think that the TMC method provides the advantage that, working at the scale of a single tree, it better describes site-specific conditions, and, unlike the roughness method, it is directly applicable to mixed stands (Hale et al., 2015). In contrast, the approach using TOPEX indices yielded better results despite the simplifications that we introduced. We explored relationships between the calculated TOPEX indices and the wind data of the different weather stations using either linear or more complex statistical models, but the complexity of the topography and the impact that this had on the behaviour of storm Vaia over the Italian Alps (Davolio et al., 2020; Giovannini et al., 2021) led us to opt for the simple ratio shown in Eq. 10. The two key factors for the higher SI values using the TOPEX approach were the distance to the horizon and the chosen wind directions. When using TOPEX from all directions the results were below the selected threshold of SI. However, if TOPEX direction was restricted to the angles of the prevailing winds during storm Vaia (i.e., S + SE+ E) the results were significant, i.e., over the SI threshold of 0.7 at the cutpoint. This approach relies on some assumptions and simplifications that we believe could overcome the complexity of the orography of the alpine scenario. If possible, however, we would suggest comparing directional TOPEX indices such as that used in our study with more accurate - but likely much more computationally demanding - airflow models in the future, as suggested by other authors

(Usbeck et al., 2012). The best values of SI were obtained using a TOPEX with a 1000m distance from the horizon and using the S + SE + E wind directions. Under these conditions, we consider the new parametrisation validated. Reducing the distance from the horizon yielded still acceptable SI values, but these slightly decreased along with the distance from the horizon. We compared our values of SI and PS with those obtained by Hale t al. (2015) and we found that while *fgr* performed slightly better in our case study, our cutpoint multipliers were consistently lower. This can be attributed to two main factors: (i) weather stations were located at considerable distance from each other, which influenced our decision to apply the aforementioned simplifications. We expect that a denser network of weather stations would improve the performance of the model and increase the values of the multipliers; (ii) the impact of wind gusts, which have the potential to damage trees in all vulnerability classes both due to their intensity and to the cumulative stress that they transfer on trees. The impact of wind gusts is particularly difficult to predict because of the very complex dynamics of surface wind speeds (Gardiner et al., 2016), as observed in forests on the Swiss Alps in the aftermath of the Vivian and Lothar storms (Usbeck et al., 2012). At the moment *fgr* cannot account for the cumulative effect of repeated gusts on trees' resistance to wind damage. Similarly, trees' responses to wind gusts require further study and characterisation to be added to process-based models of wind damage. Moreover, we might be underestimating wind speeds above the forest. In summary, this LiDAR centred validation procedure gave us satisfactory results. We suggest the use of a similar procedure whenever it is needed to validate future releases of the ForestGALES/fgr model or when some significant changes are made to the model, e.g., new species or conceptually different overturning coefficient (C_{reg}) values, such as in this case study for trees growing on steep terrain.

Post storm scenario and DoV

The workflow that we applied to *fgr* combined with LiDAR derived data has been successful, providing some of the first vulnerability maps for wind damages for the Italian Alps. Once the new parameterisation was tested and considered validated, it was possible to study the effects of storm Vaia on a municipal scale. It is known that natural disturbances can have a high impact on areas that were previously damaged (Hanewinkel et al., 2008), which is why it is of great importance both to identify damaged areas after a disturbance (Forzieri et al., 2020) and to evaluate new vulnerability to damage in the proximity to these areas. Observing the post storm scenario, we can see that the average CWS in the municipality did not change significantly after the storm. What can be observed is the widening of the distribution of CWS values, with both lower (down to 9 m/s) and higher values (over 21 m/s) after the storm, indicating higher and lower vulnerability, respectively. These lower values can be explained by the opening of new edges and new gaps, which resulted in "brown edges"

not yet acclimated to the new wind regime (Peltola et al., 1999; Quine et al., 2021). These values are mainly found in areas where the severity of the storm was high. It is also interesting to observe that the average value of CWS did not change. This can be ascribed to the decrease of CWS values in areas that were not highly susceptible before the storm but where the severity of the disturbance was still sufficiently high to promote tree instability in the forest stands.

In our DoV map, we observed that vulnerability decreased mainly where the previous disturbance had a low severity. In these areas, it was mainly the higher and more unstable trees that were windthrown by Vaia, obtaining a similar effect of a thinning from above. Decreasing the average height within a raster cell, the values of CWS increased while the vulnerability to wind decreased. Our findings seem to suggest that thinning from above could increase stand stability against wind. Thinnings are among forest practices that can heavily modify vulnerability to wind damage (Hale et al., 2004). In the last century, studies have focused on the different effects of thinnings from below and thinnings from above on stand stability (Cremer et al. 1982, Busby et al. 1965), with contrasting results. Models have also been used to better understand how vulnerability to wind may change after thinnings (Duperat et al., 2021), indicating that for some species (e.g., balsam fir) trees from the upper canopy should be removed to reduce vulnerability. Short-term stand instability might also be increased by thinnings when the supporting effect of neighbouring trees is removed (Kamimura et al., 2022). Wind risk models have also been used to study the impact on stand stability of other silvicultural interventions (Zeng et al., 2004), the aim always being to identify the best practices to decrease the probability of wind damage. The combined application of DoV and vulnerability maps is useful to identify areas in which vulnerability to wind damage changed after the storm, and where to focus the management of the surviving stands to reduce the risk of further damage from future storms. These maps can inform the production of guidelines for forest managers, for instance to identify areas where to focus forest restoration practices, where to lead silvicultural activities, such as thinning, or where to apply other interventions aimed to reduce vulnerability to wind damages. Some authors (Suvanto et al., 2019) underline the importance of having maps related with wind risk, in this work we presented a first suggestion for the creation of vulnerability maps for the Alpine scenario. To obtain more detailed risk maps, data related with wind regimes are required (Gardiner and Quine, 2000).

The importance of these maps it is likely to increase in the next future. Taking the example of the protective function of mountain forests: some authors discussed how climate change may undermine the provision of this ecosystem service and how silviculture may promote the transition toward tree species that may be more resistant to the changed climate and still maintain a protective efficiency (Moos et al., 2021). In this case, vulnerability maps may represent the ideal tool to

evaluate the future predisposition of new tree species to wind damages in stands where the priority is protection and vulnerability to wind damage should be lowered, maximising the stability of protection forests.

The key task is to connect the concept of exposure to risk to the vulnerability of future stands, i.e., to ensure that key areas for the delivery of ecosystem services besides the protective function are at low risk. This goal can be achieved by acting to identify low vulnerability areas, or to reduce vulnerability in crucial areas for ecosystem services provision. More practically, vulnerability maps can be incorporated into a decision flow that identifies areas of high priority for intervention. In these areas, it will then be necessary to identify practices aimed at:

- the timing of silvicultural interventions. To do so it would be optimal to couple mechanistic models with dynamic growth models, to observe how vulnerability may change and vary as a function of time and management;

- the spatial distribution of new edges when these cannot be avoided;

- the design of forest management units to favour the orientation of new edges relative to the predominant wind direction or, especially in complex terrain, to that of the main valleys;

- species selection when a transition to different tree species is desired. In this case similar maps should be calculated for alternative species.

4.5 Conclusions and outlooks

Our study developed a workflow for validating a new parametrisation of the *fgr* wind risk model in an alpine scenario, which led to the following results:

- We successfully validated the new parameters that we introduced in the model and thus we were able to produce vulnerability maps that we used to analyse the effect of storm Vaia, an extra tropical windstorm that affected the Alps at the end of October 2018.
- We produced two different vulnerability maps, for forest conditions before and after the storm, for a municipality in the Italian Veneto region. We used these maps to create a DoV (difference of vulnerability) raster; the observation of changes in vulnerability to wind damage allowed us to investigate damage patterns that are caused by wind disturbances in a mountainous context.
- A limitation of our work was related to the difficulty of modelling airflow in a mountainous context, which forced us to use simplifications. Our approach using topographic exposure (TOPEX) to wind was effective but we suggest that future research explore a better

understanding of wind dynamics in highly complex terrain such as through the use of computational fluid dynamic models (e.g. Desmond et al., 2017).

We advocate that future research should follow a validation procedure for new model parameterizations similar to the one set out in this study, for instance when adding to the number of broadleaved species by performing tree-pulling tests. By doing so, it will be possible to improve the model's performance in different contexts and use the model's output to evaluate silvicultural practices and wind impacts on forests, both in terms of structural-ecological, and economic aspects.

5.6 References

Ancelin, P., Courbaud, B., Fourcaud, T., 2004. Development of an individual tree-based mechanical model to predict wind damage within forest stands. For. Ecol. Manage. 203, 101–121. https://doi.org/10.1016/j.foreco.2004.07.067

Anyomi, K.A., Mitchell, S.J., Ruel, J.-C., 2016. Windthrow modelling in old-growth and multi-layered boreal forests. Ecol. Modell. 327, 105–114. https://doi.org/10.1016/j.ecolmodel.2016.02.003

Bebi, P., Seidl, R., Motta, R., Fuhr, M., Firm, D., Krumm, F., Conedera, M., Ginzler, C., Wohlgemuth, T., Kulakowski, D., 2017. Changes of forest cover and disturbance regimes in the mountain forests of the Alps. For. Ecol. Manage. 388, 43–56. https://doi.org/10.1016/j.foreco.2016.10.028

Bennett, N.D., Croke, B.F.W., Guariso, G., Guillaume, J.H.A., Hamilton, S.H., Jakeman, A.J., Marsili-Libelli, S., Newham, L.T.H., Norton, J.P., Perrin, C., Pierce, S.A., Robson, B., Seppelt, R., Voinov, A.A., Fath, B.D., Andreassian, V., 2013. Characterising performance of environmental models. Environ. Model. Softw. 40, 1–20. https://doi.org/10.1016/j.envsoft.2012.09.011

Blennow, K., Olofsson, E., 2008. The probability of wind damage in forestry under a changed wind climate. Clim. Change 87, 347–360. https://doi.org/10.1007/s10584-007-9290-z

Brang, P., Schonenberger, W., Frehner, M., Schwitter, R., Thormann, J.J., Wasser, B., 2006. Management of protection forests in the European Alps: An overview. For. Snow Landsc. Res. 80, 23–44.

Busby, J.A. 1965 Studies on the stability of conifer stands. Scott. For. 19, 86–102.

Chapman, L., 2000. Assessing topographic exposure. Meteorol. Appl. 7, 335–340. https://doi.org/10.1017/S1350482700001729

Costa, M., Marchi, N., Bettella, F., Bolzon, P., Berger, F., Lingua, E., 2021. Biological legacies and rockfall: The protective effect of a windthrown forest. Forests 12, 1–16. https://doi.org/10.3390/f12091141

Cremer, K.W., Borough, C.J., Mckinnell, F.H. et al. 1982 Effects of stocking and thinning on wind damage in plantations. N. Z. J. For. Sci. 12, 244–265.

Davolio, S., Della Fera, S., Laviola, S., Miglietta, M.M., Levizzani, V., 2020. Heavy Precipitation over Italy from the Mediterranean Storm “Vaia” in October 2018: Assessing the Role of an Atmospheric River. Mon. Weather Rev. 148, 3571–3588. https://doi.org/10.1175/MWR-D-20-0021.1

Desmond CJ, Watson SJ, Hancock PE (2017) Modelling the wind energy resources in complex terrain and atmospheres. Numerical simulation and wind tunnel investigation of non-neutral forest canopy flows. J Wind Eng Ind Aerodyn 166:48–60

Duperat, M., Gardiner, B., Ruel, J.C., 2021. Testing an individual tree wind damage risk model in a naturally regenerated balsam fir stand: Potential impact of thinning on the level of risk. Forestry 94, 141–150. https://doi.org/10.1093/forestry/cpaa023

Elie, J.G., Ruel, J.C., 2005. Windthrow hazard modelling in boreal forests of black spruce and jack pine. Can. J. For. Res. 35, 2655–2663. https://doi.org/10.1139/x05-189

Fleischer, P., Pichler, V., Flaischer, P., Holko, L., Mális, F., Gömöryová, E., Cudlín, P., Holeksa, J., Michalová, Z., Homolová, Z., Skvarenina, J., Střelcová, K., Hlaváč, P., 2017. Forest ecosystem services affected by natural disturbances, climate and land-use changes in the Tatra Mountains.

Clim. Res. 73, 57–71. https://doi.org/10.3354/cr01461

Forzieri, G., Girardello, M., Ceccherini, G., Spinoni, J., Feyen, L., Hartmann, H., Beck, P.S.A., Camps-Valls, G., Chirici, G., Mauri, A., Cescatti, A., 2021. Emergent vulnerability to climate-driven disturbances in European forests. Nat. Commun. 12, 1081. https://doi.org/10.1038/s41467-021-21399-7

Forzieri, G., Pecchi, M., Girardello, M., Mauri, A., Klaus, M., Nikolov, C., Rüetschi, M., Gardiner, B., Tomastik, J., Small, D., Nistor, C., Jonikavicius, D., Spinoni, J., Feyen, L., Giannetti, F., Comino, R., Wolynski, A., Pirotti, F., Maistrelli, F., Savulescu, I., Wurpillot-Lucas, S., Karlsson, S., Zieba-Kulawik, K., Strejczek-Jazwinska, P., Mokroš, M., Franz, S., Krejci, L., Haidu, I., Nilsson, M., Wezyk, P., Catani, F., Chen, Y.Y., Luyssaert, S., Chirici, G., Cescatti, A., Beck, P.S.A., 2020. A spatially explicit database of wind disturbances in European forests over the period 2000-2018. Earth Syst. Sci. Data 12, 257–276. https://doi.org/10.5194/essd-12-257-2020

Gardiner, B., 2021. Wind damage to forests and trees: a review with an emphasis on planted and managed forests. J. For. Res. 26, 248–266. https://doi.org/10.1080/13416979.2021.1940665

Gardiner, B., Schuck, A., Schelhaas, M.-J., Orazio, C., Blennow, K., Nicoll, B., 2013. Living with Storm Damage to Forests. What Science Can Tell Us 3. https://doi.org/10.1007/s10342-006-0111-0

Gardiner, B.A., Quine, C.P., 2000. Management of forests to reduce the risk of abiotic damage - A review with particular reference to the effects of strong winds. For. Ecol. Manage. 135, 261–277. https://doi.org/10.1016/S0378-1127(00)00285-1

Gardiner, B., Berry, P. and Moulia, B., 2016. Wind impacts on plant growth, mechanics and damage. Plant science, 245, pp.94-118.

Gardiner, B. A, 1992. Mathematical modelling of the static and dynamic characteristics of plantation trees. Mathematical modelling of forest ecosystems: 40-61.

Giovannini, L., Davolio S., Zaramella M., Zardi D., Borga M., 2021. Multi-model convection-resolving simulations of the October 2018 Vaia storm over Northeastern Italy. Atm. Res. 253 https://doi.org/10.1016/j.atmosres.2021.105455

Gopalakrishnan, R., Packalen, P., Ikonen, V.P., Räty, J., Venäläinen, A., Laapas, M., Pirinen, P., Peltola, H., 2020. The utility of fused airborne laser scanning and multispectral data for improved wind damage risk assessment over a managed forest landscape in Finland. Ann. For. Sci. 77. https://doi.org/10.1007/s13595-020-00992-8

Hale, S.A., Gardiner, B., Peace, A., Nicoll, B., Taylor, P., Pizzirani, S., 2015. Comparison and validation of three versions of a forest wind risk model. Environ. Model. Softw. 68, 27–41. https://doi.org/10.1016/j.envsoft.2015.01.016

Hale, S.E., Gardiner, B.A., Wellpott, A., Nicoll, B.C., Achim, A., 2012. Wind loading of trees: Influence of tree size and competition. Eur. J. For. Res. 131, 203–217. https://doi.org/10.1007/s10342-010-0448-2

Hale, S.E., Levy, P.E., Gardiner, B.A., 2004. Trade-offs between seedling growth, thinning and stand stability in Sitka spruce stands: A modelling analysis. For. Ecol. Manage. 187, 105–115. https://doi.org/10.1016/S0378-1127(03)00313-X

Hanewinkel, M., Breidenbach, J., Neeff, T., Hanewinkel, E.K.M., 2008. Seventy-seven years of natural disturbances in a mountain forest area - The influence of storm, snow, and insect damage analysed with a long-term time series. Can. J. For. Res. 38, 2249–2261. https://doi.org/10.1139/X08-070

Hart, E., Sim, K., Kamimura, K., Meredieu, C., Guyon, D., Gardiner, B., 2019. Use of machine learning techniques to model wind damage to forests. Agric. For. Meteorol. 265, 16–29. https://doi.org/10.1016/j.agrformet.2018.10.022

Jackson, T., Bunce, A., James, K., Wellpott, A., Van Bloem, S., Achim, A., Gardiner, B.A., 2021. The motion of trees in the wind: a data synthesis. Biogeosciences 18, 4059–4072.

Kamimura, K., Nanko, K., Matsumoto, A., Ueno, S., Gardiner, J., Gardiner, B., 2022. Tree dynamic response and survival in a category-5 tropical cyclone : The case of super typhoon Trami. Sci. Adv. 8, 1–11.

Kamimura, K., Gardiner, B., Dupont S., Guyon D., Meredieu C., 2016. Mechanistic and statistical approaches to predicting wind damage to individual maritime pine (*Pinus pinaster*) trees in forests. Can. J. For. Res. 46, 88–100. https://doi.org/10.1139/cjfr-2015-0237

Locatelli, T., Gardiner, B., Tarantola, S., Nicoll, B., Bonnefond, J.M., Garrigou, D., Kamimura, K., Patenaude, G., 2016. Modelling wind risk to Eucalyptus globulus (Labill.) stands. For. Ecol. Manage. 365, 159–173. https://doi.org/10.1016/j.foreco.2015.12.035

Locatelli, T., Tarantola, S., Gardiner, B., Patenaude, G., 2017. Variance-based sensitivity analysis of a wind risk model - Model behaviour and lessons for forest modelling. Environ. Model. Softw. 87, 84–109. https://doi.org/10.1016/j.envsoft.2016.10.010

Locatelli, T., Gardiner, B., Hale, S., Nicoll, B., 2021. fgr: R Version of the ForestGALES wind risk model. R package version 1.0. https://www.forestresearch.gov.uk/tools-and-resources/fthr/forestgales/fgr- the-forestgales-r-package/

Locatelli, T., Hale, S., Nicoll, B., and Gardiner, B., 2022. The ForestGALES wind risk model and the fgr R package. Fgr User manual. Available at: https://www.forestresearch.gov.uk/tools-and-resources/fthr/forestgales/fgr-the-forestgales-r-package

Machado Nunes Romeiro, J., Eid, T., Antón-Fernández, C., Kangas, A., Trømborg, E., 2022. Natural disturbances risks in European Boreal and Temperate forests and their links to climate change – A review of modelling approaches. For. Ecol. Manage. 509, 120071. https://doi.org/10.1016/j.foreco.2022.120071

Marchi, L., Costa, M., Grigolato, S., Lingua, E., 2022. Overturning resistance of large diameter Norway spruce (Picea abies (L.) Karst) on sloped conditions. For. Ecol. Manage. 524, 120531. https://doi.org/10.1016/j.foreco.2022.120531

Marchi, L., Trutalli, D., Mologni, O., Gallo, R., Roeser, D., Cavalli, R., Grigolato, S., 2021. Mechanical response of natural anchors in cable logging. Int. J. For. Eng. 32, 29–42. https://doi.org/10.1080/14942119.2021.1826882

Mortensen, N.G., Landberg, L., Troen, I., Petersen, E.L., Rathmann, O., Nielsen, M., Erik, L., 2004. WAsP Utility Programs. Risø Natl. Lab. Risø-I No. 2261, 52.

Moos, C., Guisan, A., Randin, C.F., Lischke, H., 2021. Climate Change Impacts the Protective Effect of Forests: A Case Study in Switzerland. Front. For. Glob. Chang. 4. https://doi.org/10.3389/ffgc.2021.682923

Motta, R., Haudemand, J.-C., 2000. Protective Forests and Silvicultural Stability. Mt. Res. Dev. 20, 180–187. https://doi.org/10.1659/0276-4741(2000)020[0180:PFASS]2.0.CO;2

Nicoll, B.C., Gardiner, B.A., Rayner, B., Peace, A.J. 2006. Anchorage of coniferous trees in relation to

species, soil type, and rooting depth. Canadian Journal of Forest Research-Revue Canadienne De Recherche Forestiere, 36, 1871-1883.

Patacca, M., Lindner, M., Lucas-Borja, M.E., Cordonnier, T., Fidej, G., Gardiner, B., Hauf, Y., Jasinevičius, G., Labonne, S., Linkevičius, E., Mahnken, M., Milanovic, S., Nabuurs, G.J., Nagel, T.A., Nikinmaa, L., Panyatov, M., Bercak, R., Seidl, R., Ostrogović Sever, M.Z., Socha, J., Thom, D., Vuletic, D., Zudin, S., Schelhaas, M.J., 2022. Significant increase in natural disturbance impacts on European forests since 1950. Glob. Chang. Biol. 1–18. https://doi.org/10.1111/gcb.16531

Peltola, H., Kellomäki, S., Väisänen, H., Ikonen, V.P., 1999. A mechanistic model for assessing the risk of wind and snow damage to single trees and stands of Scots pine, Norway spruce, and birch. Can. J. For. Res. 29, 647–661. https://doi.org/10.1139/x99-029

Piragnolo, M., Pirotti, F., Zanrosso, C., Lingua, E., Grigolato, S., 2021. Responding to large-scale forest damage in an alpine environment with remote sensing, machine learning, and Web-GIS. Remote Sens. 13. https://doi.org/10.3390/rs13081541

Quine, C.P., Gardiner, B.A., Moore, J., 2021. Wind disturbance in forests: The process of wind created gaps, tree overturning, and stem breakage, Plant Disturbance Ecology: The Process and the Response. https://doi.org/10.1016/B978-0-12-818813-2.00004-6

Quine, C.P., Humphrey, J.W., Purdy, K., Ray, D., 2002. An approach to predicting the potential forest composition and disturbance regime for a highly modified landscape: A pilot study of Strathdon in the Scottish Highlands. Silva Fenn. 36, 233–247. https://doi.org/10.14214/sf.560

R Core Team (2022). R: A language and environment for statistical computing. R Foundation for Statistical Computing, Vienna, Austria. https://www.R-project.org/.

Rau, E.P., Gardiner, B.A., Fischer, F.J., Maréchaux, I., Joetzjer, E., Sun, I.F., Chave, J., 2022. Wind Speed Controls Forest Structure in a Subtropical Forest Exposed to Cyclones: A Case Study Using an Individual-Based Model. Front. For. Glob. Chang. 5, 1–16. https://doi.org/10.3389/ffgc.2022.753100

Raupach, M. R.: 1992, 'Drag and Drag Partition on Rough Surfaces', Boundary-Layer Meteorol. 60, 375-395.

Raupach, M.R., 1994. Simplified expressions for vegetation roughness length and zero-plane displacement as functions of canopy height and area index. Boundary-Layer Meteorol. 71, 211–216. https://doi.org/10.1007/BF00709229

Sagi, P., Newson, T., Miller, C., Mitchell, S., 2019. Stem and root system response of a Norway spruce tree (Picea abies L.) under static loading. For. An Int. J. For. Res. 92, 460–472. https://doi.org/10.1093/forestry/cpz042

Schönenberger, W., Noack, A., Thee, P., 2005. Effect of timber removal from windthrow slopes on the risk of snow avalanches and rockfall. For. Ecol. Manage. 213, 197–208. https://doi.org/10.1016/j.foreco.2005.03.062

Seidl, R., Blennow, K., 2012. Pervasive growth reduction in norway spruce forests following wind disturbance. PLoS One 7. https://doi.org/10.1371/journal.pone.0033301

Seidl, R., Rammer, W., Blennow, K., 2014. Simulating wind disturbance impacts on forest landscapes: Tree-level heterogeneity matters. Environ. Model. Softw. 51, 1–11. https://doi.org/10.1016/j.envsoft.2013.09.018

Seidl, R., Thom, D., Kautz, M., Martin-Benito, D., Peltoniemi, M., Vacchiano, G., Wild, J., Ascoli, D.,

Petr, M., Honkaniemi, J., Lexer, M.J., Trotsiuk, V., Mairota, P., Svoboda, M., Fabrika, M., Nagel, T.A., Reyer, C.P.O., 2017. Forest disturbances under climate change. Nat. Clim. Chang. 7, 395–402. https://doi.org/10.1038/nclimate3303

Suarez, J., Garcia, R., Gardiner, B., Patenaude, G., 2008. The Estimation of Wind Risk in Forests Stands using Airborne Laser Scanning (ALS)(<Special Issue>Silvilaser). J. For. Plan. 13, 165–185. https://doi.org/10.20659/jfp.13.special_issue_165

Suárez, J.C., Gardiner, B.A., Quine, C.P., 1999. A comparison of three methods for predicting wind speeds in complex forested terrain. Meteorol. Appl. 6, 329–342. https://doi.org/10.1017/S1350482799001267

Suvanto, S., Peltoniemi, M., Tuominen, S., Strandström, M., Lehtonen, A., 2019. High-resolution mapping of forest vulnerability to wind for disturbance-aware forestry. For. Ecol. Manage. 453, 117619. https://doi.org/10.1016/j.foreco.2019.117619

Talkkari, A., Peltola, H., Kellomäki, S., Strandman, H., 2000. Integration of component models from the tree, stand and regional levels to assess the risk of wind damage at forest margins. For. Ecol. Manage. 135, 303–313. https://doi.org/10.1016/S0378-1127(00)00288-7

Udali, A., Andrighetto, N., Grigolato, S., Gatto, P., 2021. Economic impacts of forest storms—taking stock of after-vaia situation of local roundwood markets in northeastern italy. Forests 12. https://doi.org/10.3390/f12040414

Unterwieser, H., Schickhofer, G., 2011. Influence of moisture content of wood on sound velocity and dynamic MOE of natural frequency- and ultrasonic runtime measurement. Eur. J. Wood Wood Prod. 69, 171–181. https://doi.org/10.1007/s00107-010-0417-y

Usbeck, T., Waldner, P., Dobbertin, M., Ginzler, C., Hoffmann, C., Sutter, F., Steinmeier, C., Volz, R., Schneiter, G., Rebetez, M., 2012. Relating remotely sensed forest damage data to wind data: Storms Lothar (1999) and Vivian (1990) in Switzerland. Theor. Appl. Climatol. 108, 451–462. https://doi.org/10.1007/s00704-011-0526-5

Van Doninck J., 2018. horizon: Horizon Search Algorithm. R package version 1.2. https://rdrr.io/cran/horizon/

Venäläinen, A., Zeng, H., Peltola, H., Talkkari, A., Strandman, H., Wang, K., Kellomäki, S., 2004. Simulations of the influence of forest management on wind climate on a regional scale. Agric. For. Meteorol. 123, 149–158. https://doi.org/10.1016/j.agrformet.2003.12.005

Wickham H, Averick M, Bryan J, Chang W, McGowan LD, François R, Grolemund G, Hayes A, Henry L, Hester J, Kuhn M, Pedersen TL, Miller E, Bache SM, Müller K, Ooms J, Robinson D, Seidel DP, Spinu V, Takahashi K, Vaughan D, Wilke C, Woo K, Yutani H, 2019. Welcome to the tidyverse. Journal of Open-Source Software, *4*(43), 1686. doi: 10.21105/joss.01686 (URL: https://doi.org/10.21105/joss.01686)

Wohlgemuth, T., Schwitter, R., Bebi, P., Sutter, F., Brang, P., 2017. Post-windthrow management in protection forests of the Swiss Alps. Eur. J. For. Res. 136, 1029–1040. https://doi.org/10.1007/s10342-017-1031-x

Zeng, H., Peltola, H., Talkkari, A., Venäläinen, A., Strandman, H., Kellomäki, S., Wang, K., 2004. Influence of clear-cutting on the risk of wind damage at forest edges. For. Ecol. Manage. 203, 77–88. https://doi.org/10.1016/j.foreco.2004.07.057

6. Conclusions and outlooks for the future

This thesis work aimed to understand the impacts of natural disturbances, specifically windstorms, on protective forests in the Alps. The different chapters addressed the topic starting with a presentation of the state of the art regarding natural disturbances and their legacies, moving to a post-disturbance management phase aimed at maintaining protective function, and ending with a discussion of strategies for prevention and mitigation of future wind damage.

The systematic review presented in Chapter 2, starting from a broad point of view, sought to observe and discuss the different roles that different disturbance legacies can play. Once the definition of disturbance legacies had been harmonised according to some authors (Franklin et al., 2000; Johnstone et al., 2016), 95 papers were analysed in order to provide an up-to-date state of the art. It was chosen to start from this broad analysis because the general understanding of a disturbance is necessarily linked to post disturbance dynamics. Knowledge of these is fundamental to management; with reference to forest management, knowledge of the roles of biological legacies in the forest is fundamental to restoration processes and to target interventions that may enhance them (Seidl et al., 2014). The most studied roles were found to be related to the dynamics of post-disturbance recovery processes and species life-boating. Among the various aspects studied in the literature is also the contribution of biological legacies in maintaining certain ecosystem services, one example being the role of protection from natural hazards, a regulatory ecosystem service.

A clear example of this concept is addressed in Chapter 3, based on a work on wind disturbances in protective forests (Costa et al., 2021). The case study reported concerns a protective forest in an alpine environment, in the Dolomites. Specifically, it is a rockfall protective forest damaged by storm Vaia, a storm that hit north-eastern Italy in October 2018 (Davolio et al., 2020). The chapter highlights the key role of biological legacies, mainly dead wood and lying logs in mitigating rockfall hazards. These legacies act as a physical barrier and reduce the energy of falling rocks. The results obtained are in line with similar studies carried out in other Alpine areas following other storms, e.g., the studies carried out in Switzerland after storms Vivian and Lothar (Wohlgemuth et al., 2017). Currently, research is focused on modelling dead wood to better quantify its effect on protective efficiency (Ringenbach et al., 2022, 2021), the chapter fits into this framework and concludes by advising to avoid practices such as total removal of wood (salvage logging) in forests with a predominantly protective function, as salvage logging would in fact negate the positive effect of legacies. Moreover, it has been observed how to leave biological legacies in a damaged stand may enhance restoration processes, both regarding natural or artificial regeneration (Marangon et al., 2022; Marzano et al., 2012). Future research should analyse the evolution of wood decaying

processes and how these may undermine the physical barrier effect played by lying logs against natural hazards.

The next chapters of the thesis, Chapters 4 and 5, shift the focus from immediate post-disturbance management to the study of key elements in the prevention of future damage, again with reference to wind disturbances specifically.

Chapter 4 is based on pulling tests carried out in an alpine environment, these tests observed the different stability of spruce plants in flat and sloping terrain (Marchi et al., 2022). The results of this study show that plants grown on slopes have greater overturning resistance than those grown in a flat environment. The results of these tests made it possible to introduce a new parameterisation into a model for the assessment of susceptibility to wind impacts. In fact, it should be emphasised that overturning resistance is an important factor in calculating trees susceptibility to wind damages; different overturning coefficients correspond to different critical wind speeds (Locatelli et al., 2016; Quine et al., 2020), i.e. the minimum wind speed capable of damaging individual plants or forest stands, in this case referring in particular to the wind speed required for a tree to overturn. The new parameterisation for susceptibility assessment was therefore based on these new values of the overturning coefficients, and values of wood characteristics, modulus of elasticity and modulus of rupture, obtained from wood samples taken during field tests were also added.

Chapter 5 therefore deals with the validation of this parameterisation dedicated to the Alpine Mountain environment. The model used is the semi-empirical model ForestGales, and its most recent version '*fgr*' (Gardiner and Quine, 2000; Quine et al., 2020). The validation process was based on previous works (Hale et al., 2015), consolidating a methodology that can be replicated whenever new parameterisations need to be included in the model. Once validated, the use of this parameterisation allowed the construction of wind susceptibility maps from LiDAR data as suggested in the literature (Gopalakrishnan et al., 2020; Suarez et al., 2008). Some authors indicate how mapping risk and vulnerability to natural disturbances, in this case wind, is an essential tool for forest planning (Suvanto et al., 2019). As previously pointed out, the frequency of natural disturbances is expected to increase, as is their severity (Patacca et al., 2022; Seidl et al., 2017) and forest management need to target interventions to obtain more resistant and resilient forest stands.

This planning tool may be particularly important when considering protective forests. For while it has already been noted in the earlier chapters how despite wind damage these stands can continue to provide a protective function effectively, management should aim to apply strategies to prevent future damage in a way that ensures continued protective effectiveness, guaranteeing the preservation of local communities and infrastructures.

An example that is discussed in Chapter 5 is thinnings. In this chapter, using LiDAR data obtained before and after a storm, it was observed that the stability of a forest stand increased in areas where the severity of disturbance was low. In these areas, natural disturbance caused similar effects as thinning from above, removing taller plants. The issue of thinnings as a tool to mitigate wind damage is a hotly debated topic; the debate is currently open (Duperat et al., 2021). Models can help improve knowledge in this regard; future research should aim to consolidate these concepts to provide guidelines for forest managers.

To conclude, some aspects that can be summarized with respect to management strategies for protective forests damaged by windstorms:

- salvage logging should be avoided where the protective function of a damaged forest stand is predominant.

- Deadwood and lying logs can help maintaining a protective efficiency in the short term, moreover deadwood will have a positive effect for restoration dynamics. For what concern the wood decaying processes that may occur in the long term, and how these will affect protective efficiency, further investigation in needed.

- Models can help forest management, if necessary, it is useful to enter new parameterizations and validate them. Parameterizations should be based on field data whenever possible.

- Vulnerability to wind maps should be taken into account in the detailed planning of mountain forest areas, with the aim of maintaining stand stability.

- Thinnings can be a useful management tool for maintaining stability in protective forests, however, it is necessary to further investigate which types of thinning, with which timing and in which context it is best to perform them.

6.6 References

Costa, M., Marchi, N., Bettella, F., Bolzon, P., Berger, F., Lingua, E., 2021. Biological legacies and rockfall: The protective effect of a windthrown forest. Forests 12, 1–16. https://doi.org/10.3390/f12091141

Davolio, S., Della Fera, S., Laviola, S., Miglietta, M.M., Levizzani, V., 2020. Heavy Precipitation over Italy from the Mediterranean Storm "Vaia" in October 2018: Assessing the Role of an Atmospheric River. Mon. Weather Rev. 148, 3571–3588. https://doi.org/10.1175/MWR-D-20-0021.1

Duperat, M., Gardiner, B., Ruel, J.C., 2021. Testing an individual tree wind damage risk model in a naturally regenerated balsam fir stand: Potential impact of thinning on the level of risk. Forestry 94, 141–150. https://doi.org/10.1093/forestry/cpaa023

Franklin, J.F., Lindenmayer, D., Macmahon, J.A., Mckee, A., Perry, D.A., Waide, R., Foster, D., 2000. Threads of Continuity: Ecosystem disturbance, recovery, and the theory of biological legacies. Conserv. Pract. 1, 8–17.

Gardiner, B.A., Quine, C.P., 2000. Management of forests to reduce the risk of abiotic damage - A review with particular reference to the effects of strong winds. For. Ecol. Manage. 135, 261–277. https://doi.org/10.1016/S0378-1127(00)00285-1

Gopalakrishnan, R., Packalen, P., Ikonen, V.P., Räty, J., Venäläinen, A., Laapas, M., Pirinen, P., Peltola, H., 2020. The utility of fused airborne laser scanning and multispectral data for improved wind damage risk assessment over a managed forest landscape in Finland. Ann. For. Sci. 77. https://doi.org/10.1007/s13595-020-00992-8

Hale, S.A., Gardiner, B., Peace, A., Nicoll, B., Taylor, P., Pizzirani, S., 2015. Comparison and validation of three versions of a forest wind risk model. Environ. Model. Softw. 68, 27–41. https://doi.org/10.1016/j.envsoft.2015.01.016

Johnstone, J.F., Allen, C.D., Franklin, J.F., Frelich, L.E., Harvey, B.J., Higuera, P.E., Mack, M.C., Meentemeyer, R.K., Metz, M.R., Perry, G.L.W., Schoennagel, T., Turner, M.G., 2016. Changing disturbance regimes, ecological memory, and forest resilience. Front. Ecol. Environ. 14, 369–378. https://doi.org/10.1002/fee.1311

Locatelli, T., Gardiner, B., Tarantola, S., Nicoll, B., Bonnefond, J.M., Garrigou, D., Kamimura, K., Patenaude, G., 2016. Modelling wind risk to Eucalyptus globulus (Labill.) stands. For. Ecol. Manage. 365, 159–173. https://doi.org/10.1016/j.foreco.2015.12.035

Marangon, D., Marchi, N., Lingua, E., 2022. Windthrown elements: a key point improving microsite

amelioration and browsing protection to transplanted seedlings. For. Ecol. Manage. 508. https://doi.org/10.1016/j.foreco.2022.120050

Marchi, L., Costa, M., Grigolato, S., Lingua, E., 2022. Overturning resistance of large diameter Norway spruce (Picea abies (L.) Karst) on sloped conditions. For. Ecol. Manage. 524, 120531. https://doi.org/10.1016/j.foreco.2022.120531

Marzano, R., Lingua, E., Garbarino, M., 2012. Post-fire effects and short-term regeneration dynamics following highseverity crown fires in a Mediterranean forest. IForest 5, 93–100. https://doi.org/10.3832/ifor0612-005

Patacca, M., Lindner, M., Lucas-Borja, M.E., Cordonnier, T., Fidej, G., Gardiner, B., Hauf, Y., Jasinevičius, G., Labonne, S., Linkevičius, E., Mahnken, M., Milanovic, S., Nabuurs, G.J., Nagel, T.A., Nikinmaa, L., Panyatov, M., Bercak, R., Seidl, R., Ostrogović Sever, M.Z., Socha, J., Thom, D., Vuletic, D., Zudin, S., Schelhaas, M.J., 2022. Significant increase in natural disturbance impacts on European forests since 1950. Glob. Chang. Biol. 1–18. https://doi.org/10.1111/gcb.16531

Quine, C.P., Gardiner, B.A., Moore, J., 2020. Wind disturbance in forests: The process of wind created gaps, tree overturning, and stem breakage, Plant Disturbance Ecology: The Process and the Response. https://doi.org/10.1016/B978-0-12-818813-2.00004-6

Ringenbach, A., Bebi, P., Bartelt, P., Rigling, A., Christen, M., Bühler, Y., Stoffel, A., Caviezel, A., 2022. Modelling deadwood for rockfall mitigation assessments in windthrow areas. Earth Surf. Dyn. Discuss. 1–24.

Ringenbach, A., Stihl, E., Bühler, Y., Bebi, P., Bartelt, P., Rigling, A., Christen, M., Lu, G., Stoffel, A., Kistler, M., Degonda, S., Simmler, K., Mader, D., Caviezel, A., 2021. Full scale experiments to examine the role of deadwood on rockfall dynamics in forests 1–15.

Seidl, R., Rammer, W., Spies, T.A., 2014. Disturbance legacies increase the resilience of forest ecosystem structure, composition, and functioning. Ecol. Appl. 24, 2063–2077. https://doi.org/10.1890/14-0255.1

Seidl, R., Thom, D., Kautz, M., Martin-Benito, D., Peltoniemi, M., Vacchiano, G., Wild, J., Ascoli, D., Petr, M., Honkaniemi, J., Lexer, M.J., Trotsiuk, V., Mairota, P., Svoboda, M., Fabrika, M., Nagel, T.A., Reyer, C.P.O., 2017. Forest disturbances under climate change. Nat. Clim. Chang. 7, 395–402. https://doi.org/10.1038/nclimate3303

Suarez, J., Garcia, R., Gardiner, B., Patenaude, G., 2008. The Estimation of Wind Risk in Forests Stands using Airborne Laser Scanning (ALS)(<Special Issue>Silvilaser). J. For. Plan. 13, 165–185. https://doi.org/10.20659/jfp.13.special_issue_165

Suvanto, S., Peltoniemi, M., Tuominen, S., Strandström, M., Lehtonen, A., 2019. High-resolution mapping of forest vulnerability to wind for disturbance-aware forestry. For. Ecol. Manage. 453, 117619. https://doi.org/10.1016/j.foreco.2019.117619

Wohlgemuth, T., Schwitter, R., Bebi, P., Sutter, F., Brang, P., 2017. Post-windthrow management in protection forests of the Swiss Alps. Eur. J. For. Res. 136, 1029–1040. https://doi.org/10.1007/s10342-017-1031-x